

# Modelling of magnetic structure using interior point optimization given exchange parameters

Arthur C. Ronner

Bachelor project  
TU Delft

Delft, June 15, 2022  
Supervisors: Prof. Dr. E. Brück  
Dr. C. Urzúa Torres  
Dr. N. van Dijk  
Dr. I. Batashev

## Abstract

In this report, a model is presented to alleviate some of the computational work that goes into the effort of finding the magnetic properties of magnetocaloric materials. The model utilizes an interior point optimization routine to solve for the minimal exchange energy configuration of a system, given the exchange interactions of the material. The model is tested against four materials (Ni, MnO, Fe<sub>2</sub>P and Mn<sub>2</sub>Sb). For Ni and MnO, the exchange interactions are also computed. Three iterations of the model are compared. The base model, which only considers exchange interactions inside a chosen supercell, the base model with the inclusion of boundary conditions, and the base model with boundary conditions and the addition of an algorithm to find optimal solutions.

The algorithm analyzes the found results by the optimization routine, and if the result is considered not properly symmetric, runs the optimization routine another time, from a symmetrical starting point obtained from the outcome of the previous run.

In all versions of the model, effectiveness (percent of runs that resulted in the optimal configuration) and average run times were recorded. Three initialization methods for the model were used, and also tested for their effectiveness. For the algorithm, a parameter  $\gamma$  is introduced that changes the size of some of the moments for the new starting points. Six different values for  $\gamma$  were tested for their effectiveness against a test set of suboptimal solutions. The model with the addition of boundary conditions and the algorithm performed the best out of the three iterations of the model, with an effectiveness of 99.895%, and an average run time ranging from 0.62 s for  $2 \times 2 \times 2$  Ni, to 94.64 s for  $3 \times 3 \times 3$  Fe<sub>2</sub>P, in the case of  $\gamma = 0.3$ . To conclude, the model with the inclusion of the boundary conditions and the algorithm proves to be a robust method to evaluate the magnetic configuration of a material, especially for smaller systems.

# Contents

Abstract . . . . .	i
1. Introduction . . . . .	1
2. Theory . . . . .	2
2.1 Types of magnetism . . . . .	2
2.2 Exchange interactions . . . . .	3
2.3 Magnetocaloric effect . . . . .	4
2.3.1 Applications . . . . .	5
2.4 Magnetocrystalline anisotropy . . . . .	6
2.5 Density-functional theory . . . . .	6
2.6 Wannier functions . . . . .	6
2.7 Green's function method . . . . .	7
2.8 Bilinear form . . . . .	8
2.9 Materials . . . . .	8
2.9.1 Ni . . . . .	8
2.9.2 MnO . . . . .	8
2.9.3 Fe <sub>2</sub> P . . . . .	9
2.9.4 Mn <sub>2</sub> Sb . . . . .	9
3. Method . . . . .	10
3.1 Motivation . . . . .	10
3.2 Data acquisition . . . . .	10
3.2.1 Vienna ab-initio simulation package . . . . .	10
3.2.2 Wannier90 . . . . .	10
3.2.3 TB2J . . . . .	11
3.3 The model . . . . .	11
3.3.1 Interior Point Optimization . . . . .	11
3.3.2 Assumptions . . . . .	12
3.3.3 The basic model . . . . .	12
3.3.4 Boundary conditions . . . . .	13
3.3.5 Symmetry finding algorithm . . . . .	15
4. Results . . . . .	17
4.1 Exchange interactions . . . . .	17
4.1.1 Ni . . . . .	17
4.1.2 MnO . . . . .	17
4.2 Model results . . . . .	18
4.2.1 Basic model . . . . .	19
4.2.2 Including boundary conditions . . . . .	22
4.2.3 Symmetry finding algorithm . . . . .	24
4.2.4 Versions comparison . . . . .	27

5. Discussion . . . . .	28
6. Conclusion . . . . .	31
Appendix A: 3D representation of boundary conditions . . . . .	35
Appendix B: Symmetry finding algorithm flowchart . . . . .	36
Appendix C: Auxiliary results . . . . .	37
Appendix D: Python code . . . . .	49

# 1. Introduction

Magnets truly are curious materials. Natural magnets have already persisted throughout history for a long period of time, but have mostly only been used as a compass for the majority of time since their discovery. It was only after world war 2 that a large surge in research on magnetic materials really started to kick in [1, pp. xiii–xv]. A large reason for this change was the discovery of neutron diffraction, a groundbreaking discovery that allowed for the closer study of individual atoms in a material.

This new rise of interest in magnets, also gave rise a great amount of applications. Not the least of which is their usage in computers, which sparked even more research, applications, and so the cycle continued. More recently a lot of research is conducted in the field of magnetocaloric materials [2] [3], magnetic materials that, when their magnetic configuration is altered, heat up or cool down. These materials have the potential to play a large role in the energy transition, as they can be utilized as an alternative for current refrigerators, which utilize harmful gasses in their core cooling process [4]. Current research concerning magnetocaloric materials is still very much in the exploration phase, and the search for the best material for this application is still very much a work in process [5].

As there is an extreme amount of different potential materials, this search is an endeavor in which a lot of testing has to be done per material considered. This means that, in the search for these new materials, there are a lot of computationally intensive steps to take before the required information about a given material is known.

Therefore, in this study, an attempt is made to simplify this process, specifically, the finding of the magnetic properties of a material. A model is proposed that, when the exchange interactions of a material are known; models the magnetic structure of the material by utilizing the interior point optimization routine. The model is subsequently tested to a number of materials (Ni, MnO, Fe<sub>2</sub>P and Mn<sub>2</sub>Sb), to test its effectiveness at predicting a magnetic structure. Three iterations of the model will be discussed; the base model, the model with the inclusion of boundary conditions, and the model with boundary conditions and a search algorithm.

This report will be structured in the following manner. First; the underlying theory supporting the model will be discussed in section 2. This will include numerous concepts from the field of magnetic materials, as well as numerical solving methods, and material properties for the materials listed above. Next, in section 3, the methodology of the model and the data acquisition for the utilized materials will be covered. This will include the methodology of each of the iterations of the model listed above. Subsequently, the results of the model and the material data acquisition will be presented in section 4, and the discussion and the conclusions in sections 5 and 6, respectively. Lastly, appendices A through D will include a 3D image of the boundary conditions, a flow chart for the model, auxiliary results and the python code of the model, respectively.

## 2. Theory

A number of closely related, separate pieces of theory are used as a basis for the model described in the next chapter. First, magnetism and related topics are discussed, followed by some computational methods, mathematical concepts, and finally some information regarding materials used in this project.

### 2.1. Types of magnetism

Materials can be magnetic in a couple of different ways. The types of magnetism considered here are the ones relevant to this project. Mainly, these types of magnetism can be subdivided into either a ordered (in about 13 different ways) or disordered state. A material is called disordered (paramagnetic) when its atoms have a random fluctuating magnetic moment in the absence of an external magnetic field, resulting in a net zero magnetic moment. As soon as a magnetic field is applied; they align with the external field<sup>1</sup>.

A material can also be ordered (see figure 1). A material is called ferromagnetic when all magnetic moments of atoms point in the same direction, and thereby creating a large magnetic field, even in absence of an external magnetic field. Antiferromagnetic materials are ordered, but their moments exactly cancel each other. Lastly (for the scope of this project;) we have ferrimagnetism, where like an antiferromagnet, moments point in opposite directions, but like a ferromagnet, does induce a net moment. This is due to the different sizes of moments. [1, pp. 87–197]

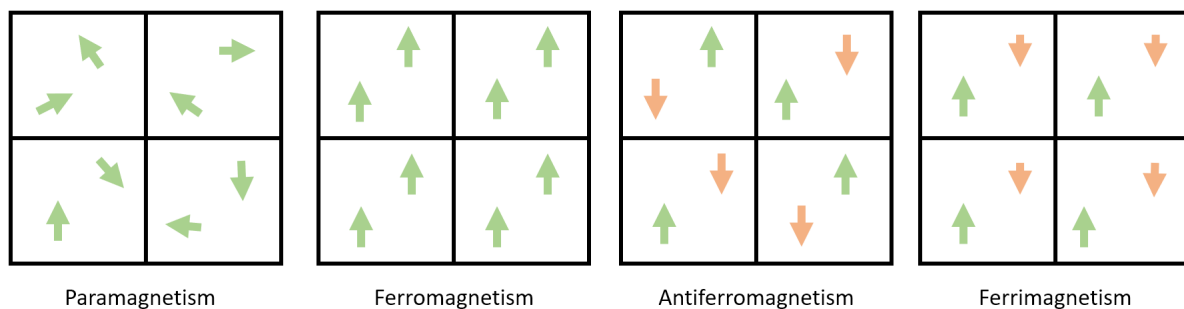


Figure 1: 2D example of the different types of magnetism. Magnetic moments of different atoms are represented by arrows. Red and green is used to emphasize direction when applicable.

Note that the above examples are not a comprehensive list, as more exotic structures also exist (for instance spin spirals, among others).

Each 'ordered' magnetic material, only has this ordered property up until a certain temperature, at which the material becomes paramagnetic. This is because a material is ordered as this is its lowest energy configuration. As a material heats up however, atoms gain more and more thermal motion (entropy), thereby getting less and less incentive to align their magnetic moments as the magnetic contribution to the total energy of the atom is less and less significant [5]. Each magnetically ordered material has a distinct magnetic phase transition (called the Curie ( $T_c$ ) or Néel ( $T_N$ ) temperature for ferro- and antiferromagnetic materials respectively) above which the material loses its magnetic ordering.

One may wonder why some materials are differently ordered magnetically than others, or about the origin of the magnetic order of materials. For that, we will have to look at exchange interactions.

<sup>1</sup>In general, though the temperature of a material also has to be considered. If the material is too warm, it may not be able to be pushed into order. If the material is cold enough, it may already be ordered without an external field.

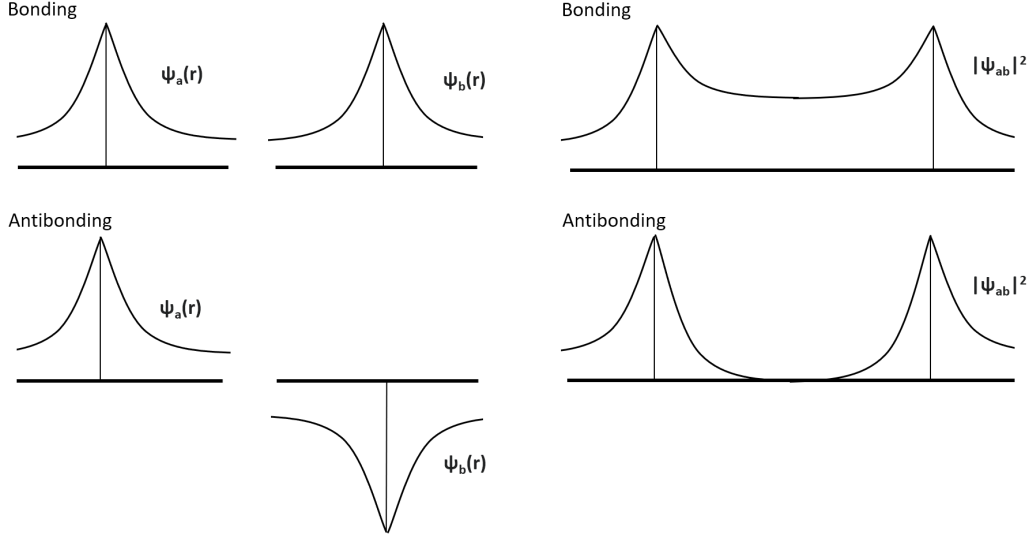


Figure 2: Different positional options for two electrons.  $\psi_a$ ,  $\psi_b$  and  $\psi_{ab}$  represent the wave functions or electron  $a$ ,  $b$  and their combined wavefunction respectively.

## 2.2. Exchange interactions

The exchange interactions are an atomic scale property of materials that couple the direction of the magnetic moments of different atoms in its crystal structure. It exists because of the principle of indistinguishability of quantum particles and the Pauli exclusion principle in the context of the electrons of a material. Indistinguishability tells us that if two identical quantum mechanical particles have an overlapping location probability, and one particle is measured in the overlapping area, there is no way of telling which one of the two was measured. Then note that the Pauli exclusion principle tells us that two fermions have an antisymmetric wavefunction with respect to exchange [6]. From this, it is clearly shown that the two interacting electrons have two options for their wavefunctions. Either their positional wavefunction is symmetric and their spin wavefunction is antisymmetric, or vice versa (as their total wavefunction can be considered a product of the two). If we then look at the combined system, note that both cases result in a different energy for the total system as the ideal position for the electrons with respect to their atoms is different (see figure 2), and hence the energy associated with its position is altered. This interaction is called the exchange interaction (1).

$$J = E_{\uparrow\uparrow} - E_{\uparrow\downarrow} \quad (1)$$

Where  $J$  is the exchange interaction, and  $E_{\uparrow\uparrow}$  and  $E_{\uparrow\downarrow}$  are the energies for parallel and antiparallel alignment, respectively. Crucially, which of the two states is optimal depends on the system. The energy associated with the exchange interaction can now be described by equation 2:

$$E = -2J_{kl}\mathbf{s}_k \cdot \mathbf{s}_l \quad (2)$$

Where  $s_k$  and  $s_l$  are the spin vectors of electron  $k$  and electron  $l$ , respectively, and  $J_{kl}$  is the exchange interaction between the two. From this, we can derive a total exchange energy for a system of multiple atoms, if we simplify the individual contributions of electrons into one exchange interaction per atom. Note that the exchange interaction is the only term that we evaluate in the Hamiltonian of the system.

$$E = -2 \sum_{i \neq j} J_{ij} \mathbf{S}_i \cdot \mathbf{S}_j \quad (3)$$

Where  $\mathbf{S}_i$  and  $\mathbf{S}_j$  are the magnetic moments of atoms  $i$  and  $j$ , and  $J_{ij}$  is the exchange interaction between the two. Where the factor 2 is a convention, though sometimes written as 1/2 or 1 in some sources [7]. The minus sign is also up to convention. In this work a minus sign and a prefactor of 2 is used, following the most common notation [8, 9, 10].

### 2.3. Magnetocaloric effect

The magnetocaloric effect (MCE), in general, is defined as a magnetic material heating or cooling due to the removal or activation of a magnetic field [11]. The MCE is especially strong at a phase transition (most commonly that of the Curie or Néel temperature), as then, the largest difference in magnetic field over the smallest difference in temperature is present. This effect is interesting, as it allows the heating or cooling of a material by changing the external magnetic field in a energy efficient manner, something that can be exploited in a number of applications.

Quantitatively, the MCE can be explained by a thermodynamic process. Consider a paramagnetic material under adiabatic conditions, i.e. a state in which the total entropy of the system is constant, for instance due to isolation of the material. The disordered magnetic state results in a high entropy [12]. If a magnetic field is applied, the magnetic configuration becomes ordered, and therefore loses part of its entropy. As the total entropy of the material has to remain constant, the material is heated up.

More explicitly, it can be derived in formulas in the following way, using the Maxwell relations in equations (4) and (5) [12].

$$\left(\frac{\partial S_M(T, H)}{\partial H}\right)_T = \left(\frac{\partial M(T, H)}{\partial T}\right)_H \quad (4)$$

Where  $S_M$  is the entropy due to magnetization  $M$ ,  $T$  is temperature,  $H$  is external magnetic field, and  $M$  is internal magnetic field.

$$\left(\frac{\partial S(T, H)}{\partial T}\right)_H = \left(\frac{C(T, H)}{T}\right)_H \quad (5)$$

Where  $S$  is the total entropy in the system, and  $C$  is the heat capacity at constant pressure. For both equations,  $T$  and  $H$  in the bottom right corner of a derivative indicates that said quantity is kept constant. Equation (4) relates the difference in entropy at a constant temperature to the change in magnetization at a constant external field. Equation (5) signifies the entropy change due to temperature  $T$ , at a constant external magnetic field  $H$ . Combining these two expressions with the expansion of the derivative of  $S$  shown in (6), where we use that the entropy of the system is constant (so  $dS = 0$ ), we obtain the following result (7).

$$TdS = T \left(\frac{\partial S(T, H)}{\partial T}\right)_H dT + T \left(\frac{\partial S(T, H)}{\partial H}\right)_T dH \quad (6)$$

$$dT(T, H) = - \left(\frac{T}{C(T, H)}\right)_H \left(\frac{\partial M(T, H)}{\partial T}\right)_H dH \quad (7)$$

Finally, we integrate the obtained result with respect to  $H$  to obtain (8).

$$\Delta T_{ad}(T)_{\Delta H} = \int_{H_I}^{H_F} dT(T, H) = - \int_{H_I}^{H_F} \left(\frac{T}{C(T, H)}\right)_H \left(\frac{\partial M(T, H)}{\partial T}\right)_H dH \quad (8)$$

Where  $\Delta T_{ad}$  is the adiabatic temperature difference, depending on temperature and the change in  $H$ .  $H_I$  and  $H_F$  are the initial and final external fields, respectively. Equation (8) gives an expression for the magnetocaloric effect. From (8), we can notice that the magnetocaloric effect dependent on temperature and the external magnetic field. Secondly, it is also material dependent, and not easily calculated using first principles [12].



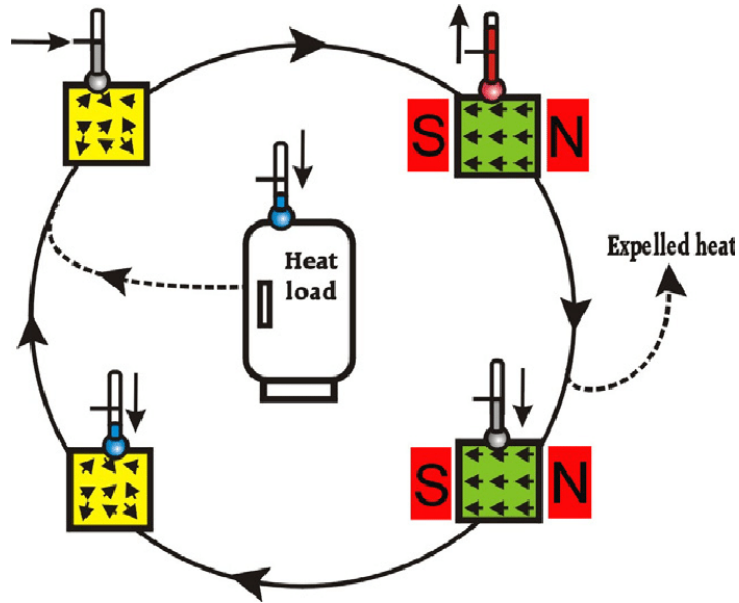


Figure 3: The magnetocaloric refrigeration cycle. Starting from the top left; activation of the magnetic field aligns and heats up the material. Then, heat is expelled, to cool down the material. Next, the external field is turned off, and the temperature of the material drops significantly. Lastly; the material extracts heat from the source, cooling down the source in the process. Image retrieved from [3].

It should also be noted, that given this expression using the change in entropy, it is also more evident that the magnetocaloric effect is largest at a magnetic phase transition, as the the change in entropy is relatively large, resulting in a large temperature change.

### 2.3.1. Applications

As per time of writing; there are three main applications/areas of research for the magnetic effect. Two of them operate near room temperature (refrigeration, and heat pumps), and one operates near the absolute zero, called adiabatic demagnetization. The latter is the only of the three that is actively used already [4]. The first two will be discussed further.

**Refrigeration** In principle, the magnetocaloric refrigeration method functions the same as a standard vapour compression devices, where the difference is that magnetocaloric refrigeration utilizes a magnetocaloric material and a (rotating) magnet attached to an electric motor as a driving force [4], where gas refrigeration uses the expanding and compression of gas (see figure 3 for the magnetocaloric refrigeration cycle). The gasses utilized for this purpose are however quite harmful for the environment [2], and their efficiency limit has been reached. Hence, this is an area where the magnetocaloric alternative has a lot of advantages over its predecessor (namely a higher efficiency and less noise while operating), although most applications are still on the expensive or experimental side [4].

**Heat pumps** Apart from providing a sustainable solution to classical refrigerators, for heat pumps, magnetocaloric materials can add to a quickly developing, already sustainable field [13]. For heat pumping, a thermodynamic cycle is used to extract heat from a reservoir, and transport it to the desired location. Most well known are the geothermal heat pumps, that have their reservoir well below the ground, and transport heat to a location at the surface. Magnetic materials are one of the many possibilities for the further development of this popular technology [14]. Another application is using this heat pumping process reversely; by turning the excess heat of industrial processes into cheap electricity [4].

## 2.4. Magnetocrystalline anisotropy

Magnetocrystalline anisotropy (MCA) is an effect related to the magnetic moment of an atom where, in contrast to the exchange parameters, the energy contribution generated by the magnetic field to a Hamiltonian is dependent on the direction in a crystal. Usually, these directions correspond to the miller indices of the crystal structure. For example: (100) and (110) could have a different MCA, thereby changing the orientation of the magnetic field of the material along the axis where the MCA energy is minimal. In general, the MCA energy is a very small contribution compared to the exchange interaction. It is therefore also hard to determine, especially using first principles<sup>2</sup> [1]. For illustration; the following approximation can be made to determine the MCA energy:

$$E = K_0 + K_1 (\alpha_1^2 \alpha_2^2 + \alpha_2^2 \alpha_3^2 + \alpha_3^2 \alpha_1^2) + K_2 (\alpha_1^2 \alpha_2^2 \alpha_3^2) + \dots \quad (9)$$

Where  $E$  is the MCA energy,  $K_i$  are the anisotropy constants, and  $\alpha_i$  are the angles between the direction of the magnetic field and the crystal axes. The anisotropy constants are the reason that the first principle determination is hard, as they depend on the spin orbit coupling, which is in general not easily described by first principles. A general theory and methodology is known however, called the force theorem. A reasoning and proof behind this method can be found in [15]. In more recent years, numerous papers have been released using a first principles method to describe the MCA energy ([16] and [17] for example). However, those methods are still in early stages and limited to the field of hard magnets, which mainly focus on rare earth metals (which are typically not readily available). As the magnetocrystalline anisotropy usually only constitutes a small energy difference compared to the exchange interactions, and it is difficult to determine using first principles, it will be disregarded in the model.

## 2.5. Density-functional theory

Density-functional theory (DFT) is a computational method to compute the Schrödinger equation for many body systems. DFT approximates the solution of the Schrödinger equation. This is extremely useful in practice, as it simplifies computation and makes solutions for other materials than the hydrogen atom possible. It usually outputs these solutions in the form of Bloch waves. Bloch waves are one of the ways to express the solution to a Schrödinger equation for a periodic structure. They are used as the solution Schrödinger equation in a crystal structure. They can be seen as a plane wave modulated by a periodic function. In this project, the Viena Ab initio simulation package (VASP) was used as an implementation of DFT, as a part of the calculation of exchange interactions of a material.

## 2.6. Wannier functions

Wannier functions, just as Bloch waves, are a solution to the Schrödinger equation in crystalline structures. Wannier functions differ from Bloch waves in that they describe the system locally [18]. When a set of Bloch waves is known, a set of Wannier functions can be constructed using the next equations. A standard Bloch wave can be described as follows:

$$\psi_{\mathbf{k}}(\mathbf{r}) = e^{i\mathbf{k}\cdot\mathbf{r}} u_{\mathbf{k}}(\mathbf{r}) \quad (10)$$

Where  $\psi_{\mathbf{k}}(\mathbf{r})$  represents Bloch wave with index  $\mathbf{k}$ , corresponding to a reciprocal lattice point.  $\mathbf{r}$  represents the location in real space, and  $u_{\mathbf{k}}$  is a function with the periodicity of the lattice in each lattice direction. Then, a Wannier function is defined as the following:

$$\phi_{\mathbf{R}}(\mathbf{r}) = \frac{1}{\sqrt{N}} \sum_{\mathbf{k}} e^{-i\mathbf{k}\cdot\mathbf{R}} \psi_{\mathbf{k}}(\mathbf{r}) \quad (11)$$

---

<sup>2</sup>First principles, or *ab initio*, is the term in physics to describe that something is calculated purely from theory, without relying on empirical data.

Where  $\phi_{\mathbf{R}}(r)$  is the Wannier function corresponding to real location  $\mathbf{R}$ ,  $N$  is the total number of Bloch waves, and  $\mathbf{R}$  represents the centers of the orbitals being described. The locality of the Wannier functions is achieved by the complex exponential function, as is common in the translation from reciprocal to real space.

## 2.7. Green's function method

The Green's function method is a general way to solve differential equations, using Green's functions. It is presented here as it is used in the general procedure of finding the exchange interactions of a material. Given a general differential equation with a source term, the Green function can be seen as the response of the system to an impulse function, as illustrated by the following example.

$$\frac{d^2x}{dt^2} + \omega^2x = f(t); \quad x(0) = 0, x'(0) = 0 \quad (12)$$

Where  $x$  is the unknown function,  $\omega$  is the frequency of the system and  $f(t)$  is a source term. Notice, that  $f(t)$  can also be written as an integral over  $\delta$ -functions without loss of generality.

$$f(t) = \int_0^\infty f(t') \delta(t' - t) dt' \quad (13)$$

Then, the Greens function is defined as follows:

$$\frac{d^2G(t, t')}{dt^2} + \omega^2G(t, t') = \delta(t' - t); \quad G(0, t') = 0, G'(0, t') = 0. \quad (14)$$

Where  $G(t, t')$  is the Greens function, dependent on time ( $t$ ) and a moment  $t'$ . Notice that  $G$  is defined to satisfy the same boundary conditions as  $x$ . Given this definition for  $G$ , one can now use  $G$  to solve for  $x$  in the following manner.

$$x(t) = \int_0^\infty G(t, t') f(t') dt' \quad (15)$$

Where one can easily check that the previous equation holds, applying 12 to 15. This gives:

$$\frac{d^2x(t)}{dt^2} + \omega^2x(t) = \int_0^\infty \left[ \frac{d^2G(t, t')}{dt^2} + \omega^2G(t, t') \right] f(t') dt' \quad (16)$$

Which is easily worked out to be the required solution (using equation 14). Now, the problem has been simplified into finding  $G$ , with which  $x$  can be determined. Solving  $G$  can be a lot of work on its own, and the mathematics behind this procedure differ from problem to problem. In some cases it is easier than finding  $x$  directly, which is why the method is utilized. [19, pp. 394–459]

A more specific version of the Greens function method is used in the field of solid state physics. This method is called the Korringa, Kohn and Rostoker (KKR) greens function method, to its inventors, who specifically used the Green's function method in solving the Schrödinger equation of a lattice system. The methodology is the same as above, as the Schrödinger equation can be rewritten in the form described in equation (17).

$$\begin{aligned} [-\nabla^2 + V(\mathbf{r}) - E] \psi(\mathbf{r}) &= 0 \\ \psi(\mathbf{r} + \mathbf{r}_s) &= \exp(i\mathbf{k} \cdot \mathbf{r}_s) \psi(\mathbf{r}) \end{aligned} \quad (17)$$

Where  $V(\mathbf{r})$  is a periodic potential,  $\mathbf{r}$  is the real space location, and  $k$  is the reciprocal space location.  $\mathbf{r}_s$  is a translation vector in real space. Then,  $\psi(\mathbf{r})$  can be described in the following form [20]:

$$\psi(\mathbf{r}) = \int_{\tau} G(\mathbf{r}, \mathbf{r}') V(\mathbf{r}') \psi(\mathbf{r}') d\tau' \quad (18)$$

A detailed description of the mathematics behind finding the actual Greens function can also be in [20].

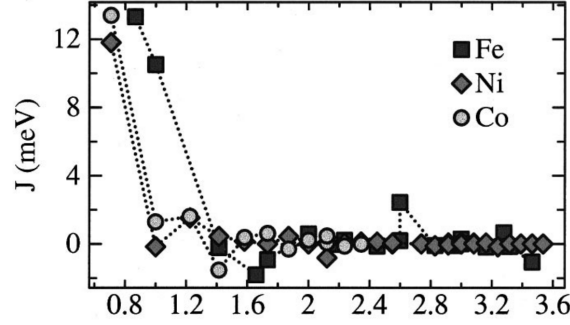


Figure 4: Exchange interactions for Nickel, Iron and Cobalt as function of distance, in units of the lattice constant (3.53 Å). Note that the exchange parameters for nickel are scaled by a factor of 4 by the author. [25]

## 2.8. Bilinear form

The bilinear form is a mapping function that maps a vector space onto a field <sup>3</sup>, and is linear in each component [22]. It is discussed, as the model represented in the next chapter will be of this form.

In pure mathematical terms, a bilinear form  $B : V \times V \rightarrow K$  has to obey the following conditions:

$$\begin{aligned} B(\mathbf{u} + \mathbf{v}, \mathbf{w}) &= B(\mathbf{u}, \mathbf{w}) + B(\mathbf{v}, \mathbf{w}) \text{ and } B(\lambda\mathbf{u}, \mathbf{v}) = \lambda B(\mathbf{u}, \mathbf{v}) \\ B(\mathbf{u}, \mathbf{v} + \mathbf{w}) &= B(\mathbf{u}, \mathbf{v}) + B(\mathbf{u}, \mathbf{w}) \text{ and } B(\mathbf{u}, \lambda\mathbf{v}) = \lambda B(\mathbf{u}, \mathbf{v}) \end{aligned} \quad (19)$$

Where  $\mathbf{u}, \mathbf{v}$  and  $\mathbf{w} \in V$ . One example of a bilinear form is the dot product in  $\mathbb{R}^n$ . The bilinear form is a way to characterize a nonlinear optimization problem. Every bilinear form can be rewritten into a quadratic form, which is a form for which other solving methods are available, as it requires more symmetry from  $B$ . Oftentimes, the bilinear form can be written as a matrix product (20).

$$B(\mathbf{v}, \mathbf{w}) = \mathbf{v}^T A \mathbf{w} \quad (20)$$

To then obtain the quadratic form, one must, in the general case, extend the matrix  $A$  to make it symmetric, as is required for a quadratic form. This means, that it is not always clear if this method, as it enlarges the matrix utilized, will help in the computation of the problem [23].

## 2.9. Materials

For this project, a number of commonly known materials were utilized to test the model. Below is some information about the listed materials.

### 2.9.1. Ni

Nickel, with atomic number 28, is a common transition metal that is mostly found in the Earth's outer and inner core. In this project, we will study nickel with a face centered cubic structure with a lattice parameter of 3.53 Å. This configuration of nickel is ferromagnetic [24], and its exchange interactions can be seen in figure 4. It is studied in this project as it is one of the most simple cases of a ferromagnet.

### 2.9.2. MnO

<sup>3</sup>A field is a space where basic addition, subtraction, multiplication and division can take place as defined on  $\mathbb{Q}$  [21, pp. 13–21] by  $V \times V \rightarrow K$ , For the purposes of this project, the field considered is  $\mathbb{R}$ .

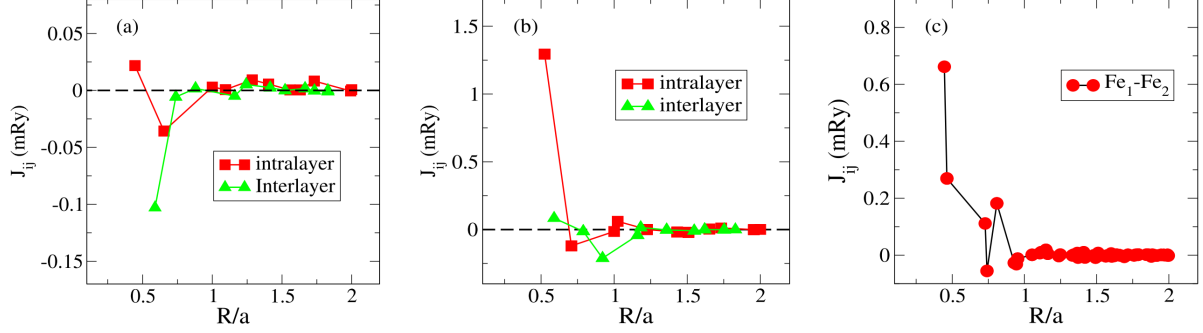


Figure 5: Exchange interactions for  $\text{Fe}_2\text{P}$ . The first, second and third plots show the  $\text{Fe}_1\text{-Fe}_1$ ,  $\text{Fe}_2\text{-Fe}_2$  and  $\text{Fe}_1\text{-Fe}_2$  interactions, respectively [29]. The x axis shows the relative distance, divided by the lattice constant  $5.813 \text{ \AA}$ .  $\text{Fe}_1$  and  $\text{Fe}_2$  are located at the  $3f$  and  $3g$  site, respectively.

Manganese oxide is a chemical compound that is utilized for numerous applications across different industries. It is antiferromagnetic in the  $[\frac{1}{2}, \frac{1}{2}, \frac{1}{2}]$  plane [27], and has a NaCl like face centered cubic structure [28]. Its exchange parameters are given in table 1. Note that the values of  $J_1$  and  $J_2$  in literature do have slight variations, depending on the source [26].

### 2.9.3. $\text{Fe}_2\text{P}$

Iron phosphide is a semiconductor used in numerous fields. A lot is known about its magnetical properties, as it has recently been discovered as a potentially great material for magnetocaloric applications [29]. It has a hexagonal structure [30], with Fe atoms at the  $3f$  (0.257, 0, 0) and  $3g$  (0.5915, 0, 0.5) positions (expressed in the lattice vectors). Its exchange interactions according to previous work are shown in figure 5.

### 2.9.4. $\text{Mn}_2\text{Sb}$

$\text{Mn}_2\text{Sb}$  is a little less commonly used than the previously discussed materials. It has however been studied for its interesting magnetic phase transition (from antiferromagnetic to ferrimagnetic). Recently, it (together with  $\text{Mn}_2\text{Sb}$ -based alloys) has been studied at the TU Delft for its magnetocaloric properties [31]. It is a tetragonal type structure [32], with lattice constants  $3.928 \text{ \AA}$ ,  $3.928 \text{ \AA}$  and  $6.426 \text{ \AA}$  for  $a$ ,  $b$  and  $c$  respectively. The Mn atoms are located in the (0, 0, 0) and (0, 0.5, 0.7098) positions (in reference to the lattice vectors), and the Sb atom is located in the (0, 0.5, 0.2849) position. It is deemed a ferrimagnetic material in its ground state [33], with a magnetic propagation vector in the  $c$  direction<sup>4</sup>. The first order exchange interactions between the two different Mn sites, is determined to be  $-72.07 \text{ K}$  experimentally [34], which was determined through the Ising model.

MnO		
$n$	$E_n^{\text{ex}}$	$J_n$
1	1.20	-30.3
2	1.18	-29.8
3	0.0	0
4	0.03	-0.8
5	0.02	-0.5
6	-0.01	0.3
7	-0.01	0.3

Table 1: The exchange parameters  $J_N$  (in  $\text{K} \approx 0.0862 \text{ meV}$ ) and exchange energy  $E_n^{\text{ex}}$  (in mRy) per different interaction.  $n$  indicates the  $n$ -th neighbor interaction. From source [26].

<sup>4</sup>A propagation vector in this sense means that in the  $c$  direction, the field is constant when traversing through the material

## 3. Method

### 3.1. Motivation

While the magnetocaloric effect (MCE) has no direct impact on model; the whole reason the model is put together ties into the MCE. As the research regarding the MCE is very much in the state of finding the optimal material for the listed applications, right now, researchers are sifting through known materials in search of a material that has a large MCE, at the right temperature, is cheap, readily available and that have a small environmental impact [5]. This means that, to find potential materials, one has to go through huge databases of materials and potentially calculate a gigantic amount of data. This model is proposed to alleviate some of the work that goes into this research, as the model simplifies the routine of finding the magnetic ordering<sup>5</sup> of materials.

### 3.2. Data acquisition

For the purpose of testing the validity of the model, four different well known materials were chosen to check the workings of the model. For these, we obtain the desired properties via a multi step process. The most important property for the model, the exchange parameters, are acquired as follows. First, the Vienna ab-initio simulation package (VASP) is used to approximate the density of states and Bloch wave solution of the material. Then, Wannier90 [35] is used to calculate Wannier functions from the VASP output. Then as a final step, TB2J [36] is used to calculate the exchange parameters of the material, using the output of Wannier90. The final exchange parameters are then compared to literature.

#### 3.2.1. Vienna ab-initio simulation package

There are multiple implementations of DFT. The one utilized in this study is the Vienna ab-initio simulation package (VASP) [37, 38, 39, 40]. VASP is a well known, versatile program used to model materials on an atomic scale. It does this via the only possible way, by using the DFT method. How VASP functions exactly is beyond the scope of this project.

#### 3.2.2. Wannier90

Wannier90 is a program that rewrites numerical Bloch functions into maximally localized Wannier functions (see section 2.6), which span the same space as the initial Bloch functions. It does so by minimizing a functional that represents the total spread of the Wannier functions in real space. This minimization is carried out directly from the Bloch functions represented in reciprocal space, and itself takes place in a space of unitary matrices<sup>6</sup> that describe the rotation around each  $k$  point. The exact implementation of Wannier90 goes beyond the scope of this work. Important to discuss however, is on what Wannier90 relies to obtain accurate Wannier functions from the given input. Next to inputting the Bloch functions obtained from VASP, the user is also asked to specify which orbitals from which atoms are to be taken into account. Next to that, the user also inputs a frozen window: i.e. a window in which all the orbitals specified are to be found. Generally; it is better for this window to be as large as possible. Therefore, an accurate way of presenting the density of states per atom is advised. The choice of the frozen window impacts the accuracy of the output of Wannier90, and should hence be taken seriously.

---

<sup>5</sup>The magnetic ordering is of importance for the search of materials, as it can tell a lot about the size of the magnetic response to an external field, its own magnetic moment and hence also about the size of the magnetocaloric effect, if the different structures for different temperatures are compared.

<sup>6</sup>A unitary matrix is a square (complex) matrix  $A$  for which its conjugate transpose is also its inverse, and  $AA^{-1} = I$ . The space of unitary matrices is defined by the matrix multiplication. [21, pp. 93–113]

### 3.2.3. TB2J

TB2J is a relatively new library that was developed to calculate exchange interactions, given results from a DFT calculation. It uses the green's function method to arrive at its result [36]. While TB2J does not directly support the output of VASP, it does support the output of Wannier90, hence TB2J is the last link in the data acquisition part of the project. It depends largely on the quality of the Wannier90 output to arrive at accurate results. This means that, as stated previously, the Wannier90 step is crucial for the succes of a run.

## 3.3. The model

Mainly, the goal is to solve equation (3) for a given material. To do this properly, a base model is created, to which boundary conditions and a symmetry analyzing algorithm are added to improve precision. Per step, assumptions are made to simplify computation. Firstly, the interior point optimization method used in this model is explained. Next, the base model is introduced, then extensions are discussed one by one. The model was built in python 3.7.11.

### 3.3.1. Interior Point Optimization

The model uses the Interior Point Optimization (IPOPT) [41], as its optimization program. IPOPT is an open source optimization routine for nonlinear problems. It compares in performance to industry standards (for instance, KNITRO, Lancelot and LOQO) [42], and has a user friendly implementation in python for large scale problems, called GEKKO [43]. First, the general workings of IPOPT will be discussed, after which GEKKO and its underlying library APMonitor will be presented.

**Working of IPOPT** Firstly, a short word on the workings of IPOPT. IPOPT is a deterministic optimization routine for nonlinear problems. It guarantees a global minimum when the problem is convex, and if the problem is concave, it can arrive at a local minima. Given a problem (for instance the one described in equation (21)), it first writes it into standard form<sup>7</sup>, and then introduces a barrier function for all variables in the following manner:

$$\begin{array}{ll} \min & f(\mathbf{x}) \\ \text{s.t.} & c(\mathbf{x}) = 0 \\ & x_i \geq 0, \quad i = 1, \dots, n \end{array} \quad (21)$$
$$\begin{array}{ll} \min & f(\mathbf{x}) + \mu \sum_{i=1}^n \ln x_i \\ & c(\mathbf{x}) = 0 \end{array} \quad (22)$$

To get rid of the last inequality constraints. Here,  $f(x_i)$  is the objective function,  $x_i$  are the variables and  $\mu$  is a positive constant that is lowered per iteration step.  $c(x_i)$  are the (potentially nonlinear) constraints. The barrier function  $\mu \ln x$  functions exactly as the constraint in (21) would for small values of  $\mu$ , as it runs into an asymptote at  $x = 0$ . Therefore, this is a valid simplification of the given model, and one that is central to the functioning of IPOPT. The IPOPT method does not solve the presented problem in (22) directly, but instead evaluates when its derivative is equal to zero, in a clever way. For further details, we refer to [41].

**GEKKO** GEKKO is a python package that handles machine learning and optimization. In GEKKO the user can build and run models using a couple of freely available solvers, for a number of different

---

<sup>7</sup>Standard form in optimization means that there are no inequality constraints, and all variables are  $\geq 0$ . this is done by introducing slack variables to an equation, for example  $f(x) \leq b$  will become  $f(x) + s = b$ , where  $s \geq 0$  is the slack variable.

problems. It utilizes the Advanced Process Monitor [44] package to actually work with the models provided by the user. APmonitor is an online solving method, and GEKKO offers the functionality of APmonitor for local solving also.

### 3.3.2. Assumptions

The overall model makes a couple of important assumptions. To make matters more clear, an overview is shortly listed in this section.

- Magnetic moments of atoms are considered to be one dimensional.
- Magnetocrystalline anisotropy is not taken into account.
- Materials are only checked for constant or alternating behaviour of moment configurations between unit cells.
- The ideal configuration is assumed to be magnetically symmetric to the same order in all three directions.
- We assume that the unit of repetition is smaller or equal to the used supercell, for each lattice direction.

### 3.3.3. The basic model

The basic model works as follows. The user inputs a supercell size (i.e. the amount of cells in each lattice direction), the material structural information and the exchange parameters of the material. The exchange parameters and structural information have to, as of the current version, be given in the form of TB2J (or RSPt<sup>8</sup>) output and VASP format, respectively. The program then uses this information to construct a minimization model that obeys the following equations (23):

$$\begin{aligned} \min \quad & -2 \cdot \sum_{i=1}^n \sum_{j<i} J_{ij} s_i s_j \\ \text{s.t.} \quad & |s_i| \leq |d_i|, \quad i = 1, \dots, n \end{aligned} \quad (23)$$

Where  $J_{ij}$  is the exchange interaction between the two atoms,  $s_i$  and  $s_j$  are the magnetic moments of atom  $i$  and  $j$ , respectively.  $d_i$  is the maximum magnetic moment of atom  $i$ , obtained from the input TB2J file. As  $d_i$  can be negative, the absolute value is used. The atoms, while of course present in a 3D grid, are each given an index  $\in \{1, 2, \dots, n\}$ , to make the summation in (23) easier. This does not affect other computations. The summation makes sure to sum over each interaction exactly once. Note that the term  $J_{ii} s_i s_i$  is disregarded  $\forall i \in \{1, \dots, n\}$ , as an atom does not have an exchange interaction with itself. Furthermore, the magnetocrystalline anisotropy is disregarded, and only spins in one direction are considered. For our purposes, this one dimensional moment is a logical assumption, as equation 23 is minimized for vectors for which either their dot product is maximal or minimal. Therefore the simplification to one dimension makes sense, as for vectors with the given bounds, this is the case when  $\mathbf{s}_i = \mathbf{s}_j$  or  $\mathbf{s}_i = -\mathbf{s}_j$ . Magnetocrystalline anisotropy is disregarded (see 2.4).

To start the model, GEKKO requires an initialization from which to iterate from. One of three initialization methods (24, 25, 26) is used.

$$|s_i| < |d_i| \quad (24)$$

$$0 < s_i < |d_i| \quad (25)$$

$$0 < m_i s_i < |d_i| \quad (26)$$

---

<sup>8</sup>RSPt is another method for calculating electronic structures of materials, and can also be used to find exchange interactions.



Here  $b_i$  is the bound for the magnetic moment of  $s_i$ , obtained from the TB2J file<sup>9</sup>, and  $m_i$  is the sign of  $b_i$ . Note that  $b_i$  depends solely on the position of atom  $i$  in its unit cell. Each position has a distinct bound.

The major flaw of the basic model is that it does not take into account any form of boundary conditions. This can quickly lead to errors, especially for small unit cells. This is because, for atoms that are located near the edge of the supercell, not all exchange interactions may be taken into account (as some fall outside of the supercell). As the main goal is to find a symmetric solution; the next step in the model is to impose boundary conditions.

### 3.3.4. Boundary conditions

As stated previously, the major flaw of the basic model is that it does not take into account any form of boundary conditions. This can quickly lead to sub optimal configurations, as not all relevant exchange interactions are taken into account (see figure 6). The main focus of the boundary conditions is to reduce the amount of unit cells required to get an accurate structure from the model.

The implementation of the boundary conditions is as follows.

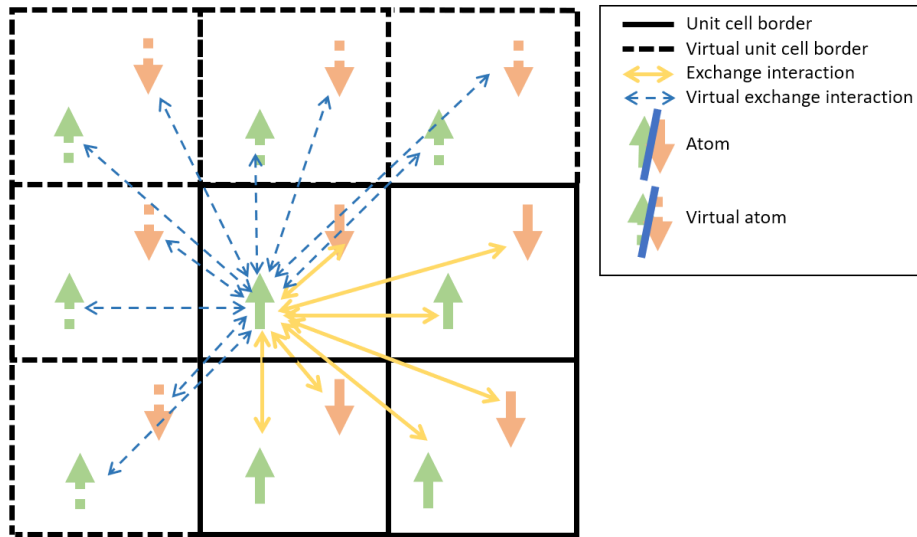


Figure 6: 2D representation of boundary conditions for one atom in a  $2 \times 2$  supercell with 2 atoms per unit cell (own work).

First a set  $A$  is created that contains all atoms at the outermost unit cells of the supercell. Then, each atom  $j \in A$  is moved to its equivalent positions at the opposite side(s) of the supercell, and the exchange interactions (between target atoms and the new position of  $j$ ) are used to add the missing interactions to the objective function. A graphical representation of this procedure given in figure 7.

The choice of which equivalent positions are used for  $j$  and which exchange interactions are considered per position is made to assure no double counting occurs. For each atom  $j \in A$ , the following set of rules is used.

Atom  $j$  has three attributed vectors that correspond to those of its unit cell;  $c_1$ ,  $c_2$  and  $c_3$ . The index of the atom in the unit cell  $o$  is also attributed. With these four parameters, each different atom is distinguishable. For each of the vectors  $c_1$ ,  $c_2$  and  $c_3$  it is checked if belongs to the outer most unit cells in its direction. Hereby it is determined if  $j$  belongs to an edge, face or corner of the supercell. For each of the three cases, the added exchange interactions are given in equations 31, 32 and 33 respectively.

<sup>9</sup>If the exchange interactions were provided via RSPT, the moments of atoms have to be provided separately.

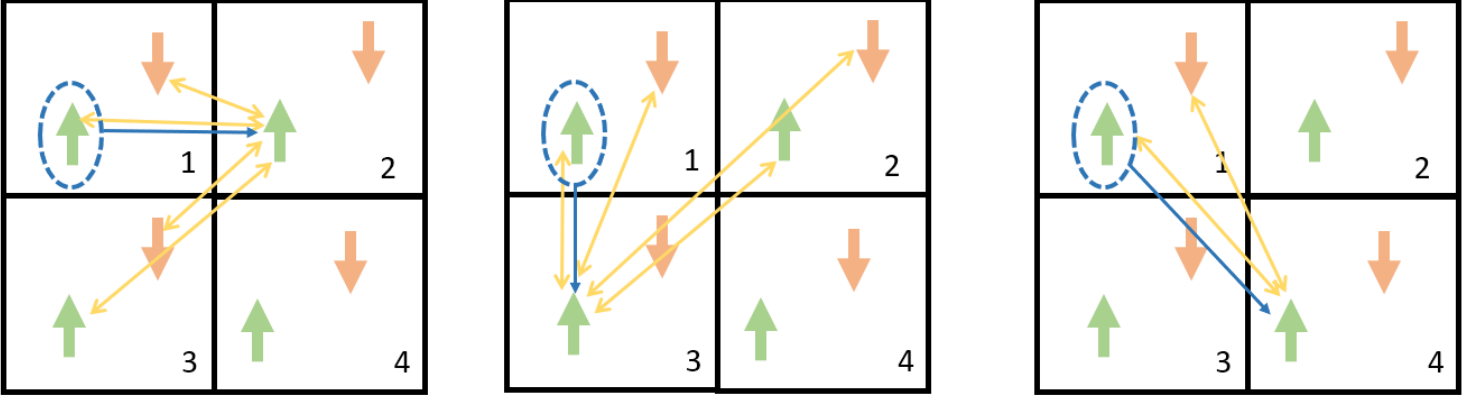


Figure 7: Graphical representation of the boundary condition implementation for one atom in a  $2 \times 2$  supercell. The circled atom is virtually moved to its equivalent location in another unit cell, shown by the blue arrow. Then, selected exchange interactions are added between the original atom and the target atoms. Hereby the virtual cells shown in figure 6 are added to the system (own work).

Let  $(b_1, b_2, b_3, b_4, b_5, b_6)$  be the set of lower and upper bounds of the supercell (with  $b_l \in \mathbb{Z}$  for  $l \in \{1, \dots, 6\}$ ), with  $(b_1, b_2, b_3)$  lower bounds and  $(b_4, b_5, b_6)$  upper bounds for the  $a, b$  and  $c$  lattice vectors respectively.  $B, M$  and  $B_l$  for  $l \in \{1, 2, 3\}$  are defined as follows (27).

$$\begin{aligned}
 B &= \{(a_1, a_2, a_3, n) : a_1 \in B_1, a_2 \in B_2, a_3 \in B_3, n \in M\} \\
 M &= \{n : n \text{ is a unique magnetic atom, per unit cell}\} \\
 B_l &= \{b_l, b_l + 1, \dots, b_{l+3} - 1, b_{l+3}\} \quad \text{for } l \in \{1, 2, 3\}
 \end{aligned} \tag{27}$$

Given these definitions and the location of atom  $j$ , sets  $C_j(l), D_j(m)$  and  $E_j$  are defined as follows  $\forall j \in A$  (28, 29, 30).

$$C_j(l) = B \setminus \{(a_1, a_2, a_3, n) : [n \in M, a_l \in B_l \setminus \{c_l\}, a_m \in B_m \text{ for } m \in \{1, 2, 3\} \setminus \{l\}]\} \tag{28}$$

$$D_j(m) = B \setminus \{(a_1, a_2, a_3, n) : [n \in M, a_l \in B_l \setminus \{c_l\}, a_m \in B_m \text{ for } l \in \{1, 2, 3\} \setminus \{m\}]\} \tag{29}$$

$$E_j = B \setminus \{(a_1, a_2, a_3, n) : n \in M, a_l \in B_l \setminus \{c_l\} \text{ for } l \in \{1, 2, 3\}\} \tag{30}$$

Graphically,  $C_j(l), D_j(m)$  and  $E_j$  all describe the supercell with the one, two or three faces that contain  $j$  cut away. With these sets, given the three options for atom  $j$  (face, edge or corner), we can construct the following boundary conditions (31, 32, 33). In all three cases;  $l \in \{p : c_p = b_p \vee c_p = p_{l+3}\}$  and  $m = \{1, 2, 3\} \setminus \{l\}$ . In words,  $l$  describes the lattice coordinates of  $j$  where  $c_p$  is at a max or minimum, and  $m$  describes the ones where  $j$  is not.

$$f_F(j) = -2 \sum_{i \in C_j(l)} J_{iq} s_i s_j \tag{31}$$

For  $j$  at a face where  $\gamma$  (with lattice vectors and atom index  $\gamma_1, \gamma_2, \gamma_3, n$ ) is the equivalent atom at the opposite face (for example  $\gamma_1, \gamma_2, n = c_1, c_2, n$  respectively and  $\gamma_3 = b_6$  when  $j$  is at the minimum

bound of the  $c$  vector in the supercell). Note that here,  $l$  is equal to the coordinate where  $j$  is at the face and hence only has one value. Only one equivalent position of  $j$  is used.

$$f_E(j) = -2 \cdot \left( \sum_l \sum_{i \in C_j(l)} J_{iq} s_i s_j + \sum_{i \in D_j(m)} J_{ir} s_i s_j \right) \quad (32)$$

For  $j$  at an edge. Here,  $q$  is the atom that is at the edge opposite to  $j$ . Note that here,  $l$  has two possible values, and  $q$  has one value. Hence a total of three equivalent positions of  $j$  are used.

$$f_C(j) = -2 \cdot \left( \sum_l \sum_{i \in C_j(l)} J_{iq} s_i s_j + \sum_m \sum_{i \in D_j(m)} J_{ir} s_i s_j + \sum_{i \in E_j} J_{it} s_i s_j \right) \quad (33)$$

For  $j$  at a corner. Here,  $t$  is the atom that is the equivalent atom at the corner opposite to  $j$ . In the corner case,  $l$  and  $q$  have three possible values, and  $t$  has one. Hence, a total of 7 equivalent positions of  $j$  are used.

The last step is to rewrite the model (23) in such a way that it includes boundary conditions. Define:

$$\begin{aligned} A_F &= \{a \in A : a \text{ is at a face}\} \\ A_E &= \{a \in A : a \text{ is at an edge}\} \\ A_C &= \{a \in A : a \text{ is at a corner}\} \end{aligned} \quad (34)$$

Where  $A$  is the set of atoms in the outermost unit cells. Then the model can be written in the following form (35):

$$\begin{aligned} \min \quad & -2 \cdot \sum_{i=1}^n \sum_{j < i} [J_{ij} s_i s_j] + \sum_{l \in A_F} f_F(l) + \sum_{l \in A_E} f_E(l) + \sum_{l \in A_C} f_C(l) \\ \text{s.t.} \quad & |s_i| \leq |d_i|, \quad i = 1, \dots, n \end{aligned} \quad (35)$$

Where all terms are as previously defined. A visualization of the exact boundary condition method in 3D is presented in appendix B.

The imposed boundary conditions add a large number of equations to the model (thereby increasing computation time), but also theoretically nets better results. The exact impact will be discussed in the results section.

### 3.3.5. Symmetry finding algorithm

Given the model including the described boundary conditions, another addition is made to make sure that the optimal solution is found, as the interior point optimization method can get stuck at a local minimum. To account for this symptom, an algorithm is implemented that, after an initial cycle of IPOPT using the model is complete, checks if the solution is properly symmetric, and if not, reruns the model with a new initialization chosen based on the previous result. A detailed flowchart for the algorithm can be found in appendix B. In this section the algorithm is discussed in detail. First, the previous solution is analyzed. From there, a new initialization is set up, after which the new initialization is used to run the program again. Lastly, the best solution is found among all the runs.

**Solution analysis** During the analysis of the first run, a couple of simplifications are made. Firstly, the algorithm only considers the sign of each magnetic moment.

The spins, as all are in one dimension, are now either +1 or -1. With this knowledge, the program now checks for a unique configurations of spins in a unit cell. With this check; the inverse of a configuration is

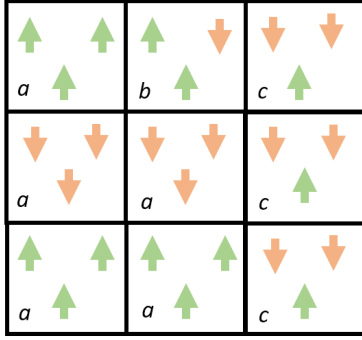


Figure 8: An example 2D structure. Different configurations are labeled in  $a$ ,  $b$  and  $c$ . As this configuration has 9 cells, both configurations  $a$  and  $c$  are considered prominent.

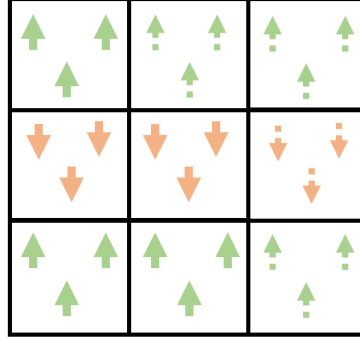
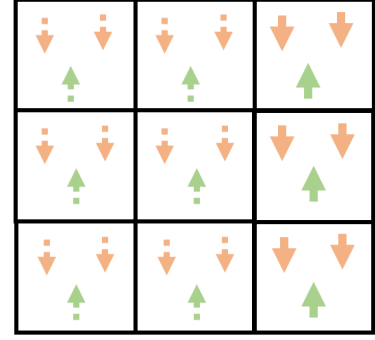


Figure 9: The new starting configurations, initialized from the structure in 8. Changed atoms are highlighted by the smaller, dotted arrows to indicate their different starting size due to  $\gamma$ . Note that the extra completely symmetric solution step is not plotted here, though in 3D this would be considered (own work).



considered the same. See figure 8 for a 2D example. As soon as all different configurations of unit cells are determined, the program finds the ones that occur most often in the supercell. The configurations that constitute more than 30% of the total amount of unit cells in the supercell are saved. If there is no configuration that meets this quota, it will run the optimization step again, from a different random initialization, in hopes of finding a better result. With all the saved configurations, the program follows the following procedure to produce a new initialization.

**Constructing new initialization(s)** Assuming a prominent configuration is given, the program now checks certain symmetry conditions. In every lattice direction, the program makes an analysis of the repetition of the current selected configuration, to determine in how many unit cells the configuration repeats. Note that as per the current version, the model only checks for constant or alternating patterns. For a 2D example, see figure 9. Then, in each direction, the material is determined to be either constant, alternating, or neither of the two. The program then runs the following analysis to construct the next starting iteration.

First it checks if the material is considered perfect. This distinction is given when the material only consists of one configuration, the pattern in all three directions is the same and the material completely obeys this pattern. If a material is perfect, no second run is executed, as the current solution is considered good enough.

If the material is not perfect, a number of steps are executed to arrive at a new initialization (or initializations).

- Firstly, if the pattern is neither constant or alternating in any direction, in the new configuration it is set to constant in that direction.
- Next, a new configuration is built by pasting the new pattern onto the material. If a unit cell is altered, its new moments are also multiplied by the parameter  $\gamma \in (0, 1)$ , see figure 9
- If the given pattern is not the same in all three directions (so either completely constant or completely alternating), a second new configuration is built by pasting the completely constant or completely alternating pattern onto the material (constant or alternating is chosen if the majority of the pattern is constant or alternating respectively).

**Running new initialization(s)** As soon as all configurations are checked and their respective new initializations are built, one by one, new runs are executed given these initializations.

## 4. Results

### 4.1. Exchange interactions

For Ni and MnO, the exchange interactions were calculated. For Fe<sub>2</sub>P and Mn<sub>2</sub>Sb, the literary values for the exchange parameters were used. In this section, the results for the exchange interactions for nickel and manganese oxide will be reported.

#### 4.1.1. Ni

For nickel, the calculated exchange interactions can be found in figure 4. The corresponding moment of the atom (only one atom as the primitive cell of nickel was used) is equal to  $0.5542 \mu_B$ .

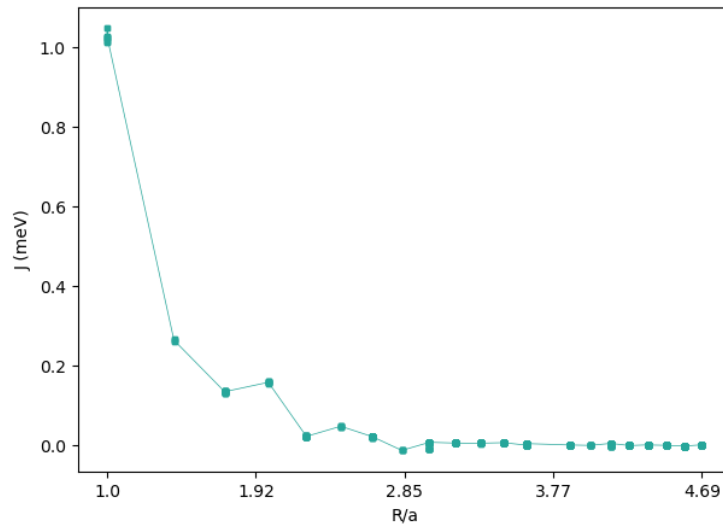


Figure 10: Exchange interactions found for Ni, plotted against distance divided by the lattice parameter ( $= 3.53 \text{ \AA}$ ).

#### 4.1.2. MnO

The exchange interactions calculated for MnO can be seen in figure 11. The moments for the Mn atoms located at  $(0,0,0)$ ,  $(0, \frac{1}{2}, \frac{1}{2})$ ,  $(\frac{1}{2}, 0, \frac{1}{2})$  and  $(\frac{1}{2}, \frac{1}{2}, 0)$  are equal to  $2.8643$ ,  $-2.8768$ ,  $-2.8399$  and  $2.8797 \mu_B$  respectively.

## 4.2. Model results

In this section, the results of the model will be discussed. First, the basic model (without the inclusion of the boundary conditions) and its outcomes will be discussed for all used materials. This will include the optimal structure found per material, the percentage of runs that arrived at this structure and the average time of a run. All quantities listed, will also be reported for each different initialization method.

Next, the same discussion will be held for the model including boundary conditions. Thereafter, the effectiveness of the symmetry finding algorithm will be discussed. Lastly, the combined results (basic model with boundary conditions and algorithm) will be presented. For all sections, the four materials described earlier were used (Ni, MnO, Fe<sub>2</sub>P and Mn<sub>2</sub>Sb) in the configurations of a 2×2×2 and a 3×3×3 supercell. These configurations were used, as the materials discussed all have a symmetry in each direction that is smaller or equal to the 2×2×2 cell. The 3×3×3 cell was also studied to check the impact of a larger supercell, as well as a cell count that is not a multiple of the materials multiplicity (i.e. 3 is not divisible by 2). For each material in each configuration, 120 runs were performed per initialization, unless stated differently. If initialization types are given, they are defined as follows (see 24, 25 and 26).

$$\begin{aligned} \text{Initialization 1:} & \quad |s_i| < |d_i| \\ 2: & \quad 0 < s_i < |d_i| \\ 3: & \quad 0 < m_i s_i < |d_i| \end{aligned}$$

For all different executed tests, the general convergence of different runs (i.e. energy per iteration) are recorded in appendix C. Secondly, appendix C also contains a note on energy differences between different versions of the model, and some examples of suboptimal configurations found in the runs for MnO. These suboptimal configurations will not be commented on further, but rather serve as an example for the reader.

As a final general comment, for all computation times holds that computations were executed on a laptop with 8 GB of DDR3 RAM, with a 4-core i5-8250U Intel CPU.

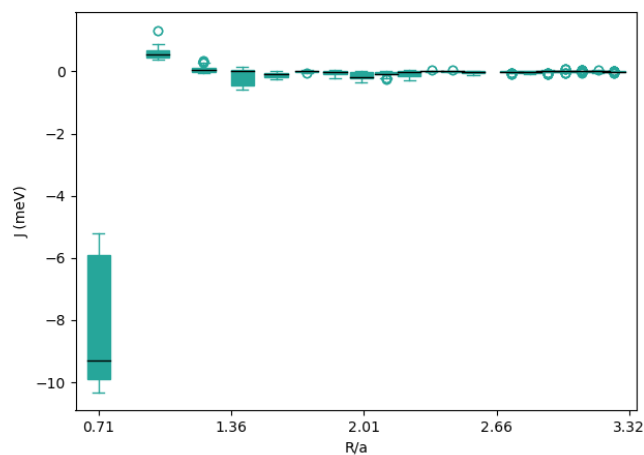


Figure 11: Exchange interactions found for MnO, plotted against distance divided by the lattice parameter ( $= 3.53 \text{ \AA}$ ). The boxes turquoise specify the 2nd and 3rd quartile, the black lines the average and the turquoise lines the 1st and 4th quartile of the data gathered per distance. The turquoise dots represent outliers from this range.

### 4.2.1. Basic model

In the runs conducted for the basic model, multiple different outcomes were found. Per outcome, the resulting exchange energies were recorded, as that is in the end the value that the model minimizes. Per distinct energy (up to a certain numerical value which is smaller than 1% of the resultant energy), the observed outcome has a different configuration. All recorded energies are shown in figure 13. Interestingly, only a select amount of energy levels are reached, and most energies are never reached as a final outcome. From the runs as shown in figure 13, each setup has a clear preferred ground state energy. These configurations are given in figure 12. Note that both the  $3 \times 3 \times 3$  and  $2 \times 2 \times 2$  configurations for all materials gave the same optimal structure, even though there is a difference in the minimal energy recorded per unit cell. This difference in energy per configuration is due to a different maximum of order of exchange interactions being taken into account, and is further elaborated upon in appendix C.

For the conducted runs, the number of times that the model reaches these optimal configurations is listed in table 2. The average run times per initialization are given in table 3.

Material	Initialization Supercell	Basic model			Total
		1 Successful runs	2 /120	3 /360	
Ni	$2 \times 2 \times 2$	118	120	120	358
	$3 \times 3 \times 3$	116	120	120	356
MnO	$2 \times 2 \times 2$	47	65	80	192
	$3 \times 3 \times 3$	28	33	65	126
Fe <sub>2</sub> P	$2 \times 2 \times 2$	54	103	96	253
	$3 \times 3 \times 3$	9	100	97	206
Mn <sub>2</sub> Sb	$2 \times 2 \times 2$	101	115	108	324
	$3 \times 3 \times 3$	84	86	90	260
Total		557	742	776	2075
Out of		960	960	960	2880
Percentage		58.02	77.29	80.83	72.05

Table 2: Amount of optimal solutions for the basic model per material and per initialization. A run counts as a successful one when it reached the optimal energy/ magnetic configuration.

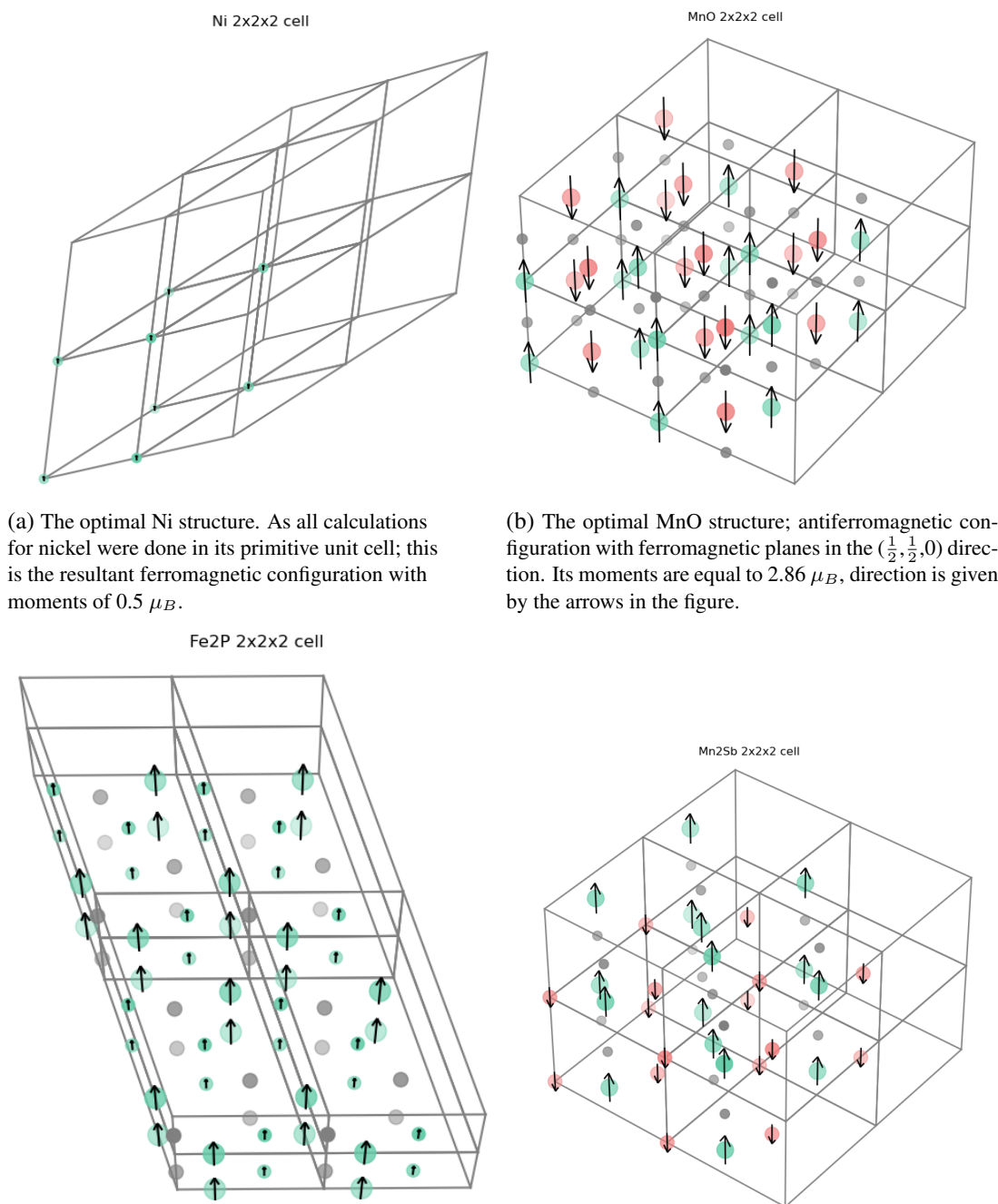
Material	Initialization Supercell	1	2	3	Total
		Average time (s)			
Ni	$2 \times 2 \times 2$	0.59	0.59	0.6	0.6
	$3 \times 3 \times 3$	0.7	0.68	0.68	0.69
MnO	$2 \times 2 \times 2$	1.14	1.18	1.1	1.14
	$3 \times 3 \times 3$	6	6.73	5.25	5.99
Fe <sub>2</sub> P	$2 \times 2 \times 2$	1.74	1.6	1.62	1.65
	$3 \times 3 \times 3$	16.59	12.32	12.59	13.83
Mn <sub>2</sub> Sb	$2 \times 2 \times 2$	0.53	0.53	0.53	0.53
	$3 \times 3 \times 3$	3.39	3.33	3.29	3.34

Table 3: Average run times of the model in seconds, per iteration.

In these results we can see that the accuracy of the basic model really depends on the material it is used on. Where for Ni, the model performs quite well, for MnO, the model has a way lower overall success rate. The different initializations also impact the final result, most evidently shown in MnO and Fe<sub>2</sub>P.

The run time per material and configuration varies heavily, as shown in table 3. The largest difference in

run time between initializations is about 30%, for  $\text{Fe}_2\text{P}$   $3 \times 3 \times 3$ . From figure 13, we can see that while MnO and  $\text{Fe}_2\text{P}$  have a lot of often occurring suboptimal solutions,  $\text{Mn}_2\text{Sb}$  and Ni only have one that is really prominent.



(a) The optimal Ni structure. As all calculations for nickel were done in its primitive unit cell; this is the resultant ferromagnetic configuration with moments of  $0.5 \mu_B$ .

(b) The optimal MnO structure; antiferromagnetic configuration with ferromagnetic planes in the  $(\frac{1}{2}, \frac{1}{2}, 0)$  direction. Its moments are equal to  $2.86 \mu_B$ , direction is given by the arrows in the figure.

(c) The optimal  $\text{Fe}_2\text{P}$  structure according to the model. It is ferromagnetic, with the  $3f$  and  $3g$  positions having a magnetic moment of  $0.81 \mu_B$  and  $2.1 \mu_B$ , respectively.

(d) The optimal configuration for  $\text{Mn}_2\text{Sb}$ . The  $(0, 0, 0)$  and  $(0, 0.5, 0.7098)$  positions have a magnetic moment of  $2.1 \mu_B$  and  $3.1 \mu_B$ , respectively.

**Figure 12:** In all structures, magnetic atoms are shown in red or green, nonmagnetic atoms in gray. The size of the red or green dots indicates the size of the moments. For all materials the exact moments per atom vary by  $\approx 0.05\%$  between unique atom positions, as they originate from a numerical input.



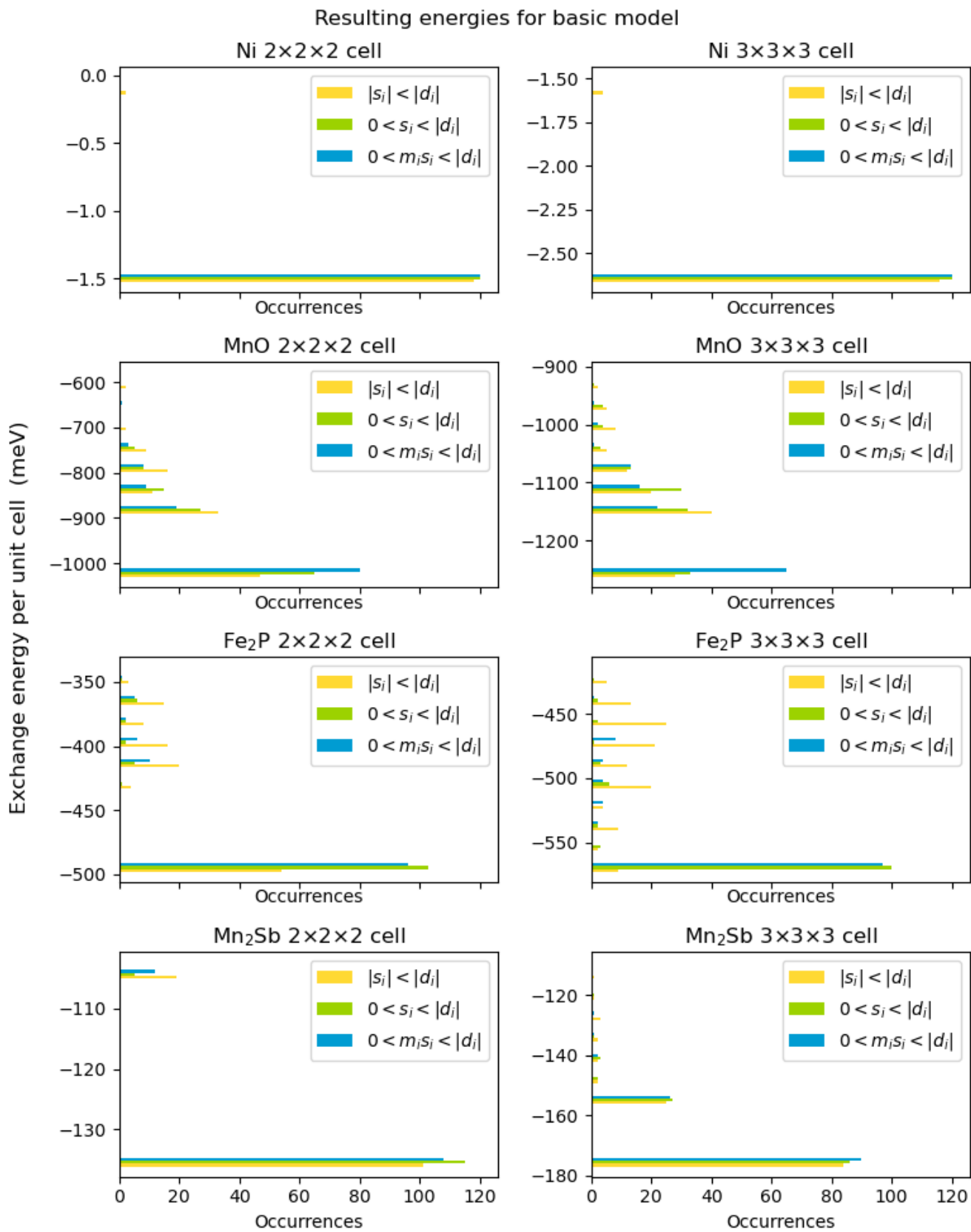


Figure 13: The full convergence results for the basic model.

#### 4.2.2. Including boundary conditions

For the model with the inclusion of boundary conditions, the same results procedure is followed as with the base model. Across the board, the boundary conditions add more accuracy to the model, but heavily increase the computation time for more complex configurations. The full final energies attained can be found in figure 14. Due to the implementation of the boundary conditions (as more exchange interactions are evaluated), the energies of the model including boundary conditions are increased compared to the base model, still the optimal solution between the two is the same. This added energy effect is further discussed in appendix C. The accuracy and time performance of the model including boundary conditions can be found in tables 4 and 5, respectively.

Material	Initialization Supercell	Basic model including BC's			Total /360
		1 Successful runs	2 /120	3 /120	
Ni	2×2×2	105	120	120	345
	3×3×3	120	120	120	360
MnO	2×2×2	80	94	96	270
	3×3×3	68	68	94	230
Fe <sub>2</sub> P	2×2×2	61	108	114	283
	3×3×3	25	110	112	247
Mn <sub>2</sub> Sb	2×2×2	104	116	112	332
	3×3×3	94	95	109	298
Total		657	831	877	2365
Out of		960	960	960	2880
Percentage		68.44	86.56	91.35	82.12

Table 4: Results for the basic model including boundary conditions, per initialization and per material configuration.

Material	Initialization Supercell	1	2	3	Total
		Average time (s)			
Ni	2×2×2	0.61	0.59	0.59	0.60
	3×3×3	1.29	1.23	1.22	1.25
MnO	2×2×2	2.37	2.54	2.17	2.36
	3×3×3	24.14	25.62	20.77	23.50
Fe <sub>2</sub> P	2×2×2	5.03	4.25	4.29	4.53
	3×3×3	72.79	52.84	52.71	59.45
Mn <sub>2</sub> Sb	2×2×2	1.84	1.81	1.78	1.81
	3×3×3	8.29	8.23	8.14	8.22

Table 5: Run times for the model with the addition of boundary conditions per initialization and material configuration.

Mostly, the same trends that were present as in the basic model are still present in the basic model with boundary conditions. Most notable is that the model with boundary conditions is more accurate than the basic model (seen by the overall percentages in table 4). Secondly, the average run time for the model with boundary conditions is a fraction higher than the run times in the basic model. Lastly, when looking at figure 14, we can see that the suboptimal solutions are differently distributed compared to the basic model.

Resulting energies for basic model with boundary conditions

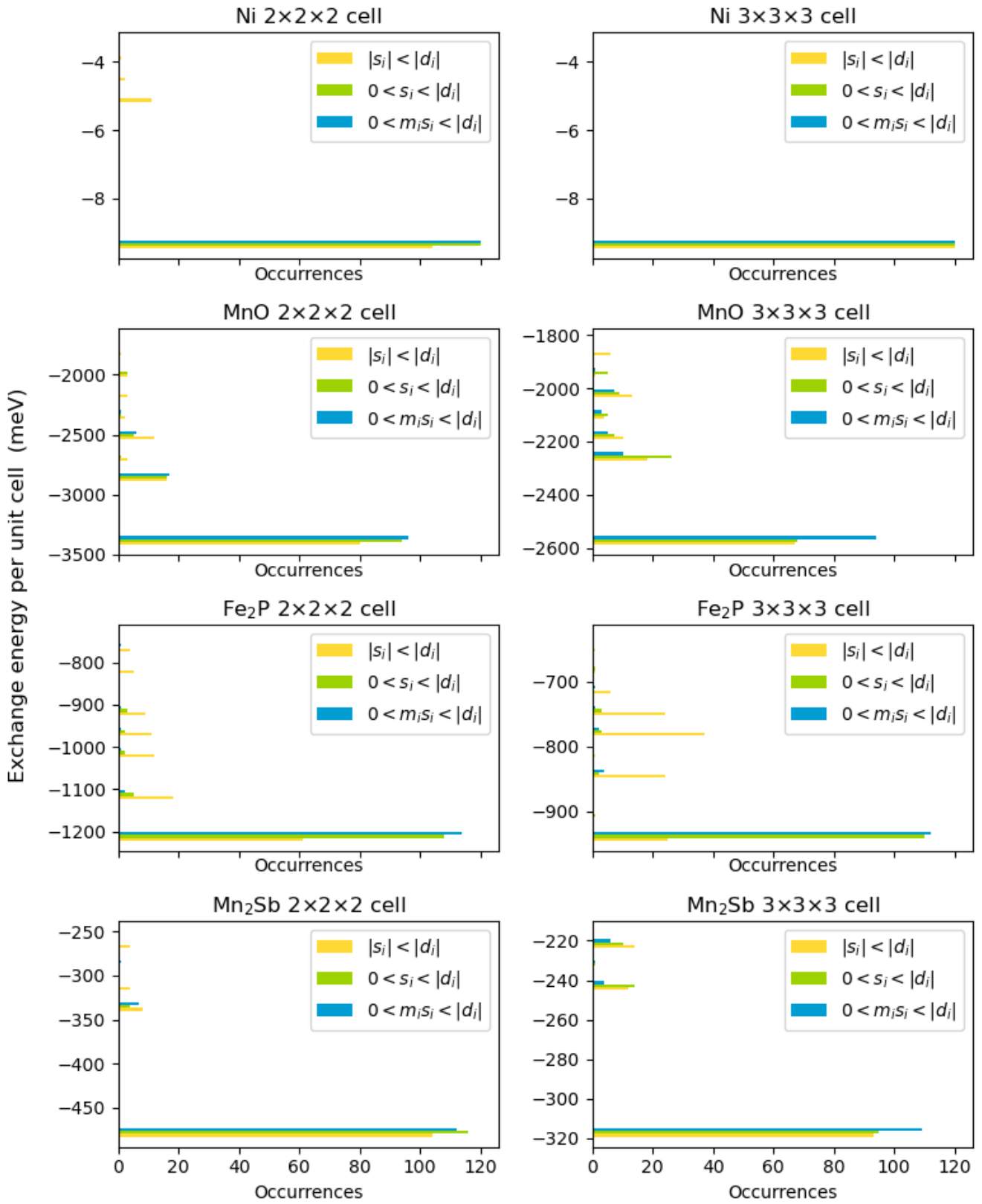


Figure 14: The full convergence results for the basic model with the inclusion of boundary conditions.

### 4.2.3. Symmetry finding algorithm

The algorithm will be evaluated in a different fashion than the previous two versions of the model. First and foremost, the algorithm was tested only with the model version that includes the boundary conditions. As it only kicks in when a solution is considered not 'optimal enough', a test set was constructed on which the algorithm was executed. The test set contains all sub-optimal solutions from the boundary conditions run, see figure 15. For the values of  $\gamma$  from 0.3 to 0.8 with increments of 0.1, the test set was executed and the success rate and running times are reported in tables 6 and 7. These values of  $\gamma$  were chosen as a logical spread of values between 0 and 1. The final attained energies of the runs are presented in 16. The convergence of the test set of each material configuration for different values of  $\gamma$  is reported in appendix C.

Material	$\gamma$ Supercell	0.3	0.4	0.5	0.6	0.7	0.8	Total runs
		Percentage of successful runs						
Ni	2×2×2	100	100	100	100	100	100	15
MnO	2×2×2	97.78	98.89	98.89	100	38.89	38.89	90
	3×3×3	100	95.38	96.15	98.46	100	98.46	130
Fe <sub>2</sub> P	2×2×2	100	100	94.81	93.51	61.04	100	77
	3×3×3	100	100	97.35	46.9	98.23	100	113
Mn <sub>2</sub> Sb	2×2×2	100	100	100	100	100	21.43	28
	3×3×3	98.39	72.58	72.58	98.39	100	98.39	62
Total successful		512	491	485	447	428	435	515
Total percentage		99.42	95.34	94.17	86.8	83.11	84.47	

Table 6: Percentage of successful runs of the algorithm, per value of  $\gamma$ . No values for Ni 3×3×3 are present, as this configuration executed perfectly for the model with boundary conditions in all 360 runs.

Material	$\gamma$ Supercell	0.3	0.4	0.5	0.6	0.7	0.8
		Average total runtime (s)					
Ni	2×2×2	1.1	1.09	1.1	1.14	1.15	1.17
MnO	2×2×2	6.08	6.01	5.95	5.99	5.84	6.2
	3×3×3	61.42	59.78	55.85	57.01	55.05	53.22
Fe <sub>2</sub> P	2×2×2	9.46	9.33	9.28	9.34	9.26	9.12
	3×3×3	171.55	157.85	165.52	166.01	160.11	165.65
Mn <sub>2</sub> Sb	2×2×2	3.58	3.72	3.98	3.84	3.65	3.82
	3×3×3	16.97	17.52	17.53	16.71	16.23	15.98

Table 7: Run times per value of  $\gamma$ , per configuration.

We can see that which value for  $\gamma$  is selected, quite heavily impacts the result of the run. This effect will be further discussed in the next section. Secondly, the average run time for the different values of  $\gamma$  differ at most around 10% of the total run time. The success rate of the algorithm on the configurations is also heavily impacted for different values of  $\gamma$ . Examples are Fe<sub>2</sub>P 3×3×3, where all values of  $\gamma$  have a (near) 100% success rate, except for  $\gamma = 0.6$  which only has one of 46.9%. The same effect seems to occur with Mn<sub>2</sub>Sb, this time with  $\gamma = 0.8$ . Overall, when comparing the figure 15 and 16, we can see that the addition of the algorithm solves a lot of the previously inaccurate cases.



### Results algorithm on test set

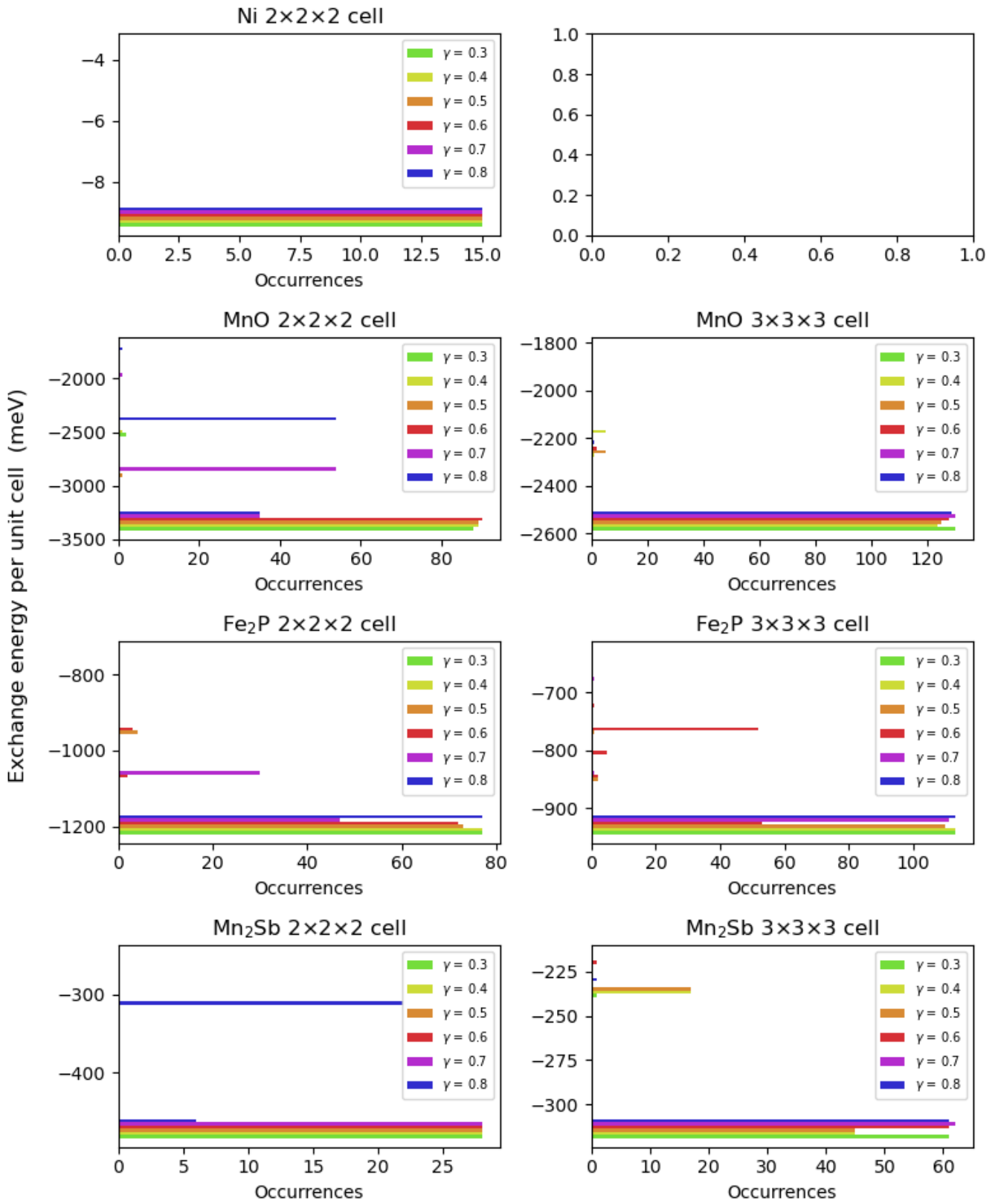


Figure 16: The full convergence results for the algorithm on the test set presented in figure 15, for different values of  $\gamma$ .

#### 4.2.4. Versions comparison

Given the results mentioned above, as the algorithm was executed on the set of sub optimal solutions of the model with boundary conditions, without loss of generality, we can combine the results to virtually construct a total average run time and accuracy per value of  $\gamma$  on the complete set of runs from the model including boundary conditions. This is done to more accurately represent real life situations, and to be able to compare its results to those from sections 4.2.1 and 4.2.2. The motivation for why this is allowed is straightforward, as each different run of IPOPT is independent and only depends on initialization, neither data set is affected by this virtual construction. The combined results can be found in tables 8 and 9.

Material	$\gamma$ Supercell	0.3	0.4	0.5	0.6	0.7	0.8	Total runs
		Percentage of successfull runs						
Ni	2×2×2	100	100	100	100	100	100	360
	3×3×3	100	100	100	100	100	100	360
MnO	2×2×2	99.44	99.72	99.72	100	84.72	84.72	360
	3×3×3	100	98.33	98.61	99.44	100	99.44	360
Fe <sub>2</sub> P	2×2×2	100	100	98.89	98.61	91.67	100	360
	3×3×3	100	100	99.17	83.33	99.44	100	360
Mn <sub>2</sub> Sb	2×2×2	100	100	100	100	100	93.89	360
	3×3×3	99.72	95.28	95.28	99.72	100	99.72	360
Total successfull		2877	2856	2850	2812	2793	2800	2880
Total percentage		99.895	99.17	98.96	97.64	96.98	97.22	

Table 8: Total accuracy as projected on the model including boundary conditions data set, value of  $\gamma$  versus material configurations.

Material	$\gamma$ Supercell	0.3	0.4	0.5	0.6	0.7	0.8
		Average total runtime (s)					
Ni	2×2×2	0.62	0.62	0.62	0.62	0.62	0.62
	3×3×3	1.25	1.25	1.25	1.25	1.25	1.25
MnO	2×2×2	3.29	3.27	3.26	3.27	3.23	3.32
	3×3×3	37.19	36.6	35.18	35.6	34.89	34.23
Fe <sub>2</sub> P	2×2×2	5.58	5.56	5.55	5.56	5.54	5.51
	3×3×3	94.64	90.34	92.74	92.9	91.05	92.79
Mn <sub>2</sub> Sb	2×2×2	1.94	1.95	1.97	1.96	1.94	1.96
	3×3×3	9.73	9.82	9.82	9.68	9.6	9.56

Table 9: Average run time of performed runs in table 8. Value of  $\gamma$  versus material configurations.

## 5. Discussion

In this section, we will discuss the obtained results, what they signify, and what further research can be conducted concerning the model.

Firstly, we discuss the exchange interactions obtained for Ni and MnO. Both findings agree on the sign of  $J$ , but differ from the exchange interactions in 4 and 1 by a factor of roughly 3 (smaller) and 5 (larger) respectively. Though inaccurate, these results are in agreement enough so that they may be used for the purposes of this study.

For the optimal structures found in figure 12, when we compare the structures to the literature structures, we find that they agree with the expected structures for Ni, Fe<sub>2</sub>P and Mn<sub>2</sub>Sb. MnO is found to be antiferromagnetic, but in a slightly different lattice direction than what is specified in literature. Where in literature, MnO is AFM in the  $[\frac{1}{2}, \frac{1}{2}, \frac{1}{2}]$  direction, the calculated structure is antiferromagnetic in the  $[\frac{1}{2}, \frac{1}{2}, 0]$  direction. This can likely be attributed to one of the processes in the gathering of the exchange interactions. This is assumed as firstly, the structure found by the model has a lower exchange energy than the literature configuration when it is compared in the model. Secondly, DFT is not a perfect representation of reality, as multiple assumptions are made, and some effects are disregarded, which will impact the resultant exchange interactions, which might have played a role in this project.

**The model** For the different versions of the model, with each extension, the accuracy is increased at the cost of also increasing run time. We will discuss the two different evaluated factors (initialization and the value of  $\gamma$ ), then compare the different versions of the model, and lastly discuss some limitations of the results.

When comparing the different initializations, the initialization  $0 < m_i s_i < |d_i|$  (initialization 3) (26) performed equally good to the other two initializations (24,25) in most, and significantly better than the others in some configurations. This is the case for both the basic model and the model with boundary conditions. Especially for Fe<sub>2</sub>P in both configurations, initialization  $|s_i| < |b_i|$  (initialization 1) performed substantially worse than the other two. For MnO  $3 \times 3 \times 3$ , initialization 3 performed remarkably better than the other two initializations. These two results can be explained intuitively by the final structure of the two materials. Where Fe<sub>2</sub>P is ferromagnetic, setting initialization 1, where moments are randomly ordered, one would expect that this is further from the optimal result. For MnO, as initialization 3 already assigns signs that would match the optimal solution, it is logical that this initialization will have to perform 'less work' to arrive at the optimal solution. Therefore, an explanation for this superior performance is that initialization 3 uses more information of magnetic moments presented, which gives it an advantage. Given this information, initialization 3 is the initialization of choice as it not only has a higher average accuracy, but it also on average has a slightly lower run time than the other two initialization methods as shown in tables 5 and 3.

When comparing the different values of  $\gamma$ ,  $\gamma = 0.3$  clearly stands out as the optimal value. While it does have a slightly higher average run time; it more than makes up for it in accuracy, where it is (comparing results on the test set), 4% more effective than its closest competitor, with a staggering 99.42% vs 95.34%. As IPOPT is a deterministic routine, and the initialization is also deterministic per run (i.e. each different value of  $\gamma$  had the exact same input), this is an extremely accurate result. Surprisingly, there is a large difference in performance for each value of  $\gamma$  per material. This effect is most noticeable when comparing  $\gamma = 0.8$  and  $\gamma = 0.7$ , as we can see that per material, the value of  $\gamma$  that performs better is different. This effect would be interesting to study, especially for other materials than the ones listed here, as there is no easy explanation for this behaviour.

Regarding the accuracy of the results, one does have to take into account that the test set did only contain 515 runs, which boils down to fairly low runs per material configuration. Next to that, only six values



for  $\gamma$  were tested.

When evaluating which model type to work with (basic, with boundary conditions or with algorithm), looking from an accuracy perspective, running the model including the boundary conditions and the algorithm is the clear winner. Even with the higher run times, the addition of the algorithm improves accuracy by a sufficiently large amount (99.895% vs 82.12% or 72.05% over all initializations), thus using it is highly recommended. The only other consideration is the model with boundary conditions using only initialization 3, which has an accuracy of 91.35%. However, to attain the same accuracy as the combined method in one run, this method would have to be run at least twice (for an accuracy of  $1 - (0.0865)^2 = 99.25\%$ ), which is still lower than the accuracy of the model including the algorithm, and, on top of that, also in a longer average run time. Therefore, the use of the algorithm is highly recommended.

It should be noted, that while individually  $\gamma = 0.3$  and the initialization  $0 < m_i s_i < |d_i|$  performed best; the combination of the two factors has not been extensively tested, as the higher accuracy of initialization method also means that there were less test cases from that set that the algorithm worked on (only 83 test cases, see table 4).

A point of concern for the model is that the computation time between small and larger configurations is impacted greatly. It is therefore advised to examine this behaviour more thoroughly in future studies.

**Recommendations** For future work, there are a lot of directions to consider. In no specific order; some of those continuations are:

- Changing the model to allow magnetic moments to independently assume any direction, instead of all adhering to the same direction. Though most likely driving up computation time, this would generalize the model to also work on more complex systems.
- Make the algorithm check for more than 2 cell repetitions. This would require a more sophisticated approach to the implementation of the algorithm, and might be a time consuming task. The usefulness of this extension also heavily depends on whether or not more complex magnetic structures are of interest to the application.
- More extensive research can be done on the exact choice of the  $\gamma$  parameter, and the model in general. As the ideal value of 0.3 works for all test materials presented in this study, however more values of  $\gamma$  could be checked against more materials to find if a more general global optimal value exists.
- As the results presented in this work are promising, we are excited to see how the model, that seems quite robust for the test cases, handles a larger sample size and a larger selection of materials. As the direction of antiferromagnetism in MnO was wrongly predicted, inputting more antiferromagnetic materials would be of interest to verify the accuracy of the model on antiferromagnetic materials.
- Concerning the algorithm, an extension that smartly determines when unit cells are similar enough that they can be considered equal may be of interest. Currently, the algorithm treats each unique configuration of a unit cell as unique, no matter how close two configurations might be. For large unit cells, this might not be optimal. This extension could be useful if the model turns out to struggle with materials with large unit cells.
- Another extension that could help the algorithm, is an immediate output of the final result is presented to either itself or the user, to check if the solution actually makes sense and is not a rare error. This could also be fixed by running the model multiple times, to achieve a near 100% accurate solution.

- And lastly, one could also check how the model reacts to the slight alteration of the input conditions (i.e. different lattice parameters) to check the magnetic response of the system, and if this is also accurately predicted by the model.

## 6. Conclusion

In this project, a model is presented that predicts the magnetic structures of materials using exchange interactions. Boundary conditions and a symmetry finding algorithm are added to a basic model to drastically increase its accuracy to 99,895% over 2880 runs. Two factors were tested, different initialization methods and the algorithm mixing parameter  $\gamma \in (0, 1)$ . The latter was tested to be optimal for  $\gamma = 0.3$ , though only six different values for  $\gamma$  were tested. Interestingly, different values of  $\gamma$  performed rather differently per material, no general trend between the four materials was observed. The initialization method  $0 < m_i s_i < |d_i|$  performed best out of the three initialization methods tested. This is likely due to it using more structural information, namely the direction of the magnetic moments of the material. The combination of using the two best performing methods was not tested. Individually however, the two performed distinctly better than their competitors, and are therefor advised to be used when using the model.

For three out of four materials tested, the optimal configuration aligned with the one shown in literature. For MnO, the result is antiferromagnetic in a different lattice direction, due to some process present in the collection of the input data.

From these findings, the model seems like a robust tool to quickly predict the magnetic structure of materials with a not too complicated structure. More testing of the model for a wider range of materials is recommended, to ensure that it functions as expected. There are also various ways to extend and to improve the model (the most prominent of which is the generalization to allow the magnetic moments to be oriented in 2 or 3 dimensions) to make it able to handle more complex systems.

## References

- [1] B. D. Cullity and C. D. Graham. *Introduction to magnetic materials*. Ed. by Abari R. et al. second. Vol. 1. John Wiley & Sons, Inc., Dec. 2008.
- [2] M. D. E. De Baar. *Potential of the ternary Fe-Mn-Y system as cooling material for room-temperature refrigeration*. 2018.
- [3] Ekkes Brück. “Developments in magnetocaloric refrigeration”. In: *Journal of Physics D: Applied Physics* 38 (23 Dec. 2005).
- [4] Andrej Kitanovski. “Energy Applications of Magnetocaloric Materials”. In: *Advanced Energy Materials* 10 (10 Mar. 2020).
- [5] Nikolai A. Zarkevich and Vladimir I. Zverev. “Viable materials with a giant magnetocaloric effect”. In: *Crystals* 10 (9 Sept. 2020), pp. 1–28.
- [6] David J. Griffiths and Darrell F. Schroeter. *Introduction to Quantum Mechanics*. Cambridge University Press, Aug. 2018. ISBN: 9781316995433.
- [7] Xueyang Li et al. “Spin hamiltonians in magnets: Theories and computations”. In: *Molecules* 26 (4 Feb. 2021).
- [8] E. K. Delczeg-Czirjak et al. “Origin of the magnetostructural coupling in  $\text{FeMnP}_{0.75}\text{Si}_{0.25}$ ”. In: *Physical Review B* 90 (21 Dec. 2014), p. 214436.
- [9] R Logemann et al. “Exchange interactions in transition metal oxides: the role of oxygen spin polarization”. In: *Journal of Physics: Condensed Matter* 29 (33 Aug. 2017), p. 335801.
- [10] I. V. Solovyev. “Exchange interactions and magnetic force theorem”. In: *Physical Review B* 103 (10 Mar. 2021).
- [11] Y. Mozharivskyj. *Magnetocaloric Effect and Magnetocaloric Materials*. Elsevier, 2016.
- [12] K. A. Gschneidner and V. K. Pecharsky. “Magnetocaloric Materials”. In: *Annual Review of Materials Science* 30 (1 Aug. 2000), pp. 387–429.
- [13] Julia Lyubina. “Magnetocaloric materials for energy efficient cooling”. In: *Journal of Physics D: Applied Physics* 50 (5 Jan. 2017).
- [14] Hicham Johra et al. “Integration of a magnetocaloric heat pump in an energy flexible residential building”. In: *Renewable Energy* 136 (June 2019), pp. 115–126.
- [15] Xindong Wang et al. “Validity of the force theorem for magnetocrystalline anisotropy”. In: *Journal of Magnetism and Magnetic Materials* 159 (3 July 1996), pp. 337–341.
- [16] Christopher E. Patrick, Munehisa Matsumoto, and Julie B. Staunton. “First-principles calculations of the magnetocrystalline anisotropy of the prototype 2:17 cell boundary phase  $\text{Y}(\text{Co}_{1-x-y}\text{Fe}_x\text{Cu}_y)_5$ ”. In: *Journal of Magnetism and Magnetic Materials* 477 (May 2019), pp. 147–155.
- [17] Haruki Okumura et al. “First-principles Calculation of Magnetocrystalline Anisotropy of  $\text{Y}(\text{Co,Fe,Ni,Cu})_5$  Based on Full-potential KKR Green’s Function Method”. In: (Apr. 2022).
- [18] Nicola Marzari et al. “Maximally localized Wannier functions: Theory and applications”. In: *Reviews of Modern Physics* 84 (4 Oct. 2012), pp. 1419–1475.
- [19] Richard Haberman. *Applied partial differential equations with fourier series and boundary value problems*. Pearson, 2014. ISBN: 9781292039855.
- [20] F. S. Ham and B. Segall. “Energy Bands in Periodic Lattices—Green’s Function Method”. In: *Physical Review* 124 (6 Dec. 1961), pp. 1786–1796.

- [21] Larry C. Grove. *Classical Groups and Geometric Algebra*. Ed. by Steven G. Krantz et al. The American mathematical society, 2002.
- [22] Marcia Fampa and Jon Lee. “Efficient treatment of bilinear forms in global optimization”. In: (Mar. 2018). URL: <http://arxiv.org/abs/1803.07625>.
- [23] Jessica Gronski. “Non-Convex Optimization and Applications to Bilinear Programming and Super-Resolution Imaging”. In: *ProQuest* 80 (9 2019).
- [24] V. P. Antropov et al. “On the calculation of exchange interactions in metals”. In: *Journal of Applied Physics* 99 (8 Apr. 2006), 08F507.
- [25] M. Van Schilfgaarde and V. P. Antropov. “First-principles exchange interactions in Fe, Ni, and Co”. In: *Journal of Applied Physics* 85 (8 II A Apr. 1999), pp. 4827–4829.
- [26] T. Oguchi, K. Terakura, and A. R. Williams. “Band theory of the magnetic interaction in MnO, MnS, and NiO”. In: *Physical Review B* 28 (11 Dec. 1983), pp. 6443–6452.
- [27] Juan Rodríguez-Carvajal and Jacques Villain. “Magnetic structures”. In: *Comptes Rendus Physique* 20 (7-8 Nov. 2019), pp. 770–802.
- [28] Pierre Villars and Karin Cenzual, eds. *MnO Crystal Structure: Datasheet from “PAULING FILE Multinaries Edition – 2012” in SpringerMaterials*. URL: [https://materials.springer.com/isp/crystallographic/docs/sd\\_1922219](https://materials.springer.com/isp/crystallographic/docs/sd_1922219).
- [29] X.B. Liu et al. “Fe magnetic moment formation and exchange interaction in Fe<sub>2</sub>P: A first-principles study”. In: *Physics Letters A* 377 (9 Mar. 2013), pp. 731–735.
- [30] Kristin Persson. *Materials Data on Fe<sub>2</sub>P (SG:189) by Materials Project*. July 2016.
- [31] Qi Shen et al. “The antiferromagnetic to ferrimagnetic phase transition in Mn<sub>2</sub>Sb<sub>1</sub>-Bi compounds”. In: *Journal of Alloys and Compounds* 866 (June 2021), p. 158963.
- [32] Kristin Persson. *Materials Data on Mn<sub>2</sub>Sb (SG:129) by Materials Project*. Feb. 2016.
- [33] Evgenii D. Chernov and Alexey V. Lukoyanov. “Magnetic Ground State and Electronic Structure of Binary Mn<sub>2</sub>Sb Compound from Ab Initio Calculations”. In: MDPI AG, Dec. 2020, p. 15.
- [34] R. Masrour et al. “Electronic and magnetic structures of ferrimagnetic Mn<sub>2</sub>Sb compound”. In: *Journal of Magnetism and Magnetic Materials* 374 (Jan. 2015), pp. 116–119.
- [35] Giovanni Pizzi et al. “Wannier90 as a community code: New features and applications”. In: *Journal of Physics Condensed Matter* 32 (16 Apr. 2020).
- [36] Xu He et al. “TB2J: a python package for computing magnetic interaction parameters”. In: *Computer Physics Communications* (Sept. 2020). URL: <http://arxiv.org/abs/2009.01910>.
- [37] G. Kresse and J. Furthmüller. “Efficient iterative schemes for *ab initio* total-energy calculations using a plane-wave basis set”. In: *Physical Review B* 54 (16 Oct. 1996), pp. 11169–11186.
- [38] G. Kresse and J. Furthmüller. “Efficiency of *ab-initio* total energy calculations for metals and semiconductors using a plane-wave basis set”. In: *Computational Materials Science* 6 (1 July 1996), pp. 15–50.
- [39] G. Kresse and J. Hafner. “*Ab initio* molecular-dynamics simulation of the liquid-metal–amorphous-semiconductor transition in germanium”. In: *Physical Review B* 49 (20 May 1994), pp. 14251–14269.
- [40] G. Kresse and J. Hafner. “*Ab initio* molecular dynamics for liquid metals”. In: *Physical Review B* 47 (1 Jan. 1993), pp. 558–561.

- [41] Andreas Wächter and Lorenz T. Biegler. “On the implementation of an interior-point filter line-search algorithm for large-scale nonlinear programming”. In: *Mathematical Programming* 106 (1 Mar. 2006), pp. 25–57.
- [42] Maame Yaa B. Poku, Lorenz T. Biegler, and Jeffrey D. Kelly. “Nonlinear Optimization with Many Degrees of Freedom in Process Engineering”. In: *Industrial & Engineering Chemistry Research* 43 (21 Oct. 2004), pp. 6803–6812.
- [43] Logan Beal et al. “GEKKO Optimization Suite”. In: *Processes* 6 (8 July 2018), p. 106.
- [44] John D. Hedengren et al. “Nonlinear modeling, estimation and predictive control in APMonitor”. In: *Computers and Chemical Engineering* 70 (Nov. 2014), pp. 133–148.

## Appendix A: 3D representation of boundary conditions

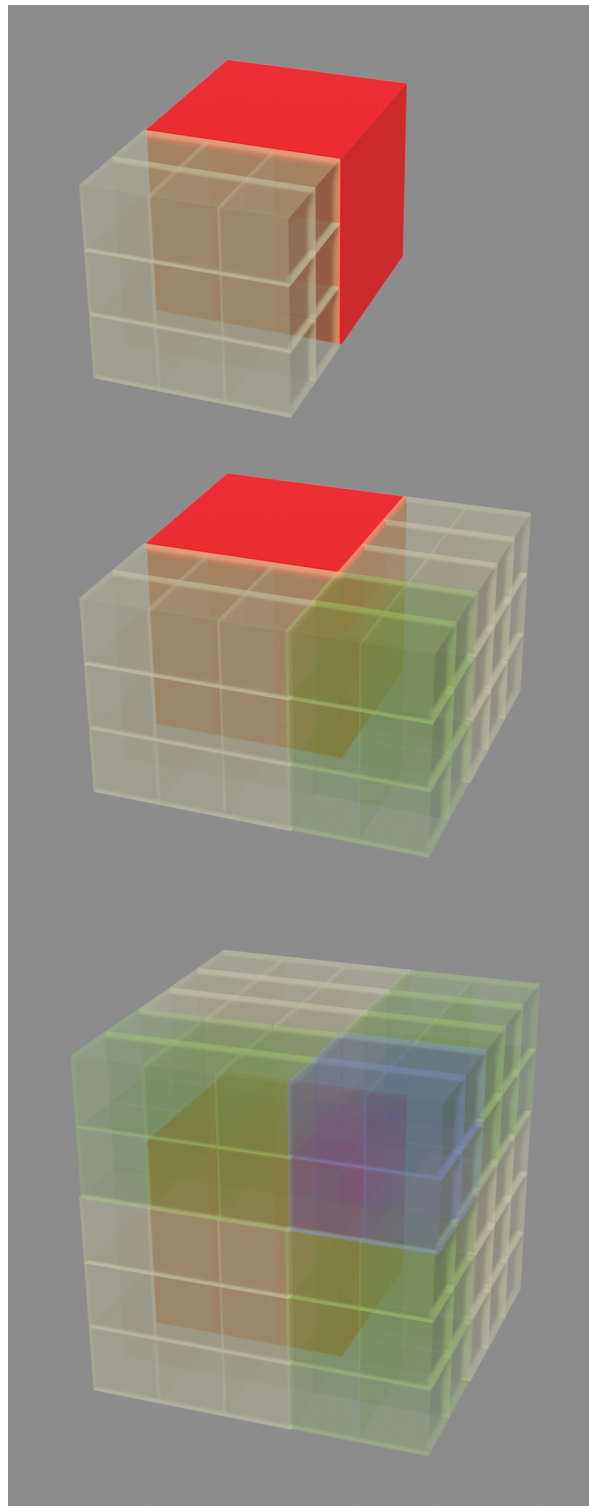


Figure 17: 3D representation of the boundary conditions. The original  $3 \times 3 \times 3$  supercell is shown in red. Added areas of types  $C_j(l)$ ,  $D_j(m)$  and  $E_j$  are shown in translucent yellow, green and blue, respectively. From top to bottom the images represent the added exchange interactions for a face, edge and corner, respectively.

## Appendix B: Symmetry finding algorithm flowchart

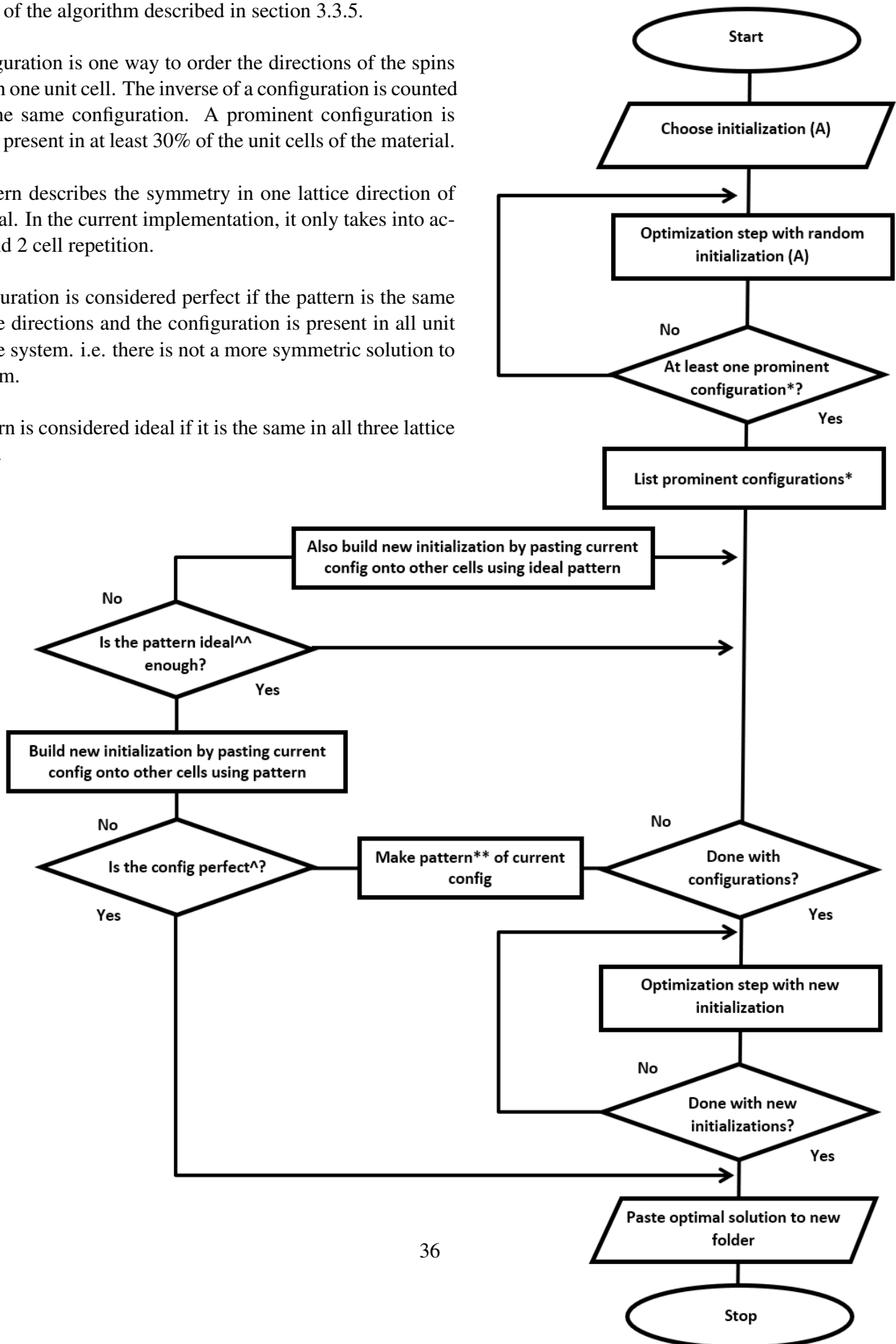
Flowchart of the algorithm described in section 3.3.5.

\* A configuration is one way to order the directions of the spins of atoms in one unit cell. The inverse of a configuration is counted towards the same configuration. A prominent configuration is one that is present in at least 30% of the unit cells of the material.

\*\* A pattern describes the symmetry in one lattice direction of the material. In the current implementation, it only takes into account 1 and 2 cell repetition.

^ A configuration is considered perfect if the pattern is the same in all three directions and the configuration is present in all unit cells of the system. i.e. there is not a more symmetric solution to the problem.

^^ A pattern is considered ideal if it is the same in all three lattice directions.





## Appendix C: Auxiliary results

In this appendix, the convergence plots, and some suboptimal configurations of the different executed runs are presented. There are 11 main figures, all spanning a page. First, the full convergence plots of the runs executed for the basic model, and the basic model including the boundary conditions are presented (figures 18 and 19). Next, the iterations of the different runs of the algorithm on the test set are shown in figures per material, as to compare the different values of  $\gamma$  (figures 20 - 26). Lastly, some frequently occurring suboptimal configurations for MnO are shown in figures 27 and 28.

For the convergence plots, note that some iterations and final exchange energies may overlap, hence the total amount of runs that end at the same energy level is not entirely evident from these plots alone. For an overview of the amount of successful runs, we refer back to the tables shown in section 4.

For the configurations plots, these are by no means all configurations found in the runs. They are presented here only to serve as examples.

### Energy differences

Due to the construction of the model, the two figures 13 and 14 contain quite different total energies. The first difference is that between the  $2 \times 2 \times 2$  and  $3 \times 3 \times 3$  configurations for the basic and boundary conditions model among itself. This effect can be explained by the order of exchange interactions that is taken into account. For a  $3 \times 3 \times 3$  cell, more exchange interactions are evaluated than in a  $2 \times 2 \times 2$  cell. Hence, a noticeable difference in total energy appears between the two configurations. The energy difference between the model with and without boundary conditions, is due to how the boundary conditions are implemented. Because the boundary conditions add equations to the total energy function, there are more exchange interactions taken into account (those that for the basic model would fall outside of the supercell). This results in a significantly higher energy for both configurations. The  $2 \times 2 \times 2$  case **benefits more** from this effect than the  $3 \times 3 \times 3$  case, as when we look back at equations (31, 32 and 33), way more boundary conditions are added for a corner than for a side or face unit cell. As the  $2 \times 2 \times 2$  only consists of corners, and the  $3 \times 3 \times 3$  does not (its outer shell consists of 8 corners, 12 edges and 6 faces), it so to speak 'gains' less net equations. Hence, for the model with boundary conditions, the  $3 \times 3 \times 3$  configurations have a consistently higher energy per unit cell, where for the base model the differences are smaller, and the  $3 \times 3 \times 3$  case has a lower energy than the  $2 \times 2 \times 2$  case.

### Convergence for basic model

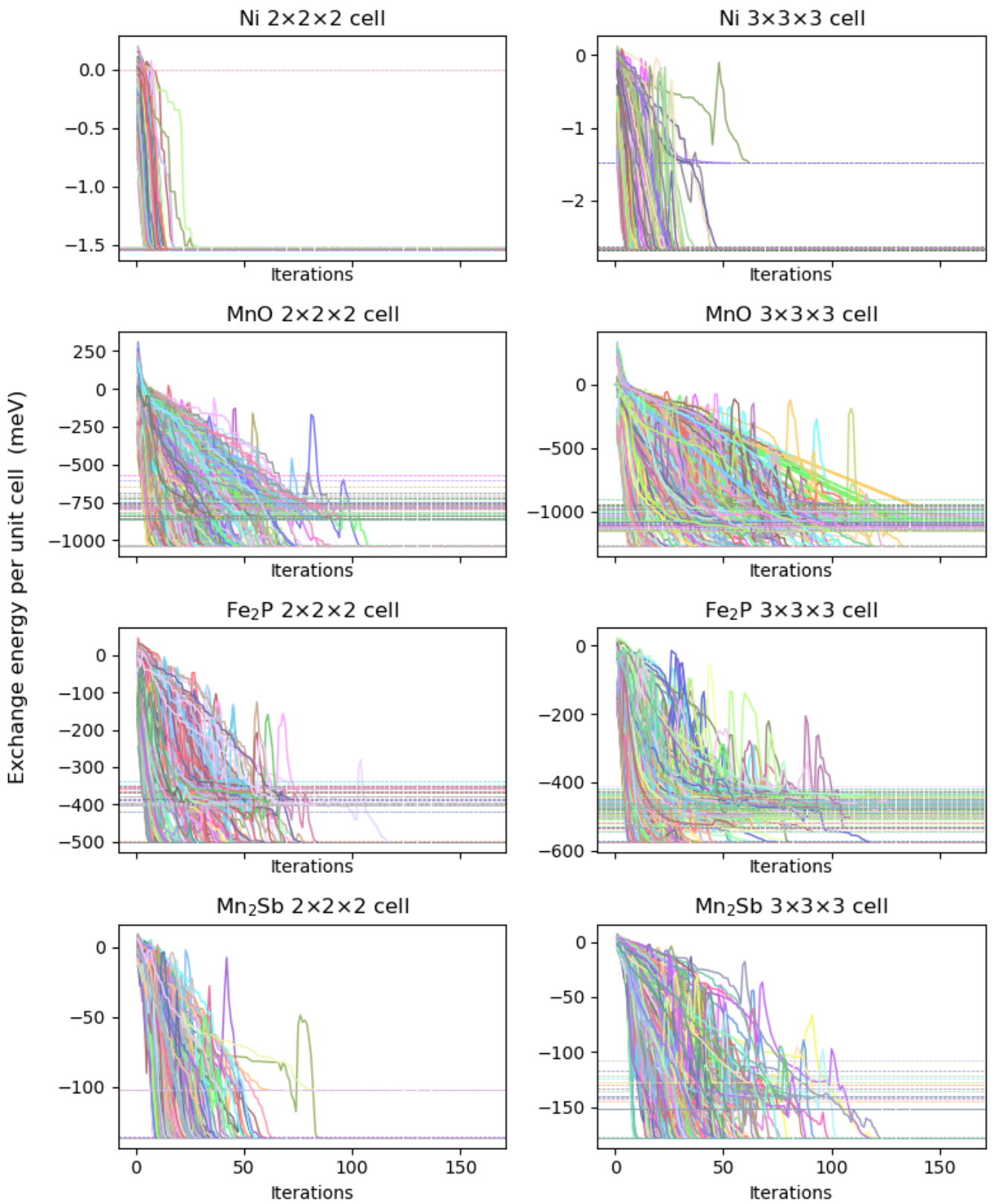


Figure 18: The full iterations for all runs executed in testing the basic model. Different runs are shown in different colours. In this plot, no distinction is made between different initializations.

### Convergence for model with boundary conditions

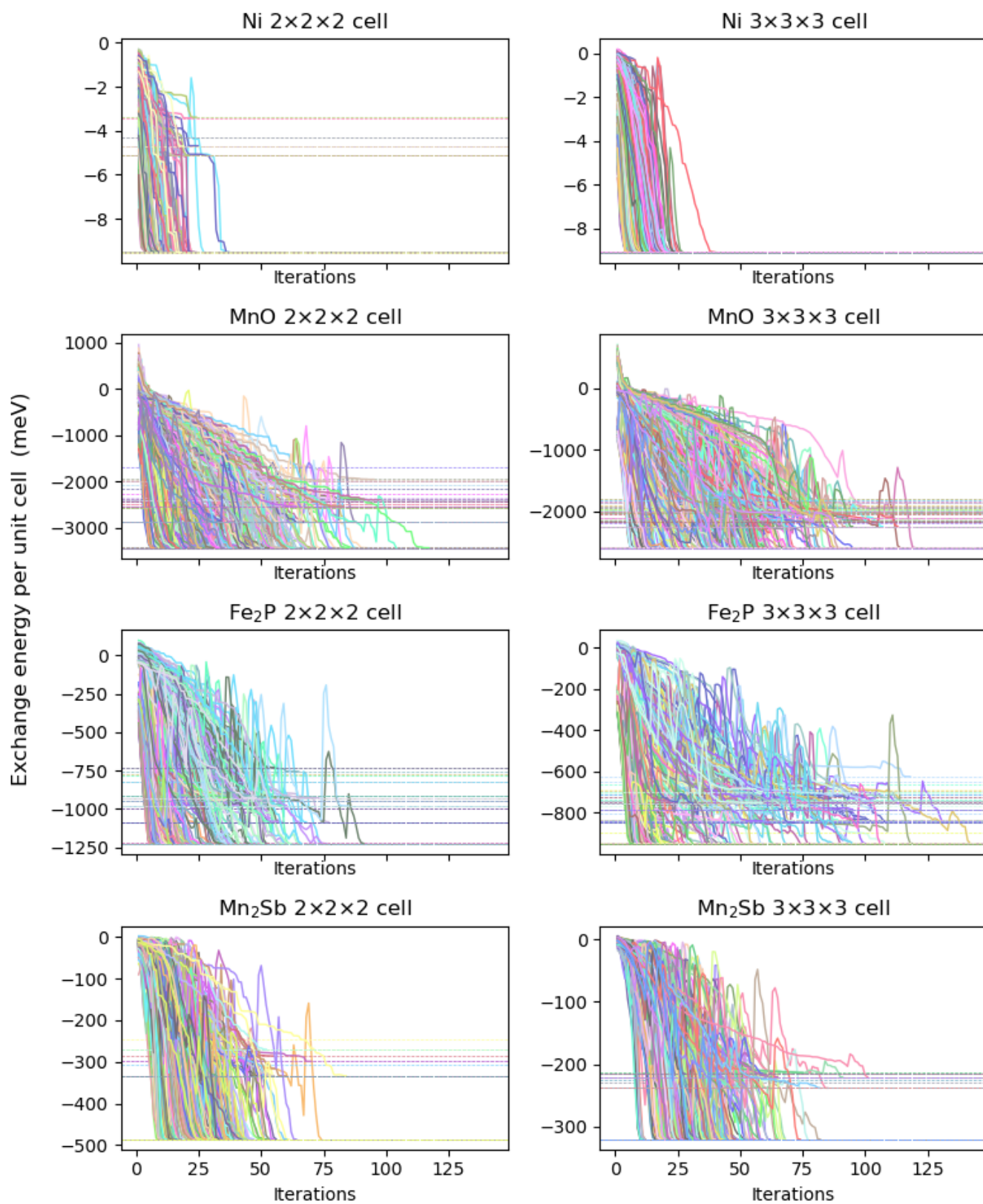


Figure 19: The full iterations for all runs executed in testing the basic model with boundary conditions. Different runs are shown in different colours. In this plot, no distinction is made between different initializations.

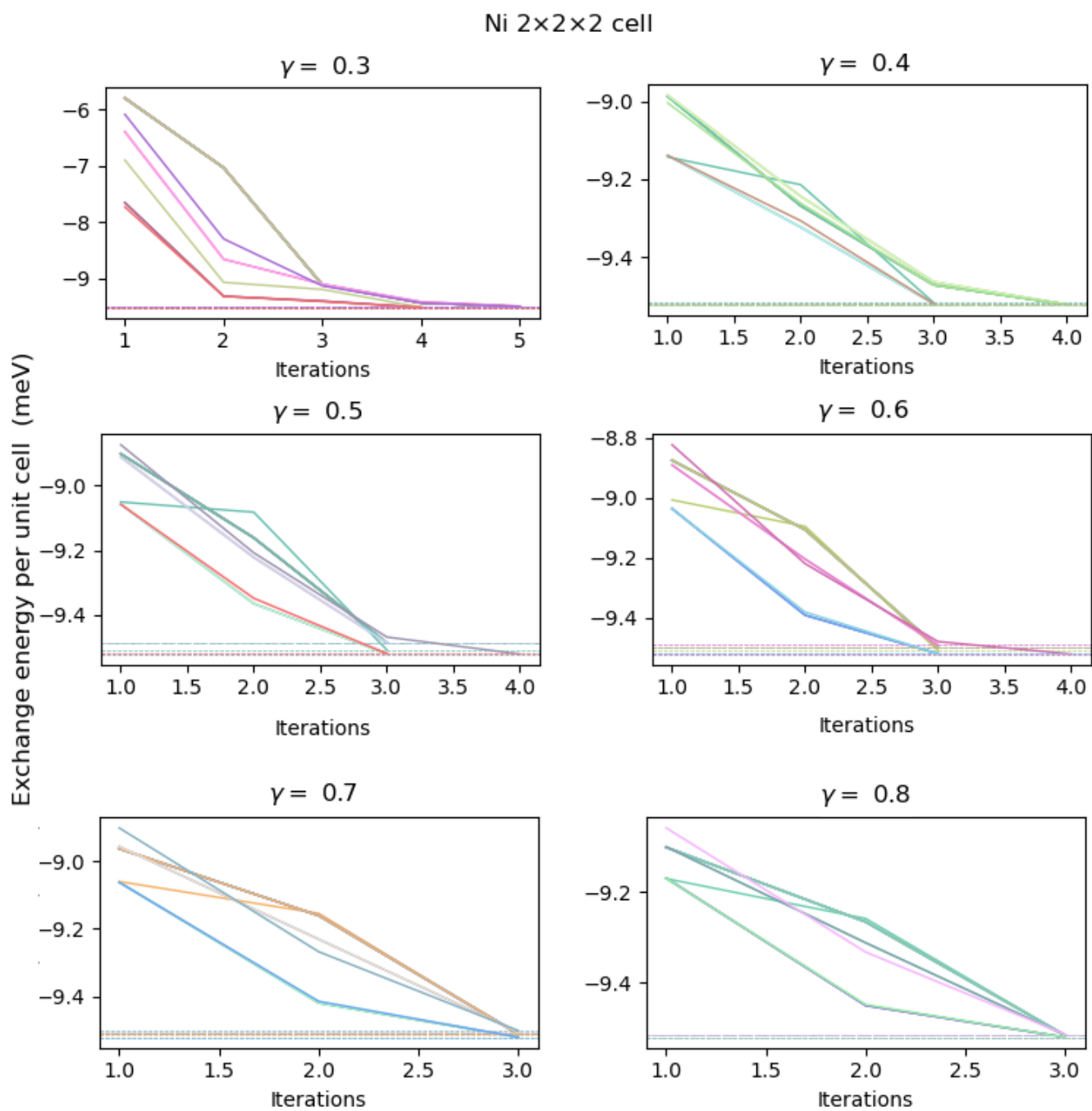


Figure 20: The full iterations for all runs executed on the test set of Ni 2×2×2.

MnO 2x2x2 cell

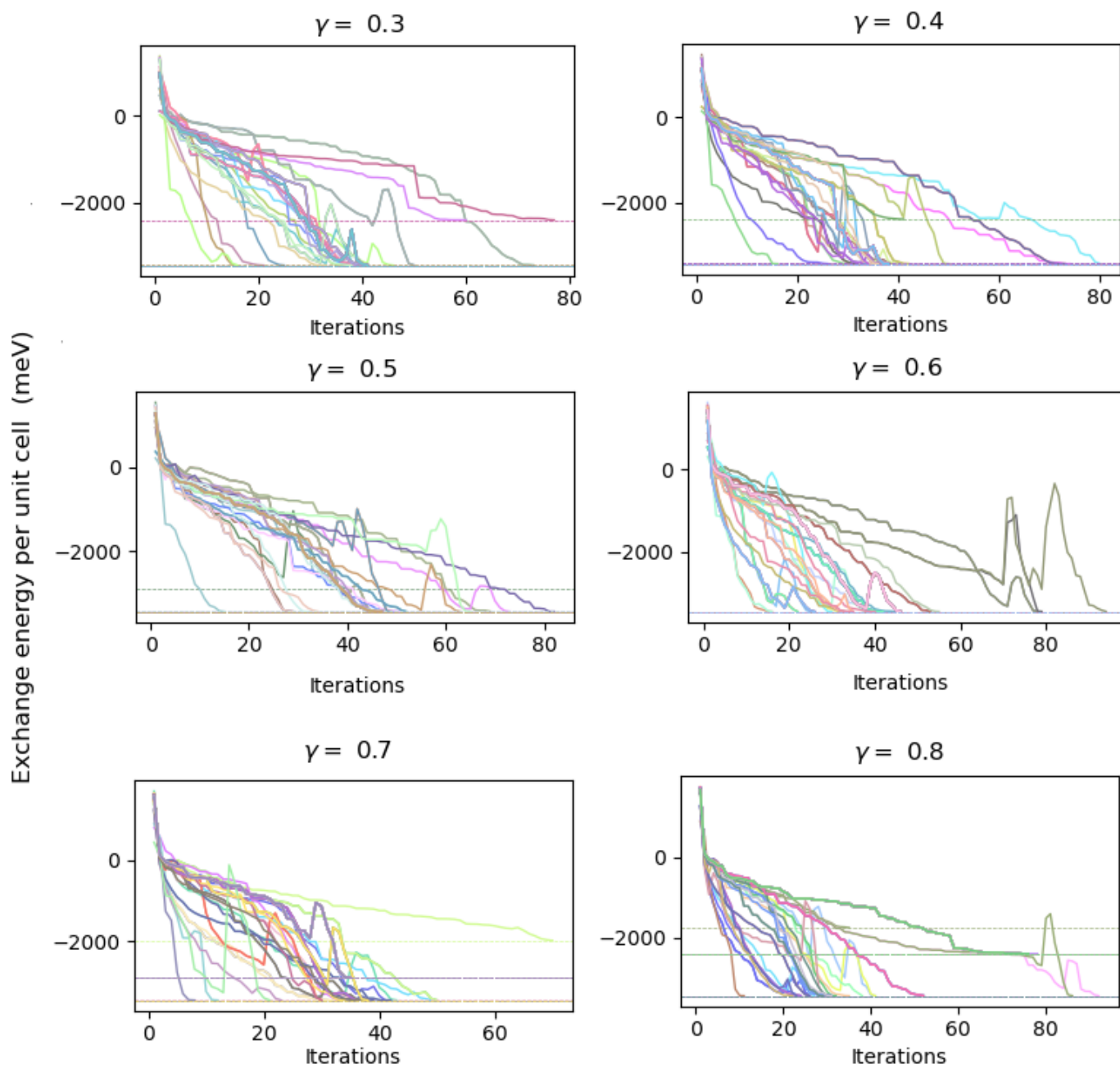


Figure 21: The full iterations for all runs executed on the test set of MnO 2x2x2.

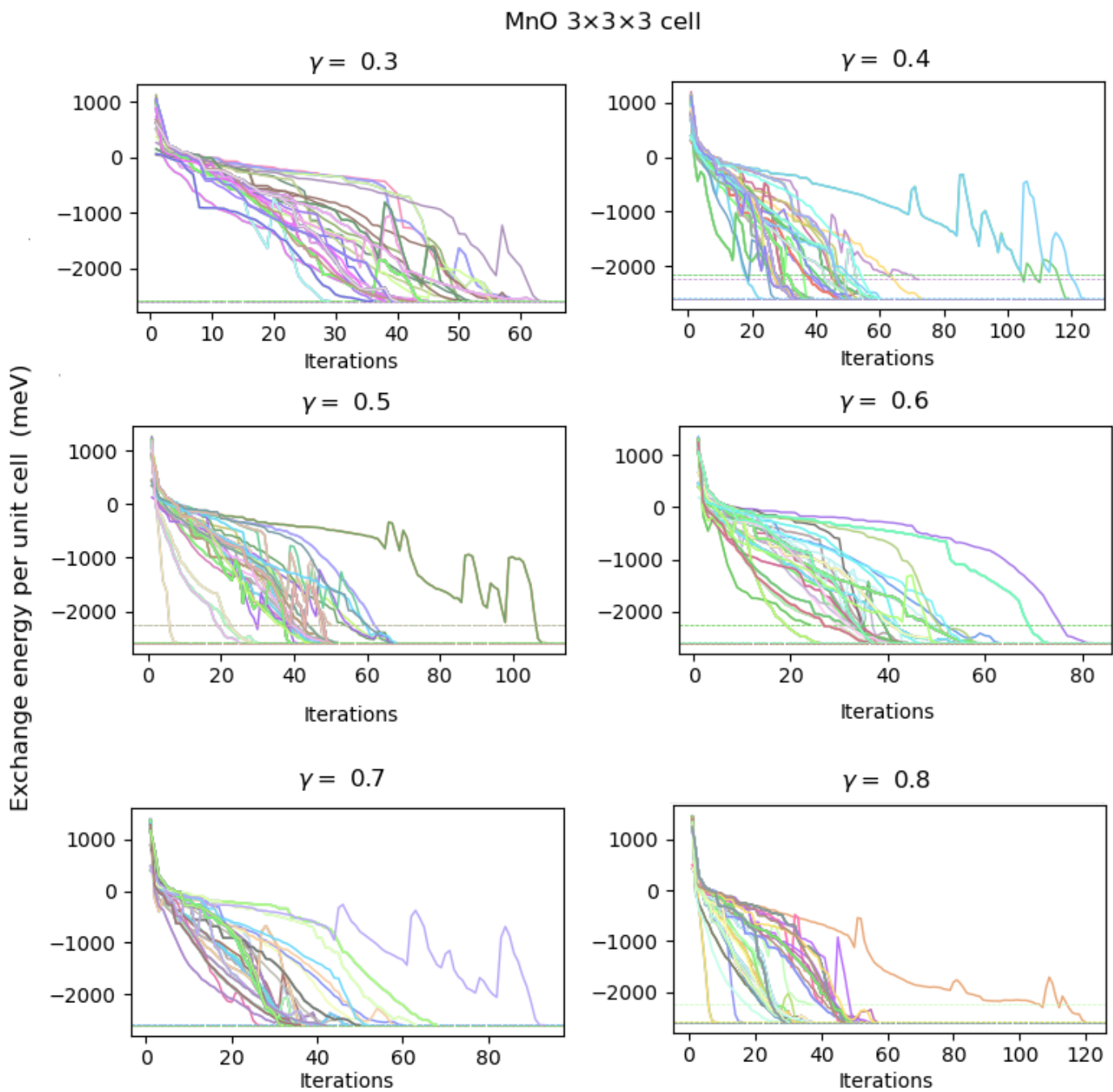


Figure 22: The full iterations for all runs executed on the test set of MnO  $3 \times 3 \times 3$ .



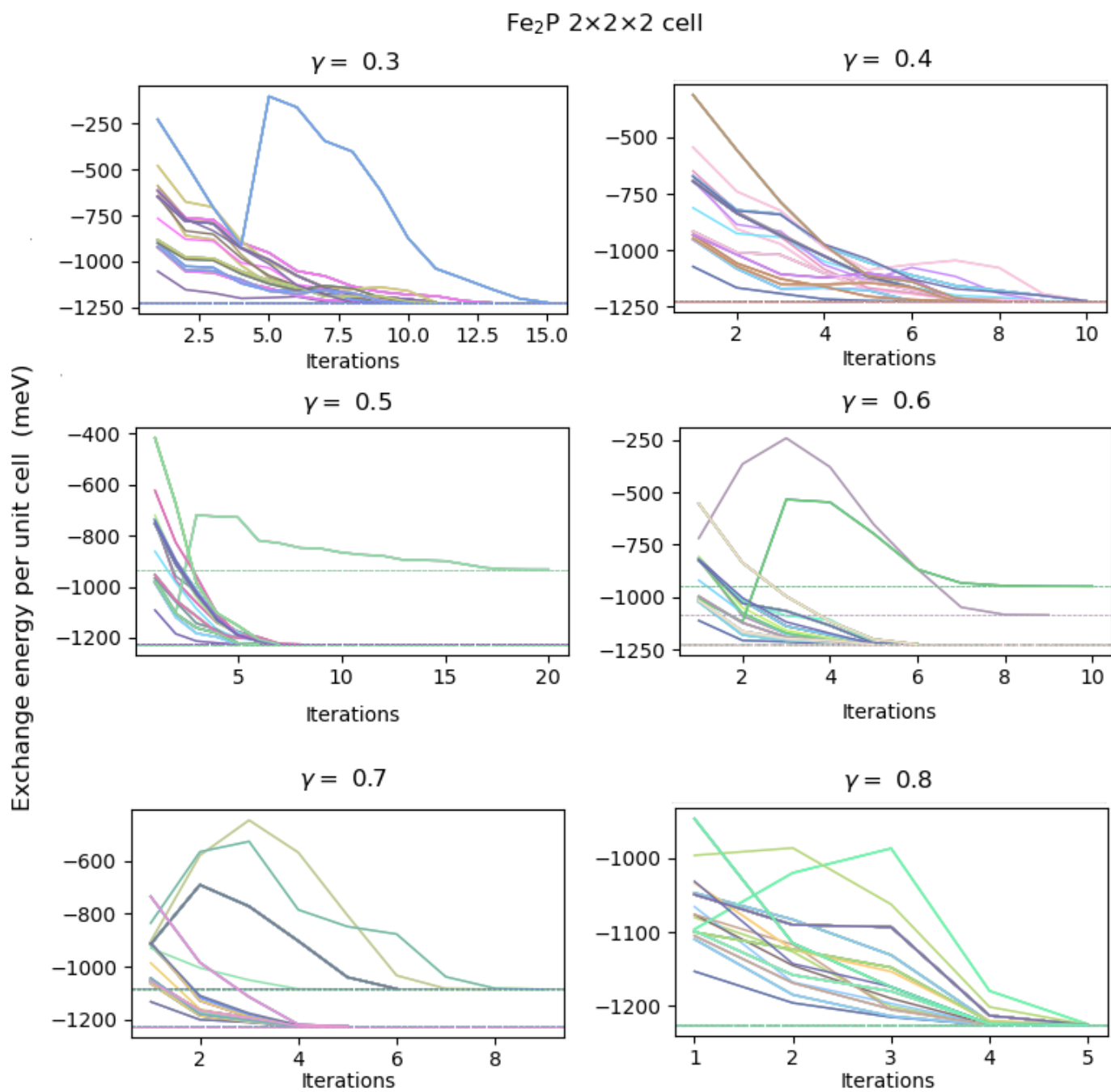


Figure 23: The full iterations for all runs executed on the test set of  $\text{Fe}_2\text{P } 2 \times 2 \times 2$ .

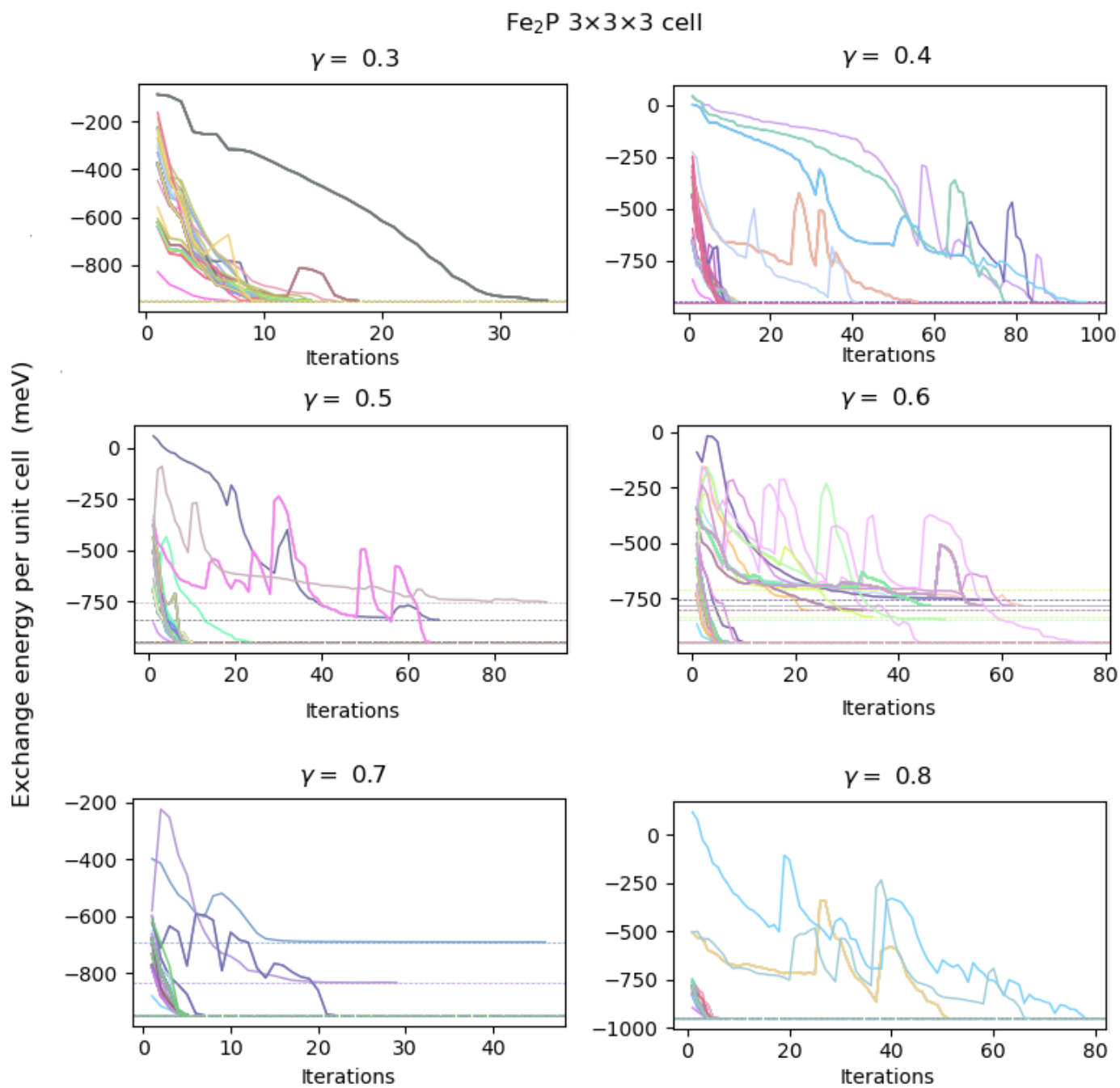


Figure 24: The full iterations for all runs executed on the test set of Fe<sub>3</sub>P 3×3×3.



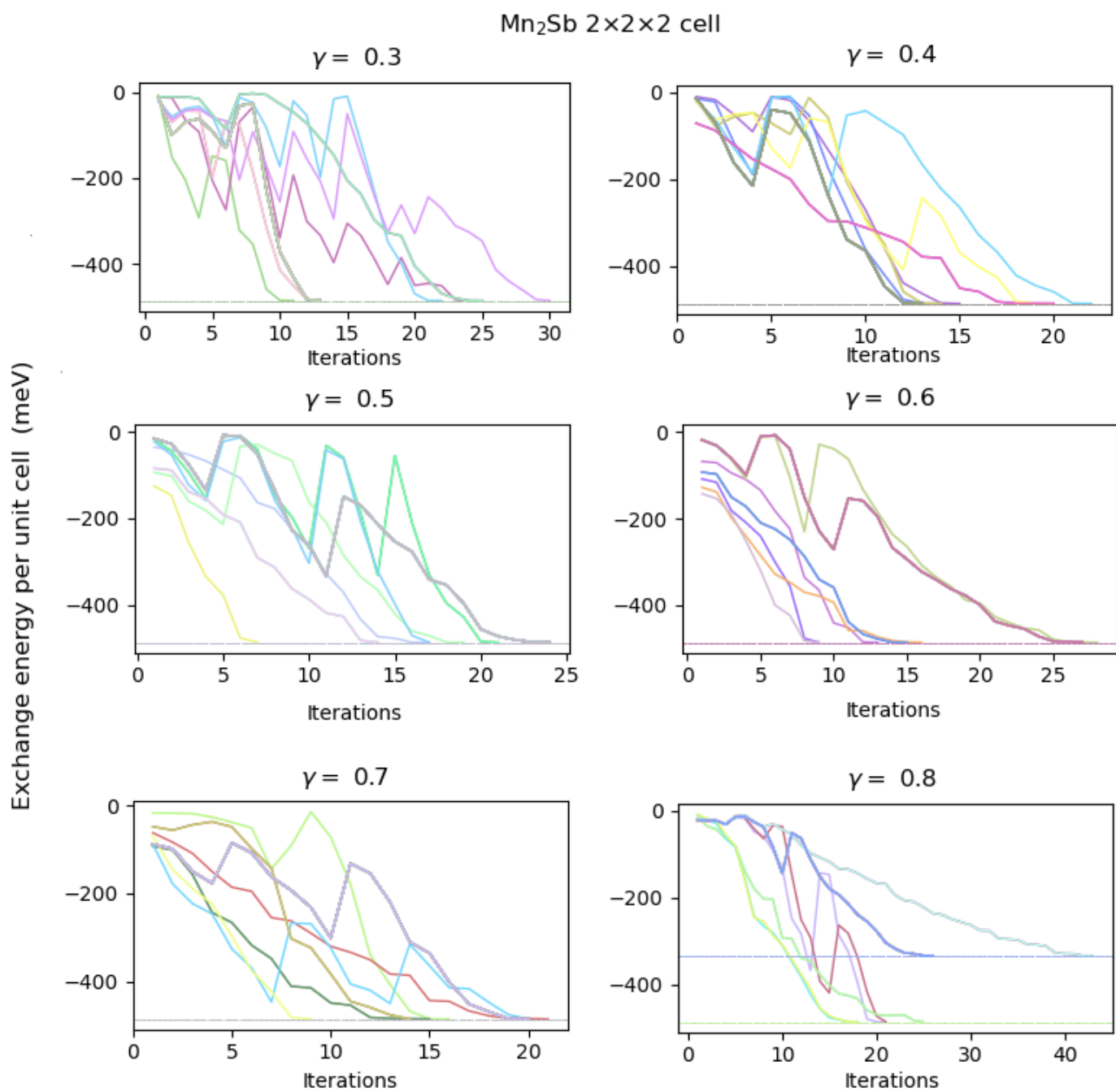


Figure 25: The full iterations for all runs executed on the test set of Mn<sub>2</sub>Sb 2×2×2.

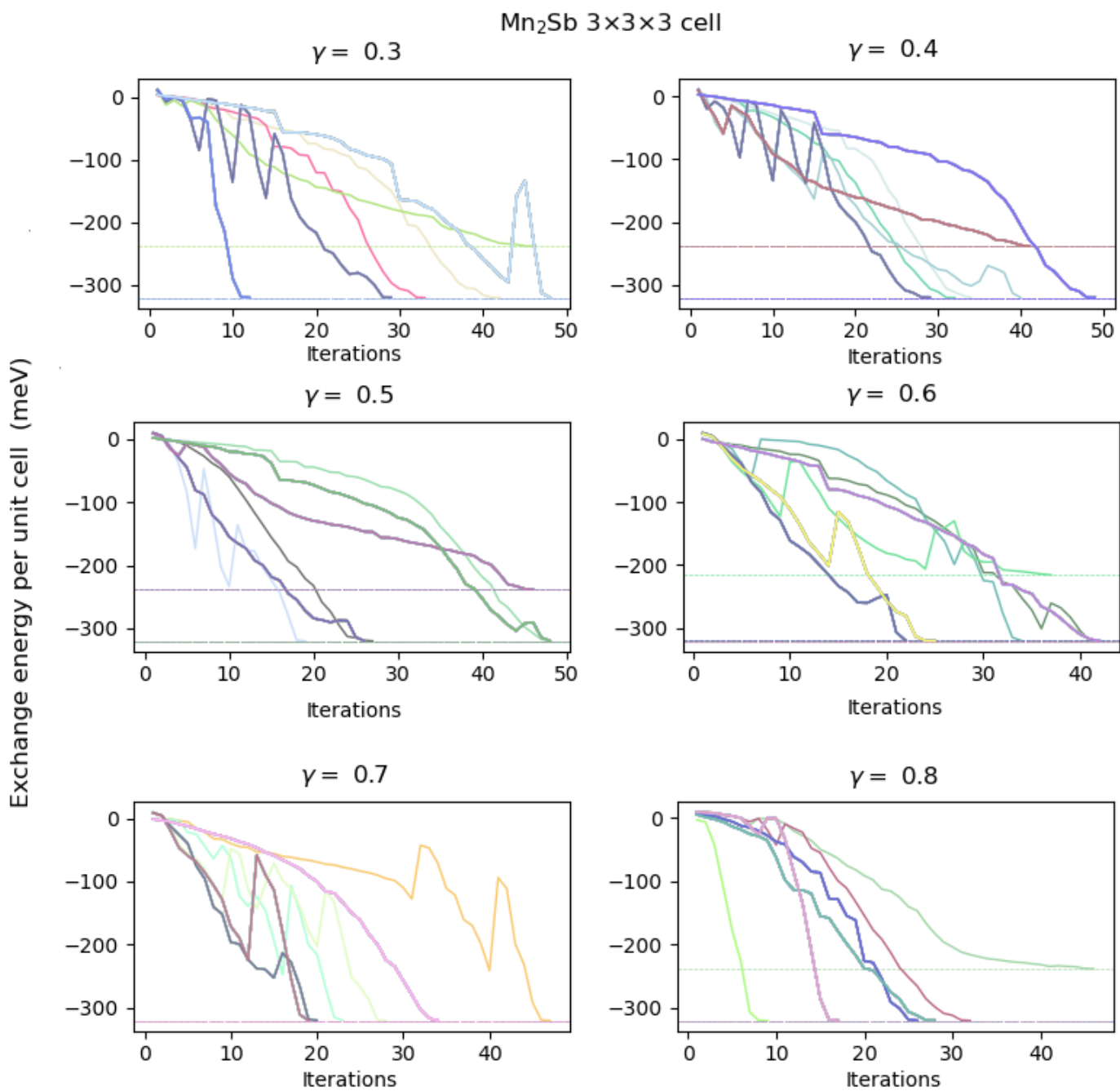


Figure 26: The full iterations for all runs executed on the test set of Mn<sub>2</sub>Sb 3×3×3.

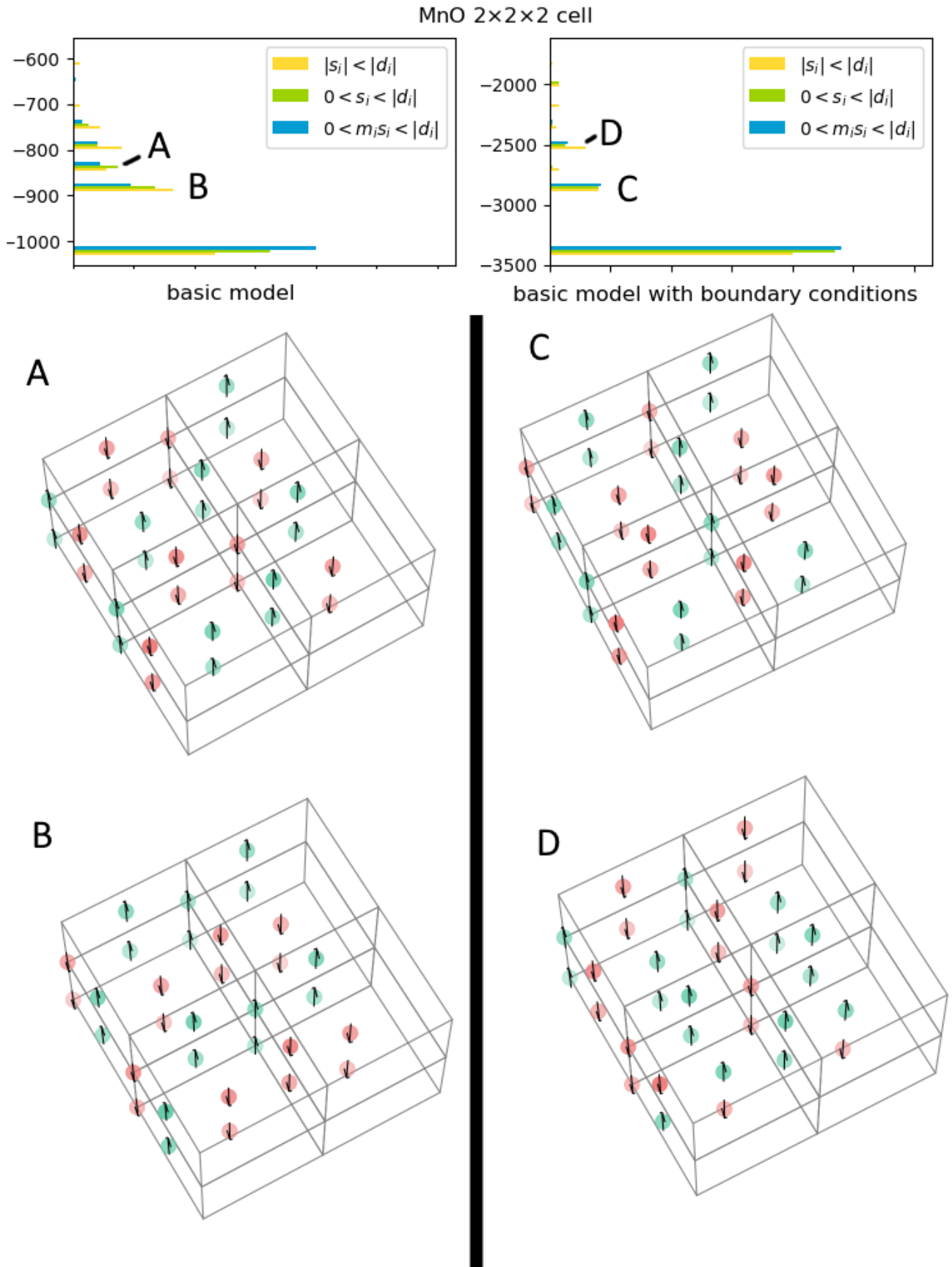


Figure 27: Two suboptimal configurations for the basic model, and the model with boundary conditions, for MnO  $2 \times 2 \times 2$ . The different energies corresponding to the different configurations are marked by A, B, C and D.

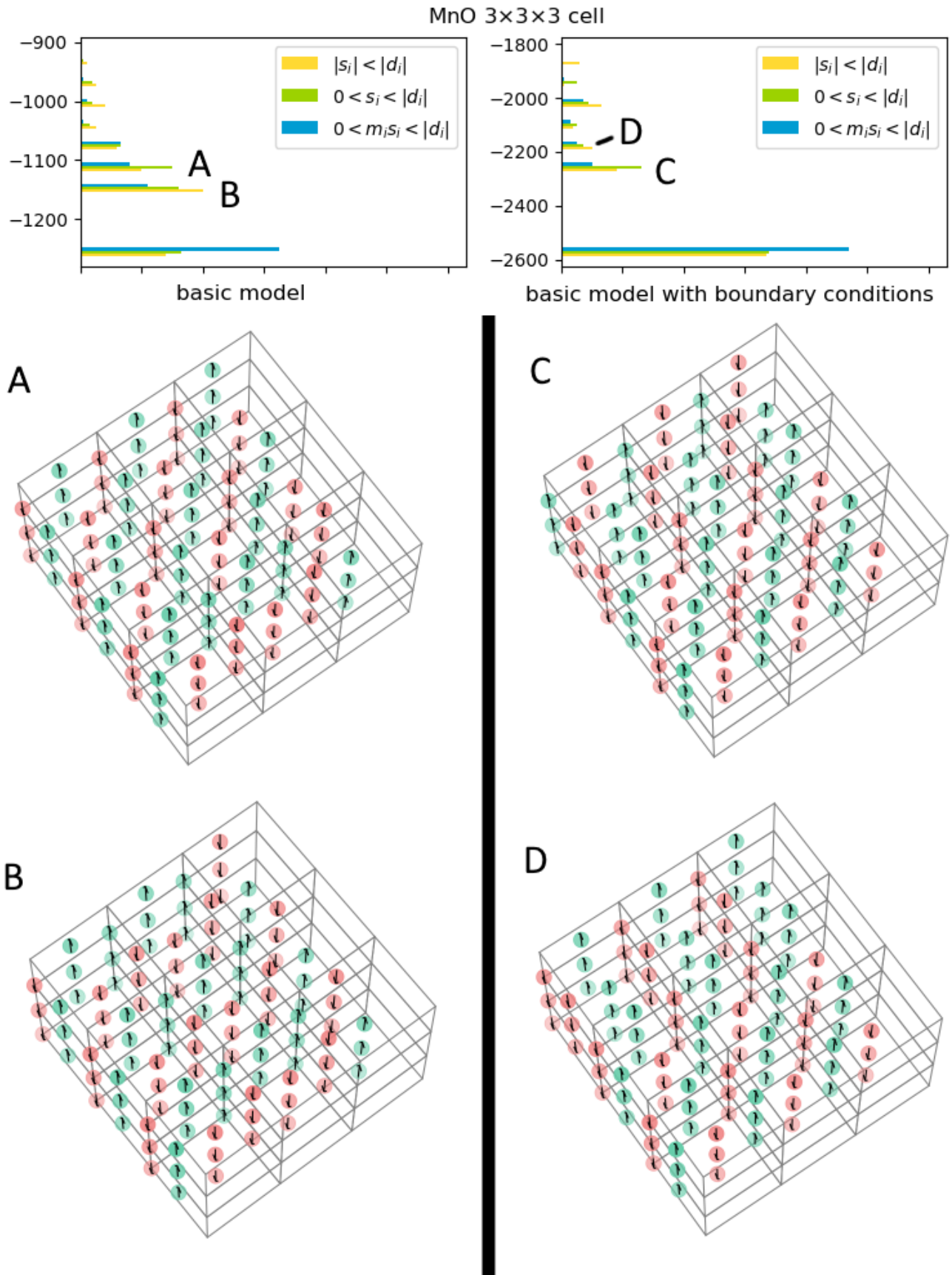


Figure 28: Two suboptimal configurations for the basic model, and the model with boundary conditions, for MnO  $3 \times 3 \times 3$ . The different energies corresponding to the different configurations are marked by A, B, C and D.

## Appendix D: Python code

```
1 # -*- coding: utf-8 -*-
2 """
3 Created on Thu May 19 21:09:22 2022
4
5 @author: Arthur C. Ronner
6 """
7 # -*- coding: utf-8 -*-
8
9 from pymatgen.io.vasp.inputs import Poscar
10 from pymatgen.core import lattice
11 import numpy as np
12 import re
13 import os
14 from pathlib import Path
15 from gekko import GEKKO
16 from contextlib import redirect_stdout
17 import mag_plotter as mp
18 import time
19 import shutil
20
21 #=====#
22 # #
23 # FILE INDEX: #
24 # files & formatting #
25 # READ FILE FUNCTION #
26 # FORMATTING FUNCTIONS #
27 # #
28 # One opt run #
29 # PERIODIC BC'S #
30 # VARIABLE INITIALIZATION #
31 # DEFINING OPTIMIZATION #
32 # SMALL HELP FUNCTIONS #
33 # MAIN RUNNER FUNCTIONS #
34 # #
35 # Multiple runs #
36 # MULTIPLE RUNS CODE #
37 # ITERATING FUNCTIONS #
38 # #
39 #=====#
40
41 #=====#
42 # READ FILE FUNCTIONS #
43 #=====#
44 def read_file(file_name,num_hor_vals, file_type, convert_names = {}):
45     """
46     :file_type: -1 = J from jdata file; 0 = J matrix short; 1 = results from Gekko;
47     ↪ 2 = APOPT; 3 = IPOPT; 4 = mag_moment file
48     """
49     #print(file_name)
50     with open(file_name) as f:
51         lines = f.readlines()
52         #Predict filesize horizontal
53         data = np.zeros((len(lines),num_hor_vals)) #initialize data vector
54         if file_type == 0 or file_type == -1: #As each file is a little different we
55             ↪ prepare different arrays
56             names = [['', ''] for i in range(len(lines))] #here we need 2 names as it
57             ↪ is J interactions
58         if file_type == 1:
```

```

56     names2 = ['' for i in range(len(lines))] #here only one as its about
        ↪ variables
57
58     for i in range(len(lines)): #per file we format lines a little differently so
        ↪ that we get the correct data
59         if file_type == 0:
60             lines[i] = re.sub(',|\(|\)', '', lines[i]) #remove comma's
61         if file_type == 1:
62             lines[i] = re.sub('\{|\}', "0 0 0 0", lines[i])
63             lines[i] = re.sub(',|\[|\]|:\|\'', '', lines[i])
64             lines[i] = re.sub('q_', '- ', lines[i])
65             lines[i] = re.sub('q', ' ', lines[i])
66             lines[i] = lines[i].title()
67         if file_type == 4:
68             lines[i] = re.sub('\s[a-z]', '_', lines[i])
69         data_frag = lines[i].split()
70         #print(lines[i])
71
72         for j in range(num_hor_vals):
73
74             try:
75                 float(data_frag[j])
76                 data[i,j] = float(data_frag[j])
77                 if file_type == -1:
78                     if j <= 1:
79                         names[i][j] = convert_names[int(data[i,j]-1)]
80             except ValueError:
81                 if file_type == 0:
82                     if j == 0:
83                         names[i][j] = re.sub(r'(-?[0-9]+\.[0-9]*)', r" \1
        ↪ ", data_frag[j].strip())
84                         names[i][j] = re.sub('\s$', '', names[i][j])
85                     elif j == 1:
86                         names[i][j] = re.sub(r'(-?[0-9]+\.[0-9]*)', r" \1
        ↪ ", data_frag[j].strip()) #capitalizes letters
87                         names[i][j] = re.sub('\s$', '', names[i][j])
88                 if file_type == 1:
89                     if j == 0:
90                         names2[i] = re.sub('_', ' ', data_frag[j])
91                 continue
92             except IndexError:
93                 continue
94         if file_type == 0:
95             return data[:,2:], np.array(names)
96         elif file_type == 1:
97             l = 2
98             for i in range(1, len(names2)):
99                 if len(re.findall('\^P\d', names2[i])) == 0:
100                     l = i
101                 break
102             return data[l:-1,1:], names2[l:-1]
103         elif file_type == 2:
104             return data[l:-2,:]
105         elif file_type == 3:
106             return data[l:-3,:]
107         elif file_type == -1:
108             return data[:, [2,3,4,5]], names
109         else:
110             return data
111

```

```

112 def read_moments(file_name, TB2J = True, N = 100):
113
114     if TB2J:
115         data = [[] for i in range(N)]
116         with open(file_name, "r") as file: # the r opens it in read mode
117             count = 0
118             for i in file:
119                 count += 1
120             N = min(count-3,N)
121         with open(file_name, "r") as file:
122             print(N)
123             for i in range(N):
124                 line = next(file).strip()
125                 if len(re.findall('Atoms', line)) > 0:
126                     start = i + 3
127                 if len(re.findall('^Total',line)) > 0:
128                     stop = i
129                 data[i] = line
130             interest = [[] for i in range(stop-start)]
131             for i in range(start,stop):
132                 interest[i-start] = data[i].split()
133             moments = {}
134             for i in range(stop-start):
135                 moments[re.sub(r'(-?[0-9]+\.[0-9]*)', r" \1",interest[i][0].strip())]
136                 ↪ = float(interest[i][-1])
137             return moments
138     else:
139         moments = {}
140         names = []
141         with open(file_name, "r") as f:
142             lines = f.readlines()
143             for i in range(len(lines)):
144                 temp = lines[i].split()
145                 if len(temp) != 2:
146                     print('ERROR!')
147                 moments[re.sub(r'(-?[0-9]+\.[0-9]*)', r" \1",temp[0].strip())] =
148                 ↪ float(temp[1])
149                 names.append(re.sub(r'(-?[0-9]+\.[0-9]*)', r"
150                 ↪ \1",temp[0].strip()))
151             return moments, names
152
153 #=====
154 #                                     FORMATTING FUNCTIONS                                     #
155 #=====
156
157 def J_short(file, new_file, ftype = 0):
158     with open(file) as f:
159         lines = f.readlines()
160     g = open(new_file, "w")
161     start = True
162     stop = False
163     if ftype == 0:
164         for i in lines:
165             x = re.findall("^\\-\\-\\-|J_iso|Orbital| \\", i)
166             if x == ['---']:
167                 start = False
168             if not x and start == False:
169                 g.write(i)
170     elif ftype == 1: #APOPT
171         for i in lines:
172             x = re.findall('Iter|Success',i)

```

```

169
170         if x == ['Iter']:
171             start = False
172         if x == ['Success']:
173             stop = True
174         if not x and start == False and stop == False and len(i)>10:
175             g.write(i)
176     elif ftype == 3: #IPOPT
177         for i in lines:
178             x = re.findall('^iter|^Number of I',i)
179             if x == ['iter']:
180                 start = False
181             if x == ['Number of I']:
182                 stop = True
183             if not x and start == False and stop == False:
184                 g.write(i)
185     g.close()
186     return
187
188
189
190 def J_as_dict(J_mat,nam_mat,latt, index):
191     J_dict_lvec = {}
192     name_dict = {}
193     #names = np.unique(nam_mat)
194     old_s = str(latt.sites[0].specie)
195     j = 1
196     for i in range(len(latt.sites)):
197         new_s = str(latt.sites[i].specie)
198         if new_s != old_s:
199             j = 1
200         name_dict[str(latt.sites[0].specie) + ' ' + str(j)] =
        ↪ latt.sites[i].coords.dot(latt.lattice.inv_matrix)
201         j += 1
202         old_s = str(latt.sites[i].specie)
203     for i in range(len(J_mat)):
204         nam = ['', '']
205         for j in range(2):
206             nam[j] = nam_mat[i][j]
207             nam[j] = re.sub('\s$', '', nam[j])
208         J_dict_lvec[nam[0]+' '+nam[1]+' '+str(int(J_mat[i,0]))+'
        ↪ '+str(int(J_mat[i,1]))+' '+str(int(J_mat[i,2]))] = J_mat[i,index]
209     #print('Done with saving Js as a dictionary')
210     return J_dict_lvec, name_dict
211
212
213
214 #=====#
215 #                               PERIODIC BC'S                               #
216 #=====#
217 def periodic_bc_2(m,J_mat, uni_at, var_vec,ind,ranges, J_reach):
218     tot = len(var_vec)
219     edge_num = len(var_vec) - (len(uni_at)*(ranges[1]-ranges[0] -
        ↪ 1)*(ranges[3]-ranges[2] - 1)*(ranges[5]-ranges[4] -1))
220     print('number of atoms at edge: ' + str(edge_num))
221     bc_fct = [None for j in range(tot)]
222     cell =
        ↪ np.array([ranges[1]-ranges[0]+1,ranges[3]-ranges[2]+1,ranges[5]-ranges[4]+1])
223     k = 1
224     for i in range(len(var_vec)):

```



```

225     if var_vec[i] is None:
226         continue
227     s_p = np.full(3,None) #s_p = saved points
228     for j in range(3):
229         if ind[i][j] == ranges[2*j] or ind[i][j] == ranges[2*j+1]:
230             temp = ind[i].copy()
231             if temp[j] == ranges[2*j]:
232                 temp[j] = ranges[2*j+1]
233             else:
234                 temp[j] = ranges[2*j]
235             orient = np.ones(4)
236             orient[3] = 0 #setting mode
237             orient[j] = 0 #setting axis to slice away
238             k = ind.index([temp[0],temp[1],temp[2],temp[3]])
239             bc_fct[i] = cut_equation(m,J_mat,uni_at,var_vec,ind,J_reach,
240                 ↪ cell,0,tot,i,typ = 1, j = k, ori = orient)
241             s_p[j] = temp[j]
242     u_c = np.where(s_p == None)[0] #u_c = unaltered coords
243     if len(u_c) == 1: #we're at an edge:
244         s_p[int(u_c)] = ind[i][int(u_c)]
245         orient = np.zeros(4)
246         orient[3] = 1
247         orient[int(u_c)] = 1
248         k = ind.index([s_p[0],s_p[1],s_p[2],ind[i][3]])
249         bc_fct[i] =
250             ↪ cut_equation(m,J_mat,uni_at,var_vec,ind,J_reach,cell,0,tot,i,typ =
251             ↪ 1, j = k, ori = orient)
252     elif len(u_c) == 0: #we're at a corner, so need 4 other configs
253         for l in range(3): #first three
254             temp = np.zeros(3)
255             orient = np.ones(4)
256             orient[l-1] = 0
257             orient[l-2] = 0 # ori will have 0's at axis that need 'slicing' and
258             ↪ 1 at unaltered axes.
259             temp[l-1] = s_p[l-1]
260             temp[l-2] = s_p[l-2]
261             temp[l] = ind[i][l]
262             k = ind.index([temp[0],temp[1],temp[2],ind[i][3]])
263             bc_fct[i] =
264             ↪ cut_equation(m,J_mat,uni_at,var_vec,ind,J_reach,cell,0,tot,i,typ
265             ↪ = 1, j = k, ori = orient)
266
267         k = ind.index([s_p[0],s_p[1],s_p[2],ind[i][3]]) #fourth
268         orient = [0,0,0,2]
269         bc_fct[i] = cut_equation(m,J_mat,uni_at,var_vec,ind,J_reach,cell,
270             ↪ 0,tot,i,typ = 1, j = k, ori = orient)
271
272     return [g for g in bc_fct if g is not None]
273
274 def J_sum_cond(coords,ori): #avoids double counting in periodic bc's
275     #ori = [x,y,z,mode] if x,y,z = 0 then these axis are to be cut away, 1 means
276     ↪ they need to be retained.
277     if ori[3] == 0: #case of a face
278         axis = np.where(ori == 0)[0]
279         return coords[axis[0]] != 0 #we remove one plane
280     if ori[3] == 1: #case of an edge
281         axis = np.where(ori == 0)[0]
282         #print(axis)
283         return (coords[axis[0]] != 0 and coords[axis[1]] != 0) #remove two planes

```

```

277     if ori[3] == 2: #case of a corner
278         return (coords[0] != 0 and coords[1] != 0 and coords[2] != 0) #remove 3
           ↪ planes
279     return
280
281
282
283 #=====
284 #                               VARIABLE INITIALIZATION                               #
285 #=====
286
287 def initial_vals(ranges,unique_ats,moments,itype, at_index = []):
288
289     a, b, c, d, r = len(unique_ats), len(ranges[0]), len(ranges[1]),
           ↪ len(ranges[2]), range(len(unique_ats))
290     ms = np.zeros(a)
291     for i in r:
292         ms[i] = moments.get(unique_ats[i]) #To shorten notations
293
294     if itype >= 0: #These are the random seeds
295         vals = np.random.rand(a,b,c,d)
296         if itype == 0: #Totally random within bounds (for antiferromagnetic?)
297             for i in r:
298                 vals[i] = vals[i]*(2*abs(ms[i]))-abs(ms[i])
299                 print("Initializing any random value within bounds")
300         if itype == 1: #Random positive values
301             for i in r:
302                 vals[i] = vals[i]*(abs(ms[i]))
303                 print("Initializing any positive random value within bounds")
304         if itype == 2: #Random pos or neg depending on moment
305             for i in r:
306                 vals[i] = vals[i]*(ms[i])
307                 print("Initializing value between 0 and the value in exchange.out (pos
           ↪ or neg)")
308     else: #These are the predetermined initialization cases
309         vals = np.zeros((a,b,c,d))
310         if itype == -1: #Initial guess is the moments obtained from the poscar file
311             for i in r:
312                 vals[i] = ms[i]
313                 print("Initializing the exact value given in exchange.out")
314         if itype == -2: #try the literature orientation ONLY WORKS FOR CELLS OF 0
           ↪ and bigger
315             for i in r:
316                 for j in range(b):
317                     for k in range(c):
318                         for l in range(d):
319                             if (j + k + 1)%2 == 0:
320                                 if i < 3:
321                                     vals[i,j,k,l] = abs(ms[i])
322                                 else:
323                                     vals[i,j,k,l] = -abs(ms[i])
324                             else:
325                                 if i < 3:
326                                     vals[i,j,k,l] = -abs(ms[i])
327                                 else:
328                                     vals[i,j,k,l] = abs(ms[i])
329                 print("Initializing the literature configuration")
330     return vals
331
332 def initialize_vars_2(ranges,m,unique_ats,la, moments, init = 0, boost = False,
           ↪ starts = {}):

```

```

333 #ranges include the cells that we want to sum over, already including the 0 if
    ↪ necessary
334 #m is the model
335 #unique_ats is the unique atoms in the unit cell
336 #la is the structure object
337 s = ' '
338 if boost == False:
339     vals = initial_vals(ranges,unique_ats,moments,init)
340 else:
341     print("Using previous ending")
342 at = [[] for i in range(len(unique_ats))]
343 x_names = [[] for i in range(len(unique_ats))]
344 for e in range(len(unique_ats)):
345     at[e] = list_3D(len(ranges[0]), len(ranges[1]), len(ranges[2]), None)
346     x_names[e] = list_3D(len(ranges[0]), len(ranges[1]), len(ranges[2]), '')
347 for h in range(len(unique_ats)):
348     for i in ranges[0]:
349         for j in ranges[1]:
350             for k in ranges[2]: #so these all walk from negative to positive
    ↪ values potentially. OUT OF RANGE ERROR -> wrap
351                 try:
352                     x_names[h][i][j][k] = f'{unique_ats[h]}q{i}q{j}q{k}'
353                     bound = abs(moments.get(unique_ats[h]))
354                     if boost == False:
355                         val = vals[h,i,j,k]
356                     else:
357                         if len(starts) == 0:
358                             print("ERROR: No data found for second run")
359                             #print(str(unique_ats[h])+s+str(i)+s+str(j)+s+str(k))
360                             val =
    ↪ starts.get(str(unique_ats[h])+s+str(i)+s+str(j)+s+str(k))
361                     at[h][i][j][k] = m.Var(lb = -bound, ub = bound, value =
    ↪ val, name = x_names[h][i][j][k])
362                 except IndexError:
363                     print("ERROR: 0 has to be part of all the ranges!!!")
364 #print("Done with initializing vars")
    ↪
365 return at, x_names
366
367 #=====
368 #                               DEFINING OPTIMIZATION                               #
369 #=====
370
371 def J_sum_2(m,J_d,q,var,star,stop,i, typ = 0, k = 0, lim = 0, ori = [1,1,1,0]):
    ↪ #main function for the objective function
372
373 s = ' '
374 # for j in range(stop-star):
375 #     if J_d.get(q[i][3] +s+ q[j][3] +s+ str(int(q[i][0]-q[j][0])) +s+
    ↪ str(int(q[i][1]-q[j][1])) +s+ str(int(q[i][2]-q[j][2]))) == None:
376 #         print(q[i][3] +s+ q[j][3] +s+ str(int(q[i][0]-q[j][0])) +s+
    ↪ str(int(q[i][1]-q[j][1])) +s+ str(int(q[i][2]-q[j][2])))
377 # J indices
378 #print(J_d.get(temp[0]))
379 #print(type(J_d.get(temp[0])))
380 if typ == 1:
381     temp = [(q[k][3] +s+ q[j][3] +s+ str(int(q[k][0]-q[j][0])) +s+
    ↪ str(int(q[k][1]-q[j][1])) +s+ str(int(q[k][2]-q[j][2]))) for j in
    ↪ range(star,stop)]
382     #print(temp)

```

```

383     length = 0
384     l = star
385     # print('max: ' +str(stop))
386     while length < lim:
387         #print('iteration: '+str(l))
388         if type(J_d.get(temp[l-star])) != None and (int(q[k][0]-q[l][0]) != 0
389             ↪ or int(q[k][1]-q[l][1]) != 0 or int(q[k][2]-q[l][2]) != 0):
390             length += 1
391         #if J_d.get(temp[l-star]) != None:
392             #print(type(J_d.get(temp[l-star])))
393         l += 1
394         if l == stop:
395             break
396     return m.Minimize(-2*sum(J_d.get(temp[j-star])*var[i]*var[j] for j in
397         ↪ range(star,l) if J_d.get(temp[j-star]) is not None and
398         ↪ (J_sum_cond([int(q[k][0]-q[j][0]),
399         ↪ int(q[k][1]-q[j][1]),int(q[k][2]-q[j][2])],ori = ori))), 1
400
401     if typ == 0:
402         temp = [(q[i][3] +s+ q[j][3] +s+ str(int(q[i][0]-q[j][0])) +s+
403             ↪ str(int(q[i][1]-q[j][1])) +s+ str(int(q[i][2]-q[j][2]))) for j in
404             ↪ range(star,stop)]
405     return m.Minimize(-2*sum(J_d.get(temp[j-star])*var[i]*var[j] for j in
406         ↪ range(star,stop) if J_d.get(temp[j-star]) is not None))
407
408
409
410
411
412
413
414
415
416
417
418
419
420
421
422
423
424
425
426
427
428
429
def optimize(J_matrix,ranges, path, atom_names, latt, moments, J_reach, solver = 1,
↪ m_name = "test", info = 1, init_ = 0, sens = False, boost = False, starts =
↪ {}):
430     m = GEKKO(name = m_name, remote = False)
431     ran = [None, None, None]
432     inc = 0
433
434     for i in range(3): #Check if we need another value due to including 0.
435         if np.sign(ranges[2*i+1]) != np.sign(ranges[2*i]):
436             inc = 1
437         ran[i] = range(int(ranges[2*i]),int(ranges[2*i+1] + inc)) #makes ranges to
438             ↪ sum over
439
440     unique_atoms = np.unique(atom_names)
441     atom_range = range(len(unique_atoms))
442     if boost == False:
443         atoms, names = initialize_vars_2(ran, m, unique_atoms,latt,moments,init =
444             ↪ init_)
445     else:
446         atoms, names = initialize_vars_2(ran, m, unique_atoms,latt,moments,init =
447             ↪ init_, boost = boost, starts = starts)
448     atoms_flat, at_index = flatten_matrix(atoms,ran, atom_range, unique_atoms)
449     cons = periodic_bc_2(m, J_matrix, unique_atoms, atoms_flat, at_index, ranges,
450         ↪ J_reach)
451     #J_par = initialize_pars(m, J_matrix)
452     test = obj_fct_3(J_matrix,atoms_flat,at_index, m)
453     p = os.path.join(os.getcwd(),path)
454     m._path = p
455     m.options.WEB = 0
456     m.options.solver = solver
457     if sens == True:
458         m.options.SENSITIVITY = 1
459     #m.options.CSV_WRITE = info
460     print("Starting optimization")

```

```

430     #m.solve (disp=True)
431     with open(path/'iterations', 'w') as f:
432         with redirect_stdout (f):
433             m.solve (disp=True)
434     print ("Finished optimization")
435
436
437
438     def obj_fct_3(J_mat, var_vec, q, m): # makes the main objective function of the
↪ system
439         cutoff = 200
440         eq_num = count (len(var_vec), cutoff)
441         obj_fct = [None for j in range(int (eq_num))]
442         k = 1
443         for i in range(1, len(var_vec)):
444             if var_vec[i] is None:
445                 continue
446             if i > cutoff:
447                 eqs = int (np.floor (i/cutoff)+1)
448                 length_eq = int (i - cutoff*(eqs-1))
449                 obj_fct [i] = J_sum_2 (m, J_mat, q, var_vec, 0, cutoff, i)
450                 for l in range(1, eqs):
451                     if l == eqs-1:
452                         obj_fct [-k] = J_sum_2 (m, J_mat, q, var_vec, l*cutoff, l*cutoff +
↪ length_eq, i)
453                     else:
454                         obj_fct [-k] =
↪ J_sum_2 (m, J_mat, q, var_vec, l*cutoff, (l+1)*cutoff, i)
455                         k += 1
456             else:
457                 obj_fct [i] = J_sum_2 (m, J_mat, q, var_vec, 0, i, i)
458     print ("Done with making obj function")
459     return obj_fct [obj_fct != 0]
460
461     #=====
462     #                               SMALL HELP FUNCTIONS                               #
463     #=====
464
465     def check_non_mag_atoms (at_dict):
466         lst = [[], []]
467         threshold = 0.1
468         for i in at_dict:
469             g = re.sub (' \d', '', i)
470             if abs (at_dict [i]) < threshold:
471                 lst [1].append (g)
472             else:
473                 lst [0].append (g)
474
475         return [list (set (lst [0])), list (set (lst [1]))]
476
477     def cut_equation (m, J_mat, uni_at, var_vec, ind, J_reach, cell, star, stop, i, typ =
↪ 0, j = 0, ori = [1,1,1,0]): #go here when we've decided upon an equation
478     # GEKKO has a max line length of 15000 characters; we prevent going over that
↪ amount here.
479     # i is the var of interest
480     # j is its equivalent brother
481     #how many equations do we really want? We want to start summing over everything
482     cutoff = 200
483     size =
↪ len (uni_at) *min (J_reach [0], cell [0]) *min (J_reach [1], cell [1]) *min (J_reach [2], cell [2])
↪ #approximate num of atoms in equations

```

```

484     eqs = int(np.floor(size/cutoff)+1)
485     fct = [None for k in range(eqs)]
486     for k in range(eqs):
487         if k == eqs -1:
488             fct[k], star = J_sum_2(m, J_mat, ind, var_vec, star, stop, i,typ = 1, k
↳ = j, lim = size/eqs, ori = ori)
489         else:
490             fct[k], star = J_sum_2(m, J_mat, ind, var_vec, star, stop, i,typ = 1, k
↳ = j, lim = size/eqs, ori = ori)
491     return fct
492
493 def list_3D(len_x,len_y,len_z,ty):
494     lst = [[ [ty for i in range(len_x)] for j in range(len_y)] for k in
↳ range(len_z)]
495     return lst
496
497 def check_line_length(filename): #To check if we go over the maximum length of one
↳ line in the optimization file.
498     filename = Path(str(filename) + ".apm")
499     with open(filename) as f:
500         lines = f.readlines()
501         lengths = np.zeros(len(lines))
502         for i in range(len(lines)):
503             lengths[i] = len(lines[i])
504         return max(lengths)
505
506 def initialize_pars(m,J_matrix): #giving each parameter a name; might only be semi
↳ usefull.
507     J_pars = {}
508     for i in J_matrix:
509         if J_pars.get(i) != None: #checking if we have extra names or not
510             print(i)
511         J_pars[i] = m.Param(value = J_matrix.get(i))
512     return J_pars
513
514 def count(var,cutoff): #function that also works in the line cut function to make
↳ sure we don't run out of space
515     tot_eq = 0
516     for i in range(int(np.floor(var/cutoff)+1)):
517         if i < np.floor(var/cutoff):
518             tot_eq += cutoff*(i+1)
519         else:
520             tot_eq += (var - cutoff*i)*(i+1)
521     return int(tot_eq)
522
523 def find_lattice_pars(im,lat): #adds the actuals lattice paramters to the J matrix.
524     J_ext = np.copy(im)
525     J_ = np.concatenate((J_ext,np.zeros((len(J_ext[:,0]),3))),axis = 1)
526     x, y, z = range(4,7)
527     c, b, a = range(-3,0)
528     for i in range(len(J_[:,0])):
529         J_[i,c:] = lat.lattice.inv_matrix.dot(J_[i,x:(z+1)])
530     return J_
531
532 #Second try; flattens the matrix and accounts for double counting
533 def flatten_matrix(mat, ra,at_ra,nam):
534     #mat is the matrix, ra are the ranges, at_ra is the atom range and nam are the
↳ unique atom names
535     lst = []
536

```

```

537 indices = [[] for i in
↳ range(len(mat[0][0][0])*len(at_ra)*len(mat[0])*len(mat[0][0]))]
538 for w in at_ra:
539     for t in ra[0]:
540         for u in ra[1]:
541             for v in ra[2]:
542                 lst.append(mat[w][t][u][v])
543                 ind = len(lst) -1
544                 indices[ind] = [t, u, v, nam[w]]
545
546 #print(len(lst))
547 #print(indices[0:10])
548 #print("Done with flattening variable matrix")
549 return lst, indices
550
551 def find_unit_cell(coords, new_names, struct_obj, which = 0, bounds =
↳ np.array([0,0,0,1,1,1])): #selects a smaller subset to print
552 '''
553 We assume here that coords are in the shape of lattice vectors (!!)
554 '''
555 needed_co = []
556 if which == 0:
557     #print(coords[0,0:3])
558     for i in range(len(coords[:,0])):
559         if np.all(coords[i,0:3] < bounds[[1,3,5]]) and np.all(coords[i,0:3] >=
↳ bounds[[0,2,4]]):
560             needed_co.append(i)
561     coords = coords[needed_co,:]
562     names = np.array(new_names)
563     names = names[needed_co]
564 return coords, names
565
566 def calculate_tot_mom(spins,out_fol,c,modn): #as mentioned; sums over all magnetic
↳ moments to find the moment per unit cell
567 tot_mom = sum(spins[:,-1])
568 off = np.zeros(3)
569 for i in range(3):
570     if np.sign(c[2*i+1]) != np.sign(c[2*i]):#WE actually always know this as we
↳ require 0 to be part of the range!
571         off[i] = 1 #Still, just to make sure though.
572 av_mom = tot_mom/((c[1]-c[0]+off[0])*(c[3]-c[2]+off[1])*(c[5]-c[4]+off[2]))
573 with open(out_fol/'mag_moment', 'w') as f:
574     with redirect_stdout(f):
575         print('Total magnetic moment: ' + str(tot_mom))
576         print('Magnetic moment per unit cell: ' + str(av_mom))
577         print('Max line length in model file: ' + str(check_line_length(out_fol
↳ / modn)))
578 print('Total magnetic moment: ' + str(tot_mom))
579 print('Magnetic moment per unit cell:' + str(av_mom))
580 print()
581 return
582
583 #=====
584 #                               MAIN RUNNER FUNCTIONS                               #
585 #=====
586
587 def used_data(in_fol,out_fol,call_type = 0): #functions that ties all the others
↳ together
588 dir_path = os.path.dirname(os.path.realpath(__file__))
589 os.chdir(dir_path)
590 file = in_fol / "POSCAR"

```

```

590 TB2J = True
591 if os.path.exists(in_fol / "exchange.out"):
592     J_file = in_fol / "exchange_short.out"
593     J_old = in_fol / "exchange.out"
594     mode = 0
595     hor_vals = 10
596 else:
597     TB2J = False
598     J_file = in_fol / "jdata"
599     mode = -1 #to read the data from jdata
600     hor_vals = 6
601 if call_type == 0:
602     try:
603         os.mkdir(out_fol)
604     except OSError:
605         print("Warning!! Out folder already exists")
606         # cont = input('Continue anyway? [y/n]')
607         # if cont == 'n':
608         #     return None
609     if os.path.exists(J_file) == False and TB2J == True:
610         J_short(J_old,J_file)
611 if TB2J:
612     at_mom = read_moments(J_old)
613     at_conv_names = None
614
615 else:
616     at_mom, at_conv_names = read_moments(in_fol / "moments_in", TB2J = TB2J)
617
618 mag_ats = check_non_mag_atoms(at_mom)
619
620 lat = Poscar.from_file(file).structure
621 lat.remove_species(mag_ats[1])
622
623 sec_lat = Poscar.from_file(file).structure
624 sec_lat.remove_species(mag_ats[0])
625 Js, at_names = read_file(J_file,hor_vals, mode, convert_names=at_conv_names)
626
627 biggest_dist = np.zeros(3)
628 if TB2J:
629     J_better = find_lattice_pars(Js, lat)
630     for i in range(3):
631         biggest_dist[i] = max(J_better[:,-3+i])
632 else:
633     J_better = Js
634     for i in range(3):
635         biggest_dist[i] = max(J_better[:,i])
636 J_dlvec, sites_dic = J_as_dict(J_better, at_names,lat, 3)
637 #print(type(J_dlvec.get("Mn 1 Mn 4 2 1 1")))
638 return lat, sec_lat, at_names, at_mom, J_dlvec, sites_dic, dir_path,
↪ biggest_dist
639
640 def full_opt(in_fol,out_fol,calc_range, modn = 'mod',title_ = "First run", initi =
↪ 0, sensitivity = False,plot = True, plot_range = np.array([0,1,0,1,0,1]), boost
↪ = False, starts = {}):
641     '''
642     Parameters
643     -----
644     in_fol : Path
645             Folder that contains the input (POSCAR and exchange.out) files of material
646     out_fol : Path()

```



```

647         Folder to print output files to
648     calc_range : list
649         1D list that contains the unit cells to consider in the calculation in the
↪ form [a_min,a_max,b_min,b_max,c_min,c_max]
650     plot_range : numpy array
651         1D array that contains the unit cells to plot in the form
↪ [a_min,a_max,b_min,b_max,c_min,c_max]
652     modn : str, optional
653         The name for the model. The default is 'mod'.
654     title_ : str, optional
655         Title for the plot. The default is "First run".
656     initi : int
657         Type of initialization.
658         0 = any val within bounds
659         1 = only positive values
660         2 = sign equal to sign in poscar
661
662     Returns
663     -----
664     None.
665
666     '''
667     # for i in np.unique(at_names):
668     #     J_dlvec[i + '+' + i + ' 0 0 0'] = 0
669     lat, sec_lat, at_names, at_mom, J_dlvec, sites_dic, dir_path, J_range =
↪ used_data(in_fol, out_fol)
670     #print(J_dlvec)
671     if lat == None:
672         print('Stopping run: wrong folder')
673         return
674     if len(re.findall('I', str(out_fol))) > len(re.findall('I', str(in_fol))):
↪ #selecting which solver to use based on the folder name (should contain a I
↪ for IPOPT and A for APOPT)
675         solve = 3
676         print("Using the IPOPT Solver") #Both A and I present defaults to IPOPT
677     elif len(re.findall('A', str(out_fol))) > len(re.findall('A', str(in_fol))):
678         solve = 1
679         print("Using the APOPT Solver")
680     else:
681         solve = 3
682     optimize(J_dlvec, calc_range, dir_path / out_fol, at_names, lat, at_mom, J_range,
↪ solver = solve, m_name = modn, init_ = initi, sens = sensitivity, boost =
↪ boost, starts = starts)
683
684     spin_states, spin_names = read_file(out_fol / 'results.json', 5, 1)
685     calculate_tot_mom(spin_states, out_fol, calc_range, modn)
686     if plot == True:
687         plotgrid, plot_names = find_unit_cell(spin_states, spin_names, lat, bounds =
↪ plot_range)
688         cols = ['gray', 'mediumaquamarine', 'lightcoral']
689         # plot_non_mag(plotgrid[:,0:3], sec_lat, show = False)
690         mp.plot_scatter(plotgrid[:,0:3], plotgrid[:,3], plot_names, sites_dic, cols,
↪ title_, latt = 1, struct_obj = lat, obj2 = sec_lat, print_lat = True,
↪ spins = True, point_scale=100)
691
692     #=====
693     #                               MULTIPLE RUNS CODE                               #
694     #=====
695
696     def run_times(in_fol, start_range, runs, inits, sensi = False, title = 'First run'):
↪ #simple loop to run the code a said number of times

```

```

697     s = '_' #also automatically makes a foldername
698     k = 0
699     for i in runs:
700         for j in inits:
701             out_fol = in_fol
702                 ↪ /('rI'+str(start_range[1]-start_range[0]+1)+s+str(i)+s+str(j))
703             full_opt(in_fol,out_fol, start_range, initi= j,plot = False,
704                 ↪ plot_range=np.array([-1,3,-1,3,-1,3]), sensitivity=sensi)
705             k += 1
706             print('Done with run number ' + str(k))
707
708 def run_thermo(in_fol,start_range,runs,inits,title = 'First run concatenated',
709     ↪ plt_range = np.array([0,2,0,2,0,2]), mod = [0], key_1 = 'r', key_2 = '\d',
710     ↪ change = 0.6):
711     s = '_'
712     t = ' '
713     k = 0
714     for i in runs:
715         for j in inits:
716             start_time = time.time()
717             new_start = {}
718             out_fol = in_fol
719                 ↪ /('rI'+str(start_range[1]-start_range[0]+1)+s+str(i)+s+str(j))
720             full_opt(in_fol,out_fol, start_range, initi= j,plot = False,
721                 ↪ plot_range=np.array([-1,3,-1,3,-1,3]))
722             spins, names = read_file(out_fol / 'results.json', 5, 1)
723             if mod[i] >= 0:
724                 spins[:,3] = boost_rand(spins[:,3], mode = mod[k])
725                 print("First run done; giving program a kick")
726                 #print(np.unique(names))
727                 for l in range(len(names)):
728                     new_start[names[l]+t+ str(int(spins[l,0]))+t+str(int(spins[l,1]))
729                         ↪ +t+str(int(spins[l,2]))] = spins[l,3]
730             if mod[i] >= 0:
731                 out_fol_2 = in_fol
732                 ↪ /('rI'+str(start_range[1]-start_range[0]+1)+s+str(i)+s+str(j)+s)
733             full_opt(in_fol,out_fol_2, start_range, initi= j,plot = False,
734                 ↪ plot_range=np.array([-1,3,-1,3,-1,3]),boost = True, starts =
735                 ↪ new_start)
736             #print(new_start)
737             if mod[i] < 0:
738                 new_starts = boost_sym(new_start, spins, names, change = change)
739                 while new_starts[0].get('rerun') == True: #this does mean that you
740                     ↪ can get really unlucky and be trapped in a loop.
741                     print('Starting solution is considered too poor; running
742                         ↪ program again')
743                     full_opt(in_fol,out_fol, start_range, initi= j,plot = False,
744                         ↪ plot_range=np.array([-1,3,-1,3,-1,3]))
745                     spins, names = read_file(out_fol / 'results.json', 5, 1)
746                     new_start = {}
747                     for l in range(len(names)):
748                         new_start[names[l]+t+
749                             ↪ str(int(spins[l,0]))+t+str(int(spins[l,1]))
750                             ↪ +t+str(int(spins[l,2]))] = spins[l,3]
751                     new_starts = boost_sym(new_start, spins, names, change =
752                         ↪ change)
753
754             if len(new_starts[0]) > 0:
755                 print(f'Running {len(new_starts)} symmetric version(s) of
756                     ↪ previous outcome')

```

```

740         n = ['a', 'b', 'c', 'd', 'e', 'f']
741         for m in range(len(new_starts)):
742             out_fol_3 = out_fol_2 = in_fol
743             ↪ / ('rI'+str(start_range[1]-start_range[0]+1)+s+str(i)+s+str(j)+n[m])
744             full_opt(in_fol, out_fol_3, start_range, initi= j, plot =
745                 ↪ False, boost = True, starts = new_starts[m])
746         else:
747             print('current solution is considered good enough symmetry
748                 ↪ wise')
749         k += 1
750         run_time = time.time() - start_time
751         minutes = int(run_time/60)
752         seconds = np.round((run_time/60 - minutes)*60, 2)
753         with open(in_fol/'runtimes', 'a') as f:
754             with redirect_stdout(f):
755                 ↪ print('rI'+str(start_range[1]-start_range[0]+1)+s+str(i)+s+str(j)+'
756                     ↪ '+str(run_time))
757             print('rI'+str(start_range[1]-start_range[0]+1)+s+str(i)+s+str(j)+'
758                 ↪ done with a runtime of '+str(minutes)+':'+str(seconds)+' minutes')
759     opt_sol_finder(in_fol, key_1, key_2)
760
761 def opt_sol_finder(in_fol, key_1, key_2, cubic = True, copy = True, prnt = True,
762     ↪ mode = 1):
763     finals = []
764     names = []
765     in_fol = Path(in_fol)
766     for fn in sorted(os.listdir(in_fol)):
767         if os.path.isdir(in_fol/fn) and len(re.findall(key_1, str(fn))) > 0 and
768             ↪ len(re.findall(key_2, str(fn))) > 0:
769             temp_fol = in_fol / fn
770             if str(fn)[-1].isnumeric():
771                 first_run = True
772             else:
773                 first_run = False
774             if len(re.findall('A', fn)) > 0: #Old colors for other method (APOPT
775                 ↪ instead of IPOPT)
776                 ft = [1, 2] #selects which mode to use of the read function
777             else:
778                 ft = [3, 3]
779             J_short(temp_fol/'iterations', temp_fol/'iter', ftype=ft[0])
780             ite = read_file(temp_fol/'iter', 10, ft[1])
781             if cubic == True:
782                 ite[:, 1] = ite[:, 1]/(int(re.findall('\d', str(fn))[0])**3) #this is
783                 ↪ not accurate probably because of extra 'ghost' interactions
784             moments = read_file(temp_fol/'mag_moment', 2, 4)
785             finals.append([str(fn), ite[-1, 1], ite[-1, 0], moments[1, 1]])
786             if mode == 1:
787                 if not first_run:
788                     if str(fn)[-5].isnumeric(): #check if run index has 2 numbers
789                         ↪ or one
790                         names.append(str(fn)[-5:-1])
791                     else:
792                         names.append(str(fn)[-4:-1])
793                 else:
794                     if str(fn)[-4].isnumeric():
795                         names.append(str(fn)[-4:])
796                     else:
797                         names.append(str(fn)[-3:])
798             if mode == 2:

```

```

789         if str(fn)[-1].isnumeric() == False:
790             names.append(str(fn)[: -1])
791
792     with open(in_fol / "results.txt", 'w') as f:
793         for i in range(len(finals)):
794             f.write(finals[i][0] + ' ' + str(finals[i][1]) + ' ' +
795                   ↪ str(finals[i][2]) + ' ' + str(finals[i][3]) + ' ' + str(names[i]) + '\n')
796
797     nam_arr = np.array(names)
798     #print(nam_arr)
799     fin_arr = np.array(finals)
800     runs = np.unique(nam_arr, return_inverse = True, return_counts = True)
801     #print(runs[1])
802     #print(runs[0])
803     #print(nam_arr)
804     if copy:
805         for i in range(len(runs[0])):
806             temp_arr = fin_arr[(runs[1]==i),:]
807             #print(temp_arr[:,1])
808             temp_win = np.argmin(temp_arr[:,1].astype(float))
809             n_t = temp_arr[temp_win,0]
810             #print(n_t)
811             if prnt:
812                 print(str(n_t) + ' is the optimal result; copying to f folder')
813
814             shutil.copytree(in_fol/str(n_t), in_fol/f'f{str(n_t)[1:-1]}')
815
816     #=====
817     #                               ITERATING FUNCTIONS                               #
818     #=====
819
820 def boost_sym(d, s, n, change = 0.6): #d = dictionary, s = spins, n = names
821     #we again assume that 0 is within each range.
822     un = np.unique(n)
823     minmax = np.zeros(6)
824     ranges = [None, None, None]
825     for i in range(3):
826         minmax[2*i] = min(s[:,i])
827         minmax[2*i+1] = max(s[:,i])
828
829     ranges[i] = range(int(minmax[2*i]), int(minmax[2*i+1]+1))
830     sym_array = np.zeros((len(ranges[0])*len(ranges[1])*len(ranges[2]), len(un)+3))
831     m = 0
832     for i in ranges[0]:
833         for j in ranges[1]:
834             for k in ranges[2]: #we sum over each unit cell and evaluate signs
835                 temp = np.zeros(len(un)+3)
836                 for l in range(len(un)):
837                     temp[l] = np.sign(d.get(un[l]+' '+str(i)+' '+str(j)+' '+str(k)))
838                 #temp = [1,-1,1,-1] each place corresponding to the sign of the
839                 ↪ spin of an atom.
840                 temp[-3] = i
841                 temp[-2] = j
842                 temp[-1] = k
843                 sym_array[m] = temp
844                 m+= 1
845     tot_length = len(sym_array[:,0]) #amount atoms
846     #print(tot_length) #should be equal to 32 for a 2x2x2 MnO cell
847     #print(sym_array)
848     abs_sym = sym_array.copy()
849     for i in range(len(abs_sym[:,0])):

```

```

847     abs_sym[i, :-3] = abs_sym[i, :-3]*abs_sym[i, 0]
848     configs = np.unique(abs_sym[:, :-3], return_inverse = True, return_counts=True,
849     ↪ axis = 0)
849     ind = []
850     # print('first: '+ str(configs[0]))
851     # print(configs[1])
852     # print(configs[2])
853     for i in range(len(configs[2])):
854         if configs[2][i] > tot_length/3: #we see this configuration as significant
855             ↪ as its at least 30% of the material
855             ind.append(i)
856     if len(ind) > 0:
857         ret_dicts = [{} for i in range(len(ind))]
858     else:
859         ret_dicts = [{'rerun': True}] #we have a very antisymmetric solution. We
860             ↪ try to run the program again with a random initialization
860     return ret_dicts
861
861     p = 0
862     for i in ind: #sum over all the prominent configurations
863         perfect = 0
864         old_ind = np.where(configs[1] == i)[0] #indices in array where its brothers
865             ↪ are present
866         cell_sym = np.zeros((len(ranges[0]), len(ranges[1]), len(ranges[2])))
867         for a in old_ind: #what does this do exactly?
868             if np.all(abs_sym[a] == sym_array[a]):
869                 cell_sym[int(sym_array[a, -3]), int(sym_array[a, -2]),
870                 ↪ int(sym_array[a, -1])] = 1
871             else:
872                 cell_sym[int(sym_array[a, -3]), int(sym_array[a, -2]),
873                 ↪ int(sym_array[a, -1])] = -1
874
875         #now the matrix is set up so we can start looking for symmetries
876         # we'll look in each direction and check each column for its dominant
877             ↪ pattern
878         # print(abs_sym)
879         # print(sym_array)
880         #print(cell_sym)
881         if len(np.where(cell_sym == 0)[0]) == 0:
882             perfect += 1 #we only have one type of unit cell -> bonus points :)
883         cs = np.zeros(3).astype(int)
884         pattern = np.zeros(3).astype(int)
885         for coord in range(3):
886             ferro = 0
887             ant_ferro = 0 #these names are misleading its more like 1 - cell
888                 ↪ symmetric and 2 - cell symmetric.
889             for cs[coord-1] in ranges[coord-1]:
890                 for cs[coord-2] in ranges[coord-2]:
891                     for cs[coord] in range(int(minmax[2*coord]), int(minmax[2*coord
892                         ↪ + 1])):
893                         ad = np.zeros(3).astype(int)
894                         ad[coord] = 1
895                         if cell_sym[cs[0], cs[1], cs[2]] ==
896                             ↪ cell_sym[cs[0]+ad[0], cs[1]+ad[1], cs[2]+ad[2]] and
897                             ↪ cell_sym[cs[0], cs[1], cs[2]] != 0:
898                             ferro += 1
899                         elif cell_sym[cs[0], cs[1], cs[2]] ==
900                             ↪ -cell_sym[cs[0]+ad[0], cs[1]+ad[1], cs[2]+ad[2]] and
901                             ↪ cell_sym[cs[0], cs[1], cs[2]] != 0:
902                             ant_ferro += 1
903

```

```

894     pattern[coord] = np.sign(ferro-ant_ferro) #-1: switching, 0 equal and 1
      ↪ is ferro
895 # print(pattern)
896 unaltered = True
897 if perfect == 1 and sum(pattern) == 1 and np.all(pattern != 0):
898     print('Solution looks good; trying other symmetric configuration to
      ↪ check optimallity')
899     pattern = [1,1,1] #try special different solution as
900     unaltered = False
901
902 if perfect == 1 and sum(pattern) == -1 and np.all(pattern != 0):
903     pattern = [-1,-1,-1]
904     print('Solution looks good; trying other symmetric configuration to
      ↪ check optimallity')
905     unaltered = False #we do this now for very neat solutions that would
      ↪ otherwise be considered
906 #we now have a list with the prominent patterns per direction.
907 #we only take the most likely one otherwise the amount of runs grows
      ↪ exponentially as we're also checking different very likely layouts
908 #so [1 1 0] -> [1 1 1] and [1 -1 0] -> [1 -1 1] as we will guess that 1
      ↪ cell symmetry is more likely
909 # only when [-1 -1 1]
910 # When are we satisfied??? [1 1 1], [-1 -1 -1]?
911
912 if np.all(pattern == pattern[0]) and unaltered:
913     check = True
914     for j in ranges[0]:
915         for k in ranges[1]:
916             for l in ranges[2]:
917                 if pattern[0]**(j+k+l)*cell_sym[0,0,0] != cell_sym[j,k,l]
      ↪ and cell_sym[0,0,0] != 0:
918                     check = False
919     #This works for our purposes, however, for larger materials this can
      ↪ still return a false positive.
920     #Hence should be altered to check each unit cell for the pattern maybe,
      ↪ or a condition should be built in
921     #that checks for irregularities
922     if check:
923         perfect += 1
924
925 if perfect == 2: #we are satisfied with the current result and return the
926     #print(pattern)
927     #print(sym_array)
928     return ret_dicts #we don't really do anything here as we assume the
      ↪ solution to be optimal
929 for j in range(3):
930     if pattern[j] == 0:
931         pattern[j] = 1
932
933 if cell_sym[0,0,0] == -1:
934     cell_sym = cell_sym*(-1) #to make sure that we dont switch/alter too
      ↪ many atoms; as -1 and 1 are similar solutions
935 new_cells = np.zeros((len(ranges[0]),len(ranges[1]),len(ranges[2])))
936
937 for j in ranges[0]:
938     for k in ranges[1]:
939         for l in ranges[2]:
940             val = pattern[0]**j*pattern[1]**k*pattern[2]**l
941             c = 1
942             if cell_sym[j,k,l] != val:

```

```

943         c = change
944         new_cells[j,k,l] = c*val
945         #print(new_cells)
946         for m in range(len(un)):
947             ret_dicts[p][un[m]+' '+str(j)+' '+str(k)+' '+str(l)] =
                ↪ c*val*abs(d.get(un[m]+' '+str(j)+' '+str(k)+'
                ↪ '+str(l)))
948     #now we have a first run; if our symmetry is not 'perfect' in each
    ↪ direction; we also try a second run to check if our solution is really
    ↪ optimal
949     if abs(sum(pattern)) != 3:
950         if sum(pattern) > 0:
951             new_pat = [1,1,1] #meaning that if we have -1, 1, 1; we also try 1
                ↪ 1 1
952         else:
953             new_pat = [-1,-1,-1] #if we have -1 -1 1, also try -1, -1, -1.
954             #NOTE that we disregard the other configurations (if we have -1 1 1
                ↪ we don't try 1 -1 1 and 1 1 -1)
955
956     new_cells_2 = np.zeros((len(ranges[0]),len(ranges[1]),len(ranges[2])))
957     ret_dicts.append({})
958     for j in ranges[0]:
959         for k in ranges[1]:
960             for l in ranges[2]:
961                 val = new_pat[0]**j*new_pat[1]**k*new_pat[2]**l
962                 c = 1
963                 if cell_sym[j,k,l] != val:
964                     c = change
965                     new_cells_2[j,k,l] = c*val
966                     #print(new_cells)
967                     for m in range(len(un)):
968                         ret_dicts[-1][un[m]+' '+str(j)+' '+str(k)+' '+str(l)] =
                            ↪ c*val*abs(d.get(un[m]+' '+str(j)+' '+str(k)+'
                            ↪ '+str(l)))
969
970     p += 1
971     #print(ret_dicts[0])
972     #print(new_cells)
973     return ret_dicts
974
975 def boost_rand(vec, mode): #previous implementation of rerun method
976     if mode == 0: #randomly select a couple of atoms to give a kick
977         rng = np.random.default_rng()
978         ind = rng.choice(len(vec),int(len(vec)/3),replace = False)
979         for i in ind:
980             vec[i] = vec[i] - vec[i]*0.6
981     if mode == 1:
982         add = np.random.rand(len(vec))
983         vec = vec - add*vec*0.2
984     if mode == 2:
985         vec = vec - vec*0.05
986         rng = np.random.default_rng()
987         ind = rng.choice(len(vec),int(len(vec)/8),replace = False)
988         for i in ind:
989             vec[i] = -vec[i]
990     if mode == 3:
991         rng = np.random.default_rng()
992         ind = rng.choice(len(vec),int(len(vec)/3),replace = False)
993         for i in ind:
994             vec[i] = vec[i] - vec[i]*1.5
995     return vec

```

```

995
996 def test_boosts(in_fol, start_fol, start_range, title = 'First test', mod = -1,
↳ change = 0.6): #testing our change function on an existing suboptimal solution
997     start_time = time.time()
998     t = ' '
999     spins, names = read_file(in_fol / start_fol / 'results.json', 5, 1)
1000     new_start = {}
1001     for l in range(len(names)):
1002         new_start[names[l]+t+ str(int(spins[l,0]))+t+str(int(spins[l,1]))
↳ +t+str(int(spins[l,2]))] = spins[l,3]
1003     if mod < 0:
1004         new_starts = boost_sym(new_start, spins, names, change = change)
1005         if new_starts[0].get('rerun') == True: #this does mean that you can get
↳ really unlucky and be trapped in a loop.
1006             print('Starting solution is considered too poor; we skip this run as it
↳ is not interesting')
1007             return
1008
1009         if len(new_starts[0]) > 0:
1010             print(f'Running {len(new_starts)} symmetric version(s) of previous
↳ outcome')
1011             n = ['a', 'b', 'c', 'd', 'e', 'f']
1012             for m in range(len(new_starts)):
1013                 out_fol_3 = in_fol / (re.sub('I',str(change)[-1], str(start_fol))
↳ +n[m])
1014                 full_opt(in_fol,out_fol_3, start_range, initi= 0,plot = False,boost
↳ = True, starts = new_starts[m])
1015             else:
1016                 print('current solution is considered good enough symmetry wise')
1017                 run_time = time.time() - start_time
1018                 minutes = int(run_time/60)
1019                 seconds = np.round((run_time/60 - minutes)*60,2)
1020                 with open(in_fol/'runtimes','a') as f:
1021                     with redirect_stdout(f):
1022                         print(re.sub('I',str(change)[-1], str(start_fol))+ ' '+str(run_time))
1023                 print(re.sub('I',str(change)[-1], str(start_fol))+ ' done with a runtime of
↳ '+str(minutes)+ ':' +str(seconds)+ ' minutes')
1024
1025
1026 def main():
1027     return
1028
1029 if __name__ == '__main__':
1030     main()

```